Review

Receptor–Mitochondria Crosstalk in the Kynurenine Metabolic Pathway: Integrating Metabolomics and Clinical Mass Spectrometry

László Juhász [†], Zsolt Galla [†], Masaru Tanaka [*,‡], László Vécsei [*,‡]

Posted Date: 12 January 2026

doi: 10.20944/preprints202601.0822.v1

Keywords: kynurenic acid (KYNA); mitochondria; citric acid cycle; nicotinamide adenine dinucleotide (NAD^+); metabolomics; liquid chromatography–mass spectrometry (LC-MS); receptors; g-protein-coupled receptors; aryl hydrocarbon receptor (AhR); N-methyl-D-aspartate (NMDA); mitophagy

Review

Receptor–Mitochondria Crosstalk in the Kynurenine Metabolic Pathway: Integrating Metabolomics and Clinical Mass Spectrometry

László Juhász [1,†], Zsolt Galla [2,†], Masaru Tanaka [3,*,‡] and László Vécsei [3,4,*,‡]

[1] Institute of Surgical Research, University of Szeged, Albert Szent- Györgyi Medical School, Szeged, Hungary

[2] Department of Pediatrics, Albert Szent-Györgyi Faculty of Medicine, University of Szeged, H-6725 Szeged, Hungary

[3] HUN-REN-SZTE Neuroscience Research Group, Hungarian Research Network, University of Szeged (HUN-REN-SZTE), Danube Neuroscience Research Laboratory, H-6725 Szeged, Hungary

[4] Department of Neurology, Albert Szent-Györgyi Medical School, University of Szeged, H-6725 Szeged, Hungary

* Correspondence: tanaka.masaru.1@med.u-szeged.hu (M.T.); vecsei.laszlo@med.u-szeged.hu (L.V.); Tel.: +36-62-342-847 (M.T.); +36-62-545-351 (L.V.)

† These authors contributed equally to this work.

‡ These authors contributed equally to this work.

Abstract

Mitochondria orchestrate energy transfer, redox poise, and cell fate. Within this landscape, tryptophan catabolism yields kynurenines (KYNs), a versatile metabolite shaping organelle function. Emerging studies implicate G protein–coupled receptor 35 (GPR35), the aryl hydrocarbon receptor (AhR), and *N*-methyl-*D*-aspartate (NMDA) receptors as conduits between extracellular cues and adenosine 5′-triphosphate (ATP) maintenance, calcium handling, mitophagy, and inflammasome restraint. Parallel work links quinolinate driven de novo nicotinamide adenine dinucleotide (NAD^+) synthesis to tricarboxylic cycle (TCA) control and sirtuin programs across tissues. Yet the field lacks an integrated view that connects receptor pharmacology to NAD^+ economics and respiration, and it lacks single run clinical assays that quantify both KYN and TCA nodes. This review addresses those gaps by mapping receptor specific mitochondrial mechanisms of KYNA, delineating pathway–cycle crosstalk, and appraising unified liquid chromatography–mass spectrometry (LC–MS) strategies for simultaneous quantification. We synthesize evidence for mitochondrial GPR35 signaling that preserves ATP, AhR programs that tune mitophagy and oxidative defenses, and NMDA antagonism that limits excitotoxic stress. These mechanisms are integrated with quinolinate dependent NAD^+ biogenesis and α-ketoglutarate checkpoints, then benchmarked against chromatographic and ionization solutions suitable for clinical workflows. Here we highlight a receptor to organelle axis that couples KYN metabolism flux to respiratory control and offer a practical roadmap for standardized, single run LC–MS panels. The framework can sharpen target validation in ischemia, neurodegeneration, psychiatry, and oncology, while de-risking biomarker qualification through harmonized analytics. More broadly, resolving temporal dynamics, compartmental signaling, and cross matrix comparability will accelerate movement from association to intervention and enable decision grade metrics for patient selection, pharmacodynamic readouts, and therapeutic design.

Keywords: kynurenic acid (KYNA); mitochondria; citric acid cycle; nicotinamide adenine dinucleotide (NAD^+); metabolomics; liquid chromatography–mass spectrometry (LC-MS); receptors; g-protein-coupled receptors; aryl hydrocarbon receptor (AhR); N-methyl-D-aspartate (NMDA); mitophagy

 doi:10.20944/preprints202601.0822.v1

1. Introduction

Mitochondria choreograph energy flux, redox poise, and fate decisions through tightly coupled metabolism, signaling, and quality control (QC) [1,2]. Nuclear factor erythroid 2–related factor 2 (Nrf2) and nuclear respiratory factor 1 (Nrf1) align bioenergetics with antioxidant defenses, tuning respiration, detoxification, and ROS setpoints to prevent maladaptive stress responses [3,4]. Proton leak via uncoupling proteins subtly tempers superoxide, reshaping signaling without collapsing adenosine 5′-triphosphate (ATP) supply [5,6]. Dynamic cycles of fission, fusion, biogenesis, and mitophagy purge damage and license apoptosis or survival, thereby preserving tissue function across development and aging [1,7,8]. In stem and neuronal lineages, mitochondrial metabolites and ROS act as instructive cues that program transcription and differentiation while guarding viability [2,9,10]. These convergent circuits constitute a master key for health and disease [11,12].

Trypt[16–18ophan (Trp)catabolism feeds the kynurenine (KYN) metabolic pathway, yielding kynurenic acid (KYNA) that operates as a pleiotropic signal aligning mitochondrial respiration, redox poise, and cellular metabolism [13–15]. KYNA engages G protein–coupled receptor 35 (GPR35) and AMP-activated protein kinase (AMPK) to modulate bioenergetics, thermogenesis, and lipid handling across adipose and muscle, with exercise-driven kynurenine aminotransferases (KATs) activity boosting KYNA output and efficiency [16–18]. Genetic or pharmacologic perturbation of KAT enzymes reveals KYNA's necessity for ATP synthesis and mitochondrial stability in brain and peripheral tissues [13,19–21]. At stress frontiers, KYNA preserves ATP, curbs mtROS, and licenses mitophagy, thereby limiting inflammasome activation and ischemic injury [21–24]. Pathway flux also supports NAD+ economy and neuroprotection, linking immune tone to mitochondrial longevity and disease modification [14,25–30].

KYNA coordinates receptor signaling that feeds directly into mitochondrial control. Through GPR35, it relocates the receptor to mitochondria, engages the ATP synthase inhibitory factor, preserves ATP, and adjusts organelle dynamics during ischemic stress [22,31]. GPR35 signaling restrains calcium mobilization, limits NLRP3 activation, and enables autophagic disposal of inflammasomes, linking immunity to mitochondrial QC [32,33]. As an AhR ligand, it reprograms redox and apoptotic set points across neural and cardiovascular contexts [34,35]. Antagonism at *N*-methyl-*D*-aspartate (NMDA) receptors and mitochondrial nicotinic acetylcholine receptors containing $\alpha 7$ subunits (α7nAChR) rewires excitatory drive and metabolic coupling, tuning respiration and protecting tissue function [36,37]. Additional endogenous ligands at GPR35 add complexity to this regulatory axis [38,39].

Trp degradation through the KYN metabolism supplies de novo NAD+, the redox currency that feeds the tricarboxylic acid cycle (TCA) and the electron transport chain, thereby tuning respiration at its core [14,40]. Flux through this pathway sets mitochondrial NAD+/NADH ratios and ROS thresholds via redox-active intermediates, stabilizing oxidative phosphorylation and ATP output [15,41]. Immune and tissue contexts reveal causality: macrophages require pathway-derived NAD+ for oxidative metabolism, while ischemia-reperfusion diverts flux and collapses antioxidant capacity until NAD+ is restored [42,43]. Enzyme control points are actionable. ACMSD inhibition elevates NAD+; kynurenine 3-monooxygenase (KMO) modulation redirects carbon to sustain TCA activity; pathway blockade diminishes SIRT1 signaling and viability[44,45]. These circuitries extend to microbiota, cardio-metabolic risk, T-cell bioenergetics, cancer, and aging [45–49].

The KYN metabolism links inflammation to mitochondrial bioenergetics, and its clinical footprint spans neurology, psychiatry, ischemic injury, metabolism, and cancer [26,50]. In neurodegeneration, skewed production of neurotoxic versus protective metabolites accelerates oxidative stress, excitotoxicity, and decline, while enzyme targeting can tilt the balance toward resilience [51–53]. Psychiatric syndromes display immune driven pathway activation with measurable biomarker shifts and actionable enzymatic nodes [50,54–57]. Cardiovascular and systemic contexts reveal redox and immune dysregulation that worsens tissue injury and aligns with ischemic vulnerability [58,59]. Metabolic disease reflects chronic low-grade inflammation that routes

 doi:10.20944/preprints202601.0822.v1

Trp away from homeostasis [26,60]. Tumors exploit pathway derived NAD+ and immunosuppression, creating therapeutic entry points under active clinical evaluation [61,62].

Capturing KYN metabolites and tricarboxylic acid intermediates in the same clinical sample remains a moving target [63–65]. Targeted LC-MS workflows for KYN species vary widely in extraction, chromatography, and calibration, and no protocol robustly spans all key metabolites or matrices [63,64,66]. Matrix effects, polarity extremes, and poor chromatographic behavior of compounds such as quinolinic acid (QA) confound accuracy and comparability [63,67]. Parallel LC-MS assays for TCA intermediates add further hurdles due to instability and matrix-dependent losses [63,68]. Alternative readouts help but fragment the picture: voltammetry and immunostrips deliver speed at the cost of scope, while capillary electrochromatography trades coverage for protracted runs [69,70]. Clinically useful panels will demand matrix-specific preparation, isotope-labeled standards, and harmonized cross-platform validation [63,71].

Current evidence offers vivid mechanistic snapshots, yet the mosaic remains disjointed across species, cell types, and measurement scales [21,55]. Elegant studies in lupus-prone T cells link Rab4A trafficking to mitophagy, cluster of differentiation 98 (CD98), and KYN-sensitive mTOR, but insights are constrained by model specificity and temporal windows [47,72]. Clinical syntheses in depression expose state-dependent metabolite signatures alongside striking heterogeneity in cohorts and methods [50,73]. Cross-phyla work in Lymnaea underscores evolutionary conservation while complicating translation to humans [74,75]. Analytical platforms further splinter datasets, with electrochemical and chromatographic approaches optimized for different matrices and targets [76,77]. Reviews connecting the pathway to NAD+ and aging highlight gaps between molecular flux, organelle dynamics, and outcomes that matter clinically [50,75,78,79].

Despite striking mechanistic vignettes, four gaps impede synthesis. First, temporal dynamics remain under-sampled: circadian, acute, and chronic windows yield nonoverlapping readouts that are rarely integrated [80]. Second, signaling is compartment-specific across tissues, cell types, and subcellular locales, complicating translation from regionally restricted or model-bound observations [81]. Third, causal links from receptors such as AhR or GPR35 to mitochondrial remodeling are inferred more often than demonstrated longitudinally in vivo [22]. Fourth, multi-analyte assays lack harmonization across matrices, throttling cross-study comparability and biomarker qualification [64]. Addressing these deficits will require time-resolved, compartment-aware designs that couple receptor activation to mitochondrial endpoints while deploying standardized, multiplexed metabolomic and signaling panels across preclinical and clinical cohorts [79,80].

Objectives are fourfold. First, chart receptor-specific mitochondrial actions of KYNA by resolving GPR35-dependent calcium control, ATP preservation, and inflammasome restraint, and by contrasting AhR-driven stress programs and synaptic α7nAChR modulation. Second, delineate pathway–cycle crosstalk by linking enzyme localization and NAD+ biogenesis to respiratory control and organelle dynamics across tissues and time. Third, appraise integrated analytics that fuse targeted LC-MS panels with multi-omics, isotope tracing, and trafficking readouts to capture mechanism and flux in matched samples. Finally, synthesize translational implications in ischemic protection, neurodegeneration, cancer immunity, and network-level metabolic resilience to guide trial design and biomarker qualification.

Bridging correlation to cure requires two pillars. First, standardized, validated quantification across matrices and cohorts so biomarker signals mean the same thing in every lab [82]. Second, causal mechanistic experiments that link receptor and enzyme perturbations to mitochondrial dynamics and clinical outcomes [83]. Harmonized LC-MS/MS panels and fit-for-purpose QC will enable longitudinal, multi-analyte readouts in neurology, psychiatry, cardiometabolic disease, and oncology, converting meta-analytic heterogeneity into actionable thresholds [84]. Interventional studies that pair enzyme inhibition or pathway rerouting with mitochondrial endpoints can validate target engagement and refine patient selection [85]. This review follows that logic: we evaluate measurement platforms, map mechanistic levers, integrate disease-area evidence, and propose trial-ready frameworks that connect pathway state to therapeutic decisions.

 doi:10.20944/preprints202601.0822.v1

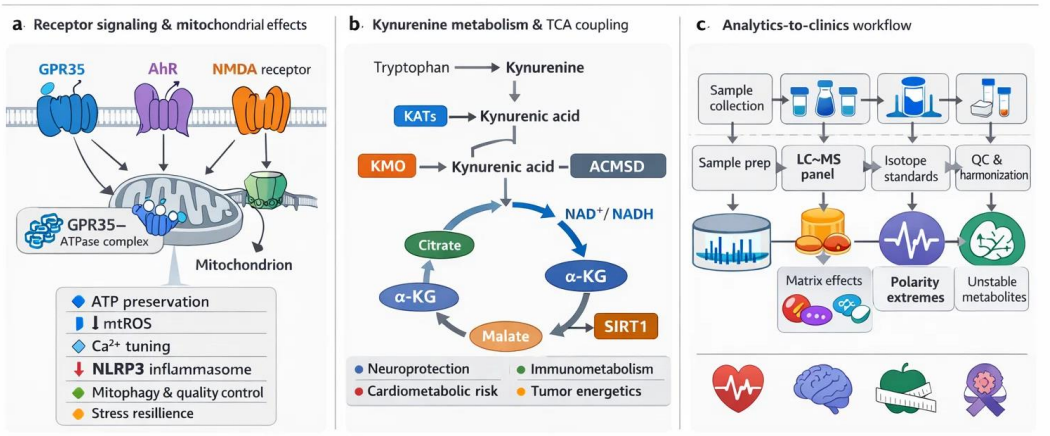

Figure 1. Kynurenic acid (KYNA) as a mitochondrial gatekeeper: receptor signaling, kynurenine (KYN) metabolism–tricyclic acid cycle (TCA) coupling, and analytics-to-clinics workflow. (A) Receptor landscape → mitochondria. KYNA engages GPR35, AhR, NMDA receptors, and mitochondrial α7nAChR to tune organelle dynamics. GPR35 activation and relocalization to mitochondria interfaces with ATP synthase inhibitory machinery to preserve ATP, limit mtROS, temper Ca^{2+} influx, and restrain NLRP3 inflammasome activity while licensing mitophagy. AhR signaling shifts redox and apoptotic programs, whereas NMDA and α7nAChR modulation recalibrates excitatory drive and respiratory coupling. Together, these inputs converge on mitochondrial quality control and stress resilience across neural, immune, and metabolic tissues. (B) KYN metabolism–TCA coupling. Tryptophan catabolism generates KYNA and de novo NAD^+, linking pathway flux to mitochondrial NAD^+/NADH ratios, ROS thresholds, and oxidative phosphorylation. Enzyme nodes—including KATs, KMO, and ACMSD—redirect carbon between KYNA synthesis, NAD^+ production, and TCA activity, shaping SIRT1 signaling and bioenergetic fitness. These interactions influence neuroprotection, immunometabolism, cardiometabolic risk, and tumor energetics, where imbalanced metabolite profiles alter mitochondrial stability and inflammatory tone. (C) Analytics-to-clinics path. Integrated measurement of KYN and TCA intermediates remains technically challenging owing to matrix effects, polarity extremes, and unstable metabolites such as quinolinic acid. Harmonized, multiplexed LC–MS panels incorporating isotope standards, matrix-specific preparation, and consistent QC—combined with multi-omics and time-resolved sampling—are required to quantify flux and receptor-mitochondria coupling. Such standardized assays underpin biomarker qualification and translational strategies across ischemia, neuropsychiatric disorders, metabolic disease, and cancer.

2. Receptor-Mediated Mitochondrial Regulation by Kynurenic Acid (KYNA)

KYNA sits at a neat signaling crossroads where surface receptors and mitochondrial targets talk to each other. Through GPR35, KYNA can trigger stress-adaptive signaling that converges on mitochondria to preserve ATP maintenance (via ATP synthase regulatory circuitry), restrain Ca^{2+} load, and dampen mtROS, with downstream effects on inflammasome tone and mitochondrial quality control. In parallel, KYNA's ligand activity at the aryl hydrocarbon receptor (AhR) reshapes transcriptional programs that promote mitophagy and redox homeostasis. As an NMDA receptor antagonist, KYNA limits excitotoxic Ca^{2+} influx, indirectly stabilizing mPTP gating and respiratory coupling. Evidence also supports mitochondrial α7nAChR-like signaling influencing Ca^{2+} handling and apoptosis. Finally, additional KYNA-sensitive "receptor-like" sites are plausible, including mitoKATP channels and redox-tunable nodes within Complex I/III.

2.1. KYNA and GPR35: Energy Homeostasis and Ischemic Protection

GPR35 has emerged as a regulator of metabolic stress responses [86–91]. It is ex-pressed in the gastrointestinal tract, immune cells, central nervous system, and heart, with expression upregulated in pathological conditions including ischemia–reperfusion injury, hypoxia, stroke, and heart failure

 doi:10.20944/preprints202601.0822.v1

[92–94]. Although GPR35 is associated with cytoprotection, evidence remains inconsistent regarding whether receptor activation or inhibition is beneficial [92,93,95,96]. Furthermore, a GPR35-dependent gut–microbe–brain metabolic axis has been identified, linking receptor activity to neuroimmune regulation and depressive-like behavior [97,98].

GPR35 interacts with several G protein families, enabling the regulation of diverse intracellular pathways with both pro- and anti-inflammatory effects [96,99–101]. Coupling to Gαi/o suppresses adenylate cyclase, decreases cyclic adenosine monophosphate (cAMP) levels [102], and reduces extracellular signal-regulated kinase (ERK) activity [103], which can limit extracellular signal-regulated kinases (ERKs) driven pro-inflammatory transcription [99]. Conversely, Gβγ subunits released from Gαi/o activate PLCβ, driving phosphoinositide hydrolysis, phosphoinositide 3-kinase (PI3K)/ protein kinase B (AKT) signaling, and nuclear factor kappa-light-chain-enhancer of activated b cells (NF-κB) activation, thereby promoting inflammatory gene expression [99]. Interaction with Gα12/13 stimulates ras homolog family protein (Rho)-dependent cytoskeletal remodeling, enhancing immune cell chemotaxis and reinforcing pro-inflammatory signaling. In addition, Gαq coupling exerts dual actions: it restricts PI3K-mediated AKT activation while facilitating ERK signaling through a PLCβ/Ca^{2+}/Src pathway [104]. These diverse and occasionally opposing mechanisms underscore the context-dependent role of GPR35 in coordinating G protein signaling and regulating mitochondrial responses [32,105–107]. Activation of these receptors has also been described to contribute to organellar damage via calpain-mediated proteolysis under various pathophysiological conditions (the GPR35–calpain signaling axis). For example, calcium overload activates calpains, which translocate to intracellular organelles, degrade target proteins, destabilize nuclear, lysosomal, and mitochondrial membranes, and release cathepsins and pro-apoptotic factors, ultimately leading to cell death [108]. Evidence implicates calpain-1 and calpain-2 in mitochondrial damage following cardiac ischemia/reperfusion [95,109,110]. Notably, GPR35 is strongly upregulated after myocardial ischemia, and its inhibition attenuates reactive oxygen species (ROS) production, reduces mitochondrial apoptosis, and preserves contractile function [111,112]. Consistently, blockade of GPR35 downregulates calpain-1 and calpain-2 expression and activity, attenuating calpain-mediated mitochondrial injury. The detrimental effects of calpain-driven proteolysis affect multiple mitochondrial sites, including increasing mitochondrial membrane permeability, inducing cytochrome c release, and initiating apoptosis [113]. In addition, calpain-1 can cleave the ATP synthase α-subunit, reducing ATP production and exacerbating oxidative stress [113].

Wyant and colleagues (2022) demonstrated that KYNA exerts cardioprotective effects during ischemia/reperfusion by acting on GPR35 [22]. Their study identified GPR35 as both necessary and sufficient for mediating KYNA-induced ischemic protection, a process tightly coupled to mitochondrial remodeling. Upon ligand binding, GPR35 activates Gi- and G12/13-dependent signaling cascades and translocates to the outer mitochondrial membrane, where it associates, likely indirectly, with ATP synthase inhibitory factor subunit 1 (ATPIF1) [100,114]. Through this interaction, activated GPR35 promotes ATP synthase dimerization and modulates oxidative phosphorylation to preserve cellular ATP content and maintain energy homeostasis under ischemic stress [115–117]. ATP synthase normally generates ATP from the proton gradient; however, during ischemia, it can reverse and hydrolyze ATP, resulting in energy loss and mitochondrial dysfunction [118–120]. ATPIF1 prevents this reverse mode without affecting ATP synthesis [92]. By stabilizing ATP synthase dimers, ATPIF1 also supports cristae integrity and prevents mitochondrial permeability transition pore (mPTP) opening [22,121]. In more detail, phosphorylation of ATPIF1 deactivates the protein, thereby permitting ATP hydrolysis, whereas dephosphorylation at Ser39 activates ATPIF1 and suppresses ATPase activity [22,122]. Mitochondrial GPR35 signaling dampens cAMP production by inhibiting adenylyl cyclase, thereby reducing PKA-mediated phosphorylation of ATPIF1 and maintaining it in its active, dephosphorylated state [22]. Collectively, these findings delineate a mitochondrial GPR35–ATPIF1–ATP synthase signaling axis that coordinates energy conservation and structural stability.

 doi:10.20944/preprints202601.0822.v1

The mitochondrial membrane potential (ΔΨm) serves as the primary driving force for ATP synthesis, generated by the proton gradient across the inner mitochondrial membrane [123–125]. A decrease in ΔΨm weakens the proton motive force, leading to diminished or even halted ATP production. Sustained depolarization of the mitochondrial membrane results in cellular energy depletion, metabolic disturbances, and ultimately, cell death [126,127]. Preservation of ATP levels under ischemic conditions is therefore closely dependent on maintaining mitochondrial membrane potential, which is essential for cell viability and the physiological function of organs [127,128]. A direct link between GPR35 modulation and alterations in ΔΨm has also been demonstrated under pathological conditions. Specifically, inhibition of GPR35 was shown to mitigate mitochondrial dysfunction not only by enhancing oxidative phosphorylation but also by preserving mitochondrial membrane potential [95]. In neonatal murine ventricular myocytes (NMVMs), JC-1 assays revealed a higher ΔΨm under ischemic or anoxic stress when GPR35 was inhibited compared to control conditions, indicating a protective mitochondrial effect [95].

Beyond its well-established role in ischemic protection, accumulating evidence indicates that KYNA–GPR35 signaling constitutes a critical regulatory axis in systemic energy homeostasis [16,129,130], particularly in the regulation of lipid catabolism [17]. Following three days of KYNA administration (a single daily intraperitoneal dose of 5 mg/kg body weight) in C57BL/6J mice, increased oxygen consumption, carbon dioxide production, and heat generation were observed, indicating enhanced metabolic activity and energy expenditure [16]. Moreover, KYNA administered on consecutive days significantly reduced white adipose tissue mass, including both inguinal and visceral (epididymal) depots, without exerting any measurable effect on brown adipose tissue mass. In adipose tissue, activation of GPR35 induces thermogenic and anti-inflammatory transcriptional programs, and thereby mitigates high-fat diet–induced adiposity while simultaneously improving glucose tolerance [16]. At the molecular level, this pathway upregulates PGC-1α expression and enhances mitochondrial oxidative capacity, thereby promoting mitochondrial biogenesis [16]. The anti-inflammatory mechanism involves KYNA signaling, which increases the expression of type 2 cytokines such as IL-4, IL-10, IL-13, and IL-33, while reducing pro-inflammatory markers such as TNFα [16,131]. This cytokine shift promotes a type 2 immune environment, supporting the resolution of inflammation and improving insulin sensitivity [17]. The KYNA–Gpr35 pathway also enhances the presence and activity of regulatory T cells (Tregs) and type 2 innate lymphoid cells (ILC2s), thereby contributing to anti-inflammatory signaling and adipose tissue being [16].

The KYNA–Gpr35 axis has emerged as a critical regulator of adipose tissue metabolism and inflammation, with considerable therapeutic relevance [16,17,34]. KYNA exerts a dual modulatory effect on metabolic efficiency and immune homeostasis by promoting adipose tissue beiging and enhancing mitochondrial oxidative capacity to support thermogenesis [16] In parallel, KYNA modulates the inflammatory milieu, directing the immune balance toward an anti-inflammatory phenotype [17,130,132]. These coordinated actions integrate metabolic and immunoregulatory mechanisms, suggesting that pharmacological activation of Gpr35 may constitute a promising therapeutic approach to augment systemic energy expenditure and mitigate metabolic disorders associated with chronic low-grade inflammation and disrupted energy balance, including obesity, type 2 diabetes, and metabolic syndrome [16].

2.2. KYNA and Aryl Hydrocarbon Receptor (AhR): Mitophagy and Organelle Quality Control (QC)

The AhR functions as a ligand-activated transcription factor that remains localized in the cytoplasm under basal conditions [133–135]. Upon ligand binding, AhR undergoes conformational changes that promote its nuclear translocation and the transcriptional regulation of a broad array of genes involved in cellular homeostasis [136–139]. AhR is well recognized for its central role in detecting xenobiotics and regulating their metabolism through cytochrome P450 enzymes (e.g., CYP1A1, CYP1A2, and CYP1B1) [140,141]. Moreover, increasing evidence indicates that AhR participates in a wide range of physiological processes, including immune regulation and

 doi:10.20944/preprints202601.0822.v1

embryogenesis [142–144]. However, its contribution to mitochondrial regulation in association with the Trp-KYN pathway has only recently come to light.

The first study identifying KYNA as an endogenous agonist of AhR was reported in the early 2010s [145,146]. Like KYNA, xanthurenic acid (XA)—another metabolite of the Trp–KYN pathway—has been shown to function as a ligand that can activate the AhR at physiologically relevant concentrations [145,147]. Recent evidence has demonstrated that AhR directly contributes to hepatic energy preservation by modulating mitophagy [139]. Mitophagy is a selective form of autophagy occurring within lysosomes and is responsible for the removal of damaged mitochondria [148–152]. This process reduces mitochondrial ROS overproduction, limits inflammasome activation, decreases apoptosis, maintains proper ATP synthesis, and promotes mitochondrial turnover [153–155]. In both AhR knockout mice and hepatocyte models, the loss of AhR expression resulted in impaired mitochondrial respiration, decreased substrate utilization, and dysregulation of mitochondria-associated gene networks [139,155]. Under pathophysiological conditions, a study conducted in intestinal porcine enterocytes (IPEC-J2 cells) further illustrated that activation of the Trp–KYN pathway via Trp-induced AhR signaling ameliorates lipopolysaccharide (LPS)-induced inflammatory responses [156,157]. This work also provided mechanistic insight into the interplay between AhR activation and mitochondrial QC by demonstrating that AhR functions as a direct transcriptional activator of PINK1 [139,156,158].

Mitophagy, in addition to being initiated through the ubiquitin-dependent PINK1–Parkin pathway, can also occur via receptor-mediated mechanisms involving BCL2-interacting protein 3 (BNIP3) and NIX [159–163]. In this pathway, LC3 binds to these receptors through its LC3-interacting region (LIR), ensuring the targeted recruitment of autophagosomes to mitochondria and enabling selective mitochondrial degradation [164]. Fasting strongly induced Bnip3 expression in livers obtained from wild-type samples, whereas this response was completely absent in AhR-deficient mice [139]. Activation of AhR by its endogenous ligand KYN significantly increased Bnip3 mRNA and protein levels in primary hepatocytes and AML12 cells [139]. Moreover, inhibition of AhR elevated mitochondrial ROS production—an effect entirely reversed by BNIP3 overexpression—and decreased LC3A expression [139]. Together, these results indicate that AhR plays a crucial role in regulating receptor-mediated mitophagy in the liver.

Excessive mitochondrial ROS promote mitochondrial dysfunction [165–167], a mechanism previously linked to AhR activation and AhR-dependent ROS generation induced by dioxins [168]. One potential source of these ROS is the accumulation of damaged or dysfunctional mitochondria, highlighting the importance of their removal for proper cellular function, including ATP production [169,170]. Physiological AhR activity appears to play a significant role in controlling mitochondrial stress responses, as its inhibition or loss has been associated with ROS imbalance and disturbance in oxidative metabolism [168,171]. In the liver, results suggests that AhR contributes to hepatic metabolic adaptation by maintaining mitochondrial efficiency and redox balance under nutrient, environmental, or hypoxic stress. Activation of AhR supports oxidative metabolism and preserves energy homeostasis, whereas its inhibition disrupts metabolic balance and promotes ROS accumulation, which can reduce cell viability [139].

The AhR plays a cellular-context–dependent role in mitochondrial biology, mediating both protective and deleterious outcomes. Under physiological conditions, AhR supports mitochondrial homeostasis: in hepatocytes, AhR loss impairs mitophagy, increases mitochondrial ROS, and reduces electron transport system function [139]. Similarly, in human melanocytes following H_2O_2-induced oxidative injury, AhR activation promotes mitochondrial biogenesis, mtDNA synthesis, and ATP production via NRF1 upregulation [172]. Conversely, toxic or xenobiotic ligands, such as PM2.5 or elevated kynurenine, trigger AhR-mediated mtROS production, mPTP opening, and $\Delta\Psi m$ collapse, leading to apoptosis in mouse neuronal cells and zebrafish heart [173,174]. These findings raise key questions: how do cell type, tissue context, and metabolic state dictate whether AhR signaling is protective or deleterious? How do ligand characteristics, dose, and exposure time affect

 doi:10.20944/preprints202601.0822.v1

mitochondrial outcomes? Resolving these issues is critical for understanding AhR's divergent role in mitochondrial physiology.

2.3. Kynurenic Acid (KYNA) and N-methyl-D-aspartate (NMDA) Receptors: Calcium Regulation and Excitotoxicity

NMDA-R are glutamate receptors and ligand-gated channels, widely recognized for their roles in synaptic signaling, calcium (Ca^{2+}) regulation, and excitotoxicity. Although they are predominantly expressed in the central nervous system, receptor subunits have also been detected in peripheral organs, including the heart, stomach, and intestine. Emerging evidence indicates that NMDA receptor localization is not restricted to the plasma membrane, as these receptors have also been identified in the inner mitochondrial membrane, suggesting a potential role in regulating mitochondrial function.

KYNA acts as an NMDA receptor antagonist by exerting its inhibitory effect at the glycine co-agonist site of the receptor [41,175,176], resulting in pleiotropic protective effects that include the modulation of mitochondrial function through this mechanism [13,177,178]. Under resting membrane potential, the NMDA receptor is blocked by magnesium ions (Mg^{2+}); however, upon depolarization, the binding of glutamate and glycine displaces the Mg^{2+} block, thereby allowing Ca^{2+} entry into the cell [179–181]. Overactivation of NMDA receptors leads to excessive calcium influx into the cytosol, which can trigger the opening of the mPTP, whose opening is tightly regulated by both calcium and ROS [182–184]. The mPTPs are high-conductance channel located in the inner mitochondrial membrane that allows the passage of molecules up to 1.5 kDa, leading to dissipation of the mitochondrial membrane potential, mitochondrial swelling, and the release of cytochrome c into the cytosol, thereby initiating the intrinsic apoptotic pathway [185–188]. In parallel, mPTP opening allows the release of mitochondrial DNA (mtDNA), which functions as a damage-associated molecular pattern (DAMP), capable of triggering innate immune responses and exacerbating cell death [189–191]. Based on these findings, preventing or delaying the opening of these channels could also represent an important therapeutic target.

By limiting NMDA receptor–mediated calcium influx, KYNA may indirectly reduce the probability of mPTP opening, thereby preventing the release of both cytochrome c and mtDNA into the cytosol [13,192]. This dual action not only attenuates pro-apoptotic signaling but also mitigates inflammatory processes associated with mitochondrial damage, emphasizing the potential cyto- and mitoprotective roles of KYNA. Recent studies further support the anti-apoptotic effects linked to its mitoprotective actions, although these mechanisms are not solely mediated by NMDA receptors. In H9c2 cells and primary rat cardiomyocytes exposed to simulated ischemia/reperfusion [31,107], KYNA exerted a dose-dependent effect on cell viability, with the most effective concentration being 64 μM [107]. Specifically, KYNA attenuated intramitochondrial Ca^{2+} accumulation, reduced ROS generation, and alleviated alterations in mitochondrial network architecture following simulated ischemia/reperfusion. Moreover, apoptosis markers such as caspase-3/7 and BAX (a pro-apoptotic modulator) were reduced, while the expression of the anti-apoptotic protein Bcl-XL was increased following KYNA treatment [107]. Therefore, a reduction of neuronal apoptosis in microglial cultures via attenuation of CXCL10 expression by KYNA and its analogue (SZR-104) cannot be ruled out [193].

NMDA receptors are not limited to the plasma membrane but have also been detected in mitochondria [194]. It was reported that the presence of NR1 and NR2B subunits, together with GABAA (alpha-6) and GABAB (R2) receptors, in rat heart mitochondria. Besides, extensive NR2a subunit immunoreactivity was observed on hippocampal mitochondria using immunogold electron microscopy [195]. Although the precise role of these receptors within mitochondria remains unclear, they are hypothesized to regulate calcium fluxes, modulate ROS production, and contribute to metabolic adaptation under hypoxic or ischemic conditions [195,196]. An additional layer of regulation may involve direct interactions between NMDA receptor subunits and mitochondrial complex I components, such as ND2, mediated via Src adaptor proteins [197–199]. This receptor–complex I crosstalk establishes a direct molecular link between receptor activity and mitochondrial

 doi:10.20944/preprints202601.0822.v1

energy metabolism, providing a mechanistic framework for how glutamatergic signaling influences mitochondrial bioenergetics. Collectively, these findings suggest that mitochondrial NMDA receptors may serve as critical modulators of organelle function, integrating cellular signaling with energy generation and oxidative stress responses, with potential implications for pathophysiological conditions such as ischemia, hypoxia, and neurodegeneration.

Taken together, these findings suggest that KYNA exerts multifaceted, receptor-mediated effects on mitochondria. Through interactions with GPR35, AhR, and NMDA receptors, KYNA helps preserve energy homeostasis, supports mitochondrial quality control, and protects against calcium-induced mitochondrial dysfunction—highlighting its therapeutic potential in conditions associated with mitochondrial stress or impairment [30,200–203]. Mitochondrial dysfunction has been implicated in various pathologies, including neurodegenerative diseases such as Alzheimer's, Huntington's, and Parkinson's diseases, as well as psychiatric disorders linked to mood disturbances, such as bipolar depression and migraine [13,41,204–208]. Therefore, maintaining mitochondrial homeostasis appears to be a promising therapeutic strategy for these conditions [158].

Future studies should investigate the role of mitochondrial NMDA receptors and their modulation by KYNA and its analogues, as it remains unclear whether these channels are sensitive to conventional NMDA receptor inhibitors. Likewise, the potential for targeting mitochondrial GPR35 and AhR receptors under stress conditions warrants further exploration, particularly regarding how their trafficking influences mitochondrial membrane dynamics and transport processes. Elucidating these mechanisms may provide crucial insights into how KYNA and its signaling pathways regulate mitochondrial function and could reveal novel therapeutic targets for diseases characterized by impaired bioenergetics or oxidative stress.

2.3. Nicotinic Acetylcholine Receptors (α7nAChR-like)

α7nAChRs, a type of ligand-gated ion channel previously thought to be localized only to the plasma membrane, are also present in the outer mitochondrial membrane [209]. Electron microscopy and binding assays (α-bungarotoxin, α-cobratoxin) have confirmed their presence in this organelle; however, their precise role remains to be characterized.

These α7nAChRs are thought to interact with voltage-dependent anion channels (VDAC1). Kalashnyk et al. confirmed this interaction, identifying α7 nAChR–Bax and α7 nAChR–VDAC1 complexes in mitochondria isolated from human glioblastoma astrocytoma cells [210]. Pharmacological studies demonstrated that inhibition of α7nAChRs using antagonists such as methyllycaconitine or α7-specific antibodies suppressed mitochondrial cytochrome c release, whereas stimulation with the receptor agonist PNU 282987 enhanced it in isolated mouse liver mitochondria [211]. Furthermore, mitochondrial ROS production was reduced following both receptor inhibition (methyllycaconitine) and stimulation with acetylcholine [211]. The α7nAChRs exhibit relatively high permeability to calcium ions (Ca^{2+}), which can influence mitochondrial function by stimulating calcium influx and efflux through the mitochondrial calcium uniporter and mPTPs [212]. In addition, modulation of various kinase pathways—including PI3K/Akt, calcium–calmodulin, and Src kinase–dependent signaling—appears to influence mPTP activity via these receptors, thereby supporting the OXPHOS machinery and maintaining cellular energy production [211].

Surprisingly, KYNA has also been reported to inhibit α7nAChRs; however, these findings remain controversial [37], as several research groups have failed to reproduce the original results. One possible explanation for these discrepancies may arise from the distinct pharmacological profiles of the kynurenate analogues most frequently used, such as 7-chloro-kynurenic acid (7-CKA) and 5,7-dichloro-kynurenic acid, which act at different sites on the NMDA receptor. A similar mechanism might account for the observed inconsistencies in the context of α7nAChRs as well.

It remains an important question, given conflicting experimental data [213], whether modulation of the α7nAChR—by inhibition or activation—can provide sustained neuroprotection and anti-inflammatory effects, and how these mechanisms interact with each other. At the same time, the

 doi:10.20944/preprints202601.0822.v1

potential role of mitochondrial α7nAChRs in mediating the cellular and mitoprotective effects of KYNA or its synthetic analogues has yet to be comprehensively characterized and requires further investigation to bridge the gap between cellular and subcellular mechanisms.

2.5. Other Potential KYNA-Sensitive Sites

Beyond the canonical receptor set, KYNA likely engages a wider mitochondrial "sensing" network. Additional receptors and redox-tunable targets—especially those shaping ion homeostasis and respiratory control—could help explain KYNA-linked phenotypes in ischemia and inflammation, and may open testable directions for neurodegenerative and psychiatric disease mechanisms.

Mitochondrial ATP-sensitive potassium (mitoKATP) channels are crucial mediators of cardioprotection induced by ischemic preconditioning and neuroprotection following cerebral ischemia-reperfusion. Pharmacological blockade of these channels with 5-hydroxydecanoate abolishes cardioprotective effects, whereas activation with the mitoKATP opener diazoxide confers neuroprotection [214,215]. Mechanistically, mitoKATP channel opening attenuates mitochondrial Ca^{2+} overload and delays or inhibits the opening of mPTP. Given that reactive oxygen species (ROS) and elevated Ca^{2+} are major triggers of mPTP opening, and that GPR35 modulates Ca^{2+} flux while ROS can induce mitoKATP opening and upregulate GPR35 [216], a potential crosstalk between these two mitochondrial receptors—both of which influence mPTP function—may underlie coordinated cytoprotective signaling in these disease conditions.

Mitochondrial ROS originate from 16 distinct redox sites within the organelle, with Complexes I and III of the electron transport system representing the principal ROS generators [217,218]. Redox-sensitive cysteine residues in Complex I subunits, such as NDUFS1, NDUFS2, and ND3, fine-tune ROS generation (superoxide and H_2O_2) by acting as redox switches. In contrast to excessive ROS production, transient Complex I–derived ROS induction enhances stress tolerance and lifespan in C. elegans [219]. KYNA, which scavenges hydroxyl radicals and superoxide [220], may reduce mitochondrial ROS at Complexes I and III by preserving electron transport integrity.

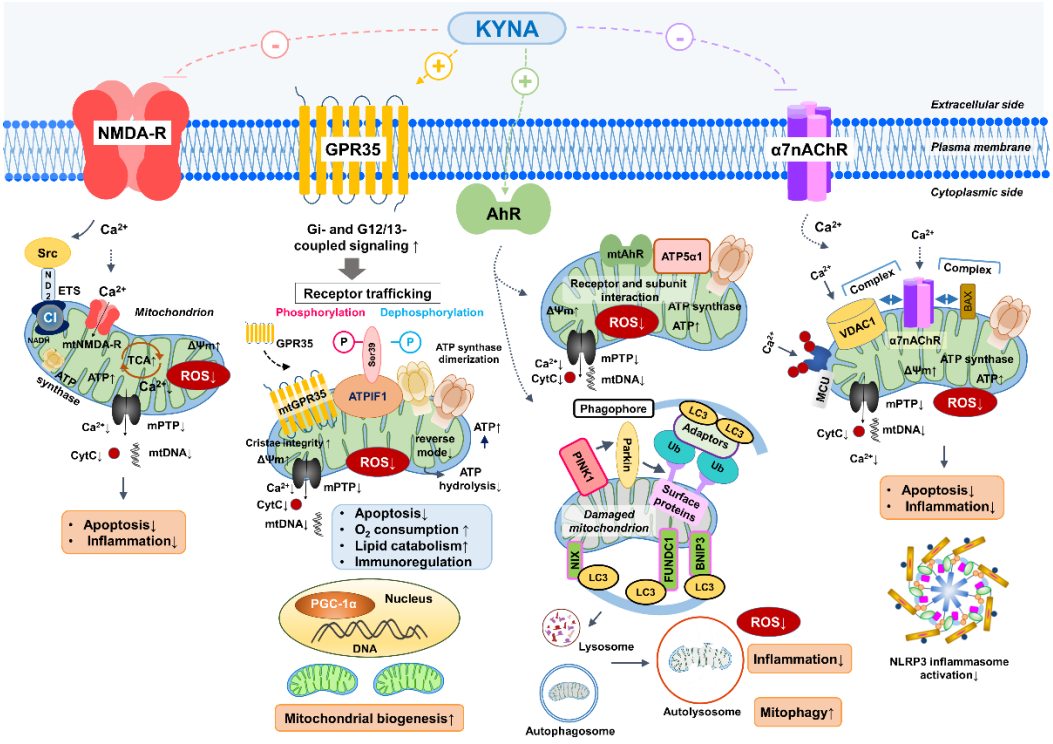

Figure 2. Receptor-mediated mitochondrial regulation by kynurenic acid (KYNA) integrates ATP preservation, redox balance, Ca^{2+} control, and mitophagy through coordinated actions at GPR35, the aryl hydrocarbon

 doi:10.20944/preprints202601.0822.v1

receptor (AhR), NMDA receptors, and mitochondrial α7nAChR. These pathways converge to stabilize bioenergetics, limit apoptosis, and restrain inflammation during metabolic or ischemic stress. (A) GPR35: KYNA engagement can promote GPR35 relocalization toward mitochondria, where it interfaces with ATPIF1 to favor ATP synthase dimer stability, reducing ATP synthase reverse activity, preserving ΔΨm, lowering mtROS, and dampening NLRP3-linked inflammatory tone; downstream PGC-1α signaling supports mitochondrial biogenesis and metabolic efficiency. (B) AhR: KYNA–AhR signaling shifts redox/apoptotic setpoints and promotes BNIP3-dependent mitophagy, enabling selective removal of damaged mitochondria and sustaining quality control. (C) NMDA receptors: KYNA antagonism reduces excitotoxic Ca^{2+} influx, limiting mitochondrial Ca^{2+} overload, stabilizing mPTP closure, and suppressing ROS escalation. (D) Mitochondrial α7nAChR: KYNA modulation can tune VDAC-associated Ca^{2+} entry, shape ΔΨm, and reduce Complex I/III ROS output. (E) Additional sites: mitoKATP channels and redox-sensitive ETC nodes may further refine ROS thresholds and tissue resilience. Abbreviations: AhR, aryl hydrocarbon receptor; ATP, adenosine triphosphate; ATP5α1, ATP synthase F1 subunit α1; ATPIF1, ATP synthase inhibitory factor 1; BAX, Bcl-2–associated X protein; BNIP3, Bcl-2/adenovirus E1B 19 kDa-interacting protein 3; Ca^{2+}, calcium ion; CI, Complex I; CytC, cytochrome c; ΔΨm, mitochondrial membrane potential; DNA, deoxyribonucleic acid; FUNDC1, FUN14 domain-containing protein 1; GPR35, G protein-coupled receptor 35; LC3, microtubule-associated protein 1A/1B-light chain 3; MCU, mitochondrial calcium uniporter; mpTP, mitochondrial permeability transition pore; mtAhR, mitochondrial aryl hydrocarbon receptor; mtDNA, mitochondrial DNA; mtGPR35, mitochondrial G protein-coupled receptor 35; ND2, NADH dehydrogenase subunit 2; NIX, Nip3-like protein X; NLRP3, NOD-, LRR- and pyrin domain-containing protein 3; NMDA-R, N-methyl-D-aspartate receptor; PGC-1α, peroxisome proliferator-activated receptor-γ coactivator-1α; PINK1, PTEN-induced putative kinase 1; ROS, reactive oxygen species; Ser39, serine 39; Src, proto-oncogene tyrosine-protein kinase Src; TCA, tricarboxylic acid cycle; Ub, ubiquitin; VDAC1, voltage-dependent anion channel 1; α7nAChR, α7 nicotinic acetylcholine receptor.

Table 1. Receptor Targets of Kynurenic Acid (KYNA) and Primary Mitochondrial Outcomes: Endpoints, Models, and Representative Evidence. **Columns:** Target; Mitochondrial effect (ATP, Ca^{2+}/mPTP, ROS, mitophagy); Model/cell type; Key finding; Reference anchors.

Target	Mitochondrial effects	Animal model/Cell type	Key findings	References
GPR35	-ATP preservation -ATP turnover ↑ -Mitochondrial oxidative capacity ↑ -ROS production ↓ -mPTP opening inhibition -Calpain-1/2 activity ↓	Myocardial ischemia/reperfusion (rat, NMVMs) Myocardial ischemia/reperfusion (mouse, heart tissue) C57BL/6J mice, adipose tissue	-KYNA–GPR35 activation stabilizes ATP synthase, maintains ΔΨm, prevents ATP hydrolysis, limits ROS and apoptosis -GPR35 blockade reduces calpain-mediated proteolysis, preserves mitochondrial integrity, and mitigates oxidative stress -KYNA–GPR35 axis enhances PGC-1α expression, promotes mitochondrial biogenesis, increases O_2 consumption, and initiate anti inflammatory cytokine production	[16,22,92,108,121,216]
mt GPR35	-ATP synthase dimerization -ATP preservation via the inhibition of ATP hydrolysis	GPR35 knoclout mice and neonaatal cardiomyocytes	-Binds to ATPIF1 and associates with the mitochondrial outer membrane -Inhibits mitochondrial adenylate cyclase and thereby PKA -Allows ATPIF1 to promote ATP synthase dimerization and prevent ATP hydrolysis	[22,121]
AhR	-Mitophagy (BNIP/PINK1–Parkin) ↑ -ROS production ↓ -ATP preservation -Oxidative metabolism ↑	Hepatocytes, AML12 cells, IPEC-J2 cells, AhR knockout mice, primary hepaocytes	-KYNA and KYN activate AhR to induce PINK1 and BNIP3 expression, promoting mitophagy and preserving mitochondrial respiration under stress -Loss of AhR impairs mitochondrial quality control and increases ROS accumulation, disrupting energy metabolism	[139,156,168,221,222]

 doi:10.20944/preprints202601.0822.v1

mtAhR	-ATP synthase regulation -Fine-tuning ROS production	Mitochondrial fraction, liver cells	-Mitochondrial AhR interacts with ATP5α1; its localization and activity depend on ligand status, possibly influencing ATP synthesis and redox balance	[221]
NMDA-R	-Ca^{2+} influx ↓ -mPTP opening ↓ -Cytochrome c release ↓ -Bcl-XL expression ↑ -Apoptosis ↓ -Complex I coupling	Neurons, Microglia, neuronal cultures	-KYNA blocks NMDA-R at the glycine site, limits Ca^{2+} overload, prevents mPTP opening, and protects against apoptosis -Potential crosstalk with complex I regulates bioenergetics	[193,197]
mt NMDA-R	-Ca^{2+} flux modulation -Fine-tuning ROS production	Rat heart mitochondria	-NR1/NR2B subunits detected in mitochondria; -Regulation of ROS production and Ca^{2+} level under hypoxia/ischemia	[194]
α7nAChR	-Regulates Ca^{2+} flux, ROS production, and cytochrome c release via interaction with VDAC1 -Influences mPTP opening and OXPHOS activity through kinase signaling (PI3K/Akt, CaM, Src). -Limits apoptosis through the regulation of Bcl-2/Bcl-xL and caspases.	Isolated mouse liver mitochondria; U373 human glioblastoma astrocytoma cells KAT II knockout (KAT II$^{-/-}$) mice	-α7nAChR–VDAC1 and α7nAChR–Bax complexes identified; receptor inhibition (methyllycaconitine) suppresses cytochrome c release; stimulation (PNU 282987) enhances it; acetylcholine reduces ROS. -Decreased KYNA levels increase α7nAChR activity; α7nAChR activation linked to neuroprotection and anti-apoptotic signaling; KYNA may physiologically regulate the receptor	[37,211,213,223,224]
mitoKATP channels (?)	-Channel opening reduces mitochondrial Ca^{2+} overload, delays mPTP opening, and supports cellular survival during ischemic or oxidative stress; -Its function is modulated by GPR35 and ROS signaling	In vivo ischemia–reperfusion models: cardiac and neuronal mitochondria	-Diazoxide (mitoKATP opener) confers neuro- and cardioprotection; inhibition (5-hydroxydecanoate) abolishes protective effects; -ROS and GPR35 signaling may crosstalk to regulate mitoKATP and mPTP.	[214–216]
Complex I / Complex III redox sites (?)	-Redox-sensitive cysteine residues regulate ROS generation (superoxide, H_2O_2); transient ROS acts as signaling for stress adaptation; -KYNAmay scavenge radicals and preserves electron transport.	Isolated mitochondria; C. elegans	-KYNA may reduce ROS at Complex I and III independent of receptor mechanisms; mild Complex I ROS prolongs lifespan in C. elegans; antioxidant effects support mitochondrial stability.	[217–220]

Abbreviations: GPR35, G protein–coupled receptor 35; KYNA, kynurenic acid; ATPIF1, ATP synthase inhibitory factor 1; PKA, protein kinase A; ΔΨm, mitochondrial membrane potential; ROS, reactive oxygen species; mPTP, mitochondrial permeability transition pore; PGC-1α, per-oxisome proliferator–activated receptor gamma coactivator 1-alpha; AhR, aryl hydrocarbon re-ceptor; mtAhR, mitochondrial aryl hydrocarbon receptor; BNIP3, Bcl-2/adenovirus E1B 19 kDa–interacting protein 3; PINK1, PTEN-induced kinase 1; NMDA-R, N-methyl-D-aspartate receptor; mtNMDA-R, mitochondrial N-methyl-D-aspartate receptor; Bcl-XL, B-cell lymphoma extra-large (anti-apoptotic protein); VDAC1, Voltage-dependent anion channel 1; α7nAChR, α7 nicotinic acetylcholine receptor; mitoKATP (mKATP), mitochondrial ATP-sensitive potassium channel; OXPHOS, oxidative phosphorylation; CI / CIII, Complex I / Complex III (electron transport cha-in).

 doi:10.20944/preprints202601.0822.v1

3. Crosstalk Between the Kynurenine (KYN) Metabolism and the TCA Cycle

This section pursues four aims: map receptor-specific mitochondrial actions of KYNA, delineate pathway–cycle crosstalk, appraise integrated analytics, and synthesize translational implications. We integrate biochemical and signaling links that couple Trp catabolism to core carbon metabolism, emphasizing QA–driven de novo NAD+ supply, sirtuin control of respiratory efficiency, and adjustments in NAD^+/NADH that set redox poise [2,7,12,30]. Receptor engagement, exemplified by GPR35, is positioned to tune electron transport and immune tone through mitochondrial signaling nodes that intersect the TCA cycle and the malate–aspartate shuttle [1,3,16]. We further evaluate IDOs and tryptophan 2,3-dioxygenase (TDO) as rate-setting checkpoints shaping α-ketoglutarate availability, ROS signaling, and tolerance versus activation states, using multi-omic and isotope-tracing frameworks to prioritize druggable targets across inflammatory and tumor contexts [4,9,11,13,21].

3.1. Shared Metabolic Intermediates and Redox Balance

Shared intermediates choreograph redox balance across compartments. TCA cycle flux supplies reducing power and precursors, while anaplerosis preserves pool sizes that sustain NADPH and glutathione buffering [3,8]. When flux falters, ATF4 programs rewire amino acid and antioxidant metabolism [1]. Malic enzyme-1 senses malate to pyruvate and tunes NADPH output [11]. Meanwhile, ROS encode signals that reshape metabolic set points and defenses [18–20].

Mitochondrial respiration reads the NAD^+/NADH ratio as a control signal that tunes flux through the TCA cycle, the electron transport chain, and fate decisions in diverse lineages [1,5]. Pool size and localization matter. mitochondrial carrier transporting NAD+ (MCART1) imports NAD+ to sustain matrix reactions, while deficits collapse dehydrogenase activity and oxygen consumption [4,6]. Oxaloacetate generated by malate dehydrogenase 2 (MDH2) selectively restrains complex II and reroutes electron flow, thereby reshaping the redox couple in real time [10]. Nicotinamide nucleotide transhydrogenase coordinates nicotinamide adenine dinucleotide (NADH) with nicotinamide adenine dinucleotide phosphate (NADPH) demand, stabilizing redox poise during shifts in glutamine and glucose use [15]. When respiration stalls, serine-driven NADH accumulates and throttles biosynthesis [11].

Immune and disease contexts expose the same logic. LKB1 dependent mitochondrial programs and thioredoxin circuits sculpt NADH turnover, with consequences for chromatin state and T cell effector function [2,13]. Cells with succinate dehydrogenase (SDH) lesions adopt alternative aspartate synthesis routes that hinge on matrix NAD^+/NADH, salvaging growth despite impaired cycling [7]. De novo NAD^+ from the KYN metabolism supports macrophage respiration and systemic redox communication, linking Trp catabolism to respiratory control across tissues [3,12,18]. ROS then operate as graded messengers downstream of the ratio, reinforcing or reprogramming signaling pathways [19,20]. Therapeutically, targeted manipulation of NAD^+/NADH can complement defective electron transport and may slow age related decline [8,16].

QA sits at the fulcrum of de novo NAD+ synthesis, converting Trp catabolism into respiratory capacity. In macrophages, intact quinolinate to NAD+ flux sustains complex I driven oxidation and immune effector programs; aging and inflammation magnify the dependence, and pathway blockade collapses oxygen consumption [1]. In tissues under ischemia reperfusion, diversion away from quinolinate depletes NAD+, weakens antioxidant defenses, and heightens oxidative injury, all reversible with NAD+ augmentation [3]. Genetic and clinical data converge on QPRT as a bottleneck whose repression or loss yields quinolinate accumulation, reduced NAD+, and vulnerability to damage [9,13]. Astrocytes and neurons similarly require quinolinate conversion to maintain SIRT activity, viability, and mitochondrial function during neuroinflammation [8].

Evolution supplies redundancy and reach. Yeast can secrete and reimport quinolinate to stabilize NAD^+ pools, and, when canonical steps fail, UMPS can substitute to complete synthesis [4,11]. Engineered circuits that route quinolinate toward NAD^+ raise cellular NAD(H) and bolster

 doi:10.20944/preprints202601.0822.v1

electron transport, illustrating design principles for metabolic support [5]. Across physiology and disease, rising mitochondrial work rates associate with higher circulating quinolinate and nicotinamide, consistent with coupled biogenesis and ETC demand [10]. Yet excess or chronic pathway activation is harmful, impairing bioenergetics in neurons and reshaping tumor growth constraints, where ubiquinol oxidation remains a nonnegotiable requirement beyond NAD^+ regeneration alone [12,17]. Together, these findings position QA as both a sensor and supplier that links Trp flux to NAD^+ homeostasis, redox poise, and sustained respiratory throughput [2,6,7,14–16,18,19].

α-Ketoglutarate sits at the crossroads of carbon flow and immune control, shaping how cells route Trp into the KYN metabolic pathway. Through IDH2 dependent reductive carboxylation, α-ketoglutarate fuels isocitrate and citrate production, generates NADPH, and thereby tunes redox poise that can favor or restrain IDOs and TDO activity through cofactor availability and metabolic context [1,2]. Inflammatory signaling rewires this hub. Type I interferon inhibits isocitrate dehydrogenase, distorting the citrate to α-ketoglutarate ratio, shifting mitochondrial electron supply, and altering the local redox environment that licenses Trp catabolic flux [3].

Macrophage polarization provides a vivid example. Network integration reveals a metabolic break at IDH in M1 cells, fragmenting the TCA cycle and lowering α-ketoglutarate regeneration; the result is constrained anaplerosis, altered NADPH production, and a redox profile conducive to heightened immune effector programs that intersect with IDOs induction [5]. In tumors, nutrient competition and hypoxia reshape the same nodes. The microenvironment modulates α-ketoglutarate levels and the balance between oxidative and reductive TCA routing, which in turn conditions IDO1 and TDO2 expression and the effectiveness of their pharmacologic blockade [4]. Across aging and chronic inflammation, these α-ketoglutarate centered adjustments integrate energy metabolism with Trp fate, coupling respiratory control to immunoregulatory enzyme flux [2].

Table 2. Integration Points Linking the Kynurenine (KYN) Metabolism to the TCA Cycle and Immune Signaling. Concise map of biochemical "nodes" where KYN-pathway flux or signaling intersects mitochondrial control, NAD^+/NADH balance, anaplerosis, and immune/ROS outcomes. Evidence class reflects the weight and modality indicated in MT 3 (mechanistic experiments, multi-omics/isotope tracing, clinical/genetic, or engineering proof-of-principle).

Node (e.g., QA → NAD^+)	Enzymes/regulators	Directionality	Impact on NAD^+/NADH or anaplerosis	Immune/ROS consequence	Evidence class	References
QA → NAD^+	QPRT → NMNAT → NADS; modulation by aging/inflammation	KYN → NAD^+ biogenesis → ETC	Increases cellular/matrix NAD(H); sustains complex I oxidation and O_2 consumption	Supports macrophage respiration; QPRT loss ↓NAD^+, ↑injury/ROS; neuroinflammation requires conversion for SIRT activity	Mechanistic (cells/animals), clinical/genetic	[14,42,225]
KYNA → GPR35 → mitochondrial nodes (incl. MAS)	KATs (KYNA production), GPR35; MAS components	KYNs ligands → receptor → mitochondria/TCA	Tunes ETC throughput and shuttle-coupled redox set-points	Sets immune tone; receptor-proximal control of inflammatory signaling	Mechanistic receptor signaling	[16,22,114]
IDO1/TDO2 rate-setting → α-KG availability	IDO1, TDO2; IFN, hypoxia, nutrient status	Immune cues → KYNs flux → TCA carbon	Pulls carbon from Trp; constrains or supports α-KG–linked anaplerosis	Biases tolerance vs activation; conditions efficacy of IDOs/TDO blockade	Multi-omic/tumor-inflammation frameworks	[26,226,227]

 doi:10.20944/preprints202601.0822.v1

MCART1-mediated NAD⁺ import (cytosol → matrix)	MCART1 (SLC25 family)	Cytosol → mitochondria	Maintains matrix NAD⁺ for dehydrogenases; prevents collapse of OXPHOS	Preserves respiratory control; supports T-cell effector programs	Mechanistic (transport/respiration)	[228–230]
MDH2 → oxaloacetate restraint of Complex II	MDH2; OAA	TCA intermediate → ETC modulation	Re-routes electron flow; dynamically resets NAD⁺/NADH coupling	Shapes graded ROS signaling downstream of ratio	Mechanistic ETC control	[217,218,231]
NNT couples NADH ↔ NADPH demand	Nicotinamide nucleotide transhydrogenase (NNT)	Matrix redox coupling	Balances NADH oxidation with NADPH generation; stabilizes redox poise	Supports antioxidant defenses; buffers ROS during substrate shifts	Mechanistic redox coupling;	[232–234]
ME1 (malic enzyme-1): malate → pyruvate (NADPH)	ME1	Cytosol anaplerosis ↔ redox	Raises NADPH; protects glutathione/NADPH buffering	Reinforces antioxidant capacity; feeds redox-encoded signaling	Mechanistic redox metabolism	[235,236]
Serine catabolism → NADH accumulation when respiration stalls	One-carbon/serine axis	Amino acid metabolism → redox	Builds cytosolic/mitochondrial NADH when ETC is limited; throttles biosynthesis	Constrains proliferative programs under low respiration	Mechanistic metabolic control	[2,9,237]
SDH lesion → alternative aspartate synthesis (matrix NAD⁺/NADH-dependent)	SDH/Complex II context; aspartate pathways	ETC defect → rerouted biosynthesis	Forces aspartate generation routes that depend on matrix NAD⁺/NADH	Salvages growth despite impaired cycling	Mechanistic pathology	[238–240]
De novo NAD⁺ from KYNs supports macrophage respiration	QPRT→NMNAT →NADS; macrophage programs	KYNs → NAD⁺ → OXPHOS	Expands NAD(H) pool; sustains respiratory control across tissues	Coordinates systemic redox communication; tunes inflammatory effectors	Mechanistic + systems	[14,42,241]
Type I IFN → IDH inhibition → citrate/α-KG ratio shift	IDH1/IDH2; Type I IFN	Immune signal → TCA wiring → KYNs context	Alters NADPH generation/redox milieu that licenses IDOs/TDO activity	Reprograms Trp catabolism vs defense state	Mechanistic immunometabolism	[26,219,231]
M1 macrophage "IDH break" → α-KG drop	IDH node; network integration	Polarization cue → TCA fragmentation	↓Anaplerosis; altered NADPH; redox favoring effector programs and IDOs induction	Heightened inflammatory activation	Network/multi-omic	[231,242]
Sirtuin activity sustained by quinolinate-derived NAD⁺	SIRTs; QPRT/NMNAT/NADS	KYNs → NAD⁺ → sirtuin deacylases	Preserves mitochondrial protein deacylation and efficiency	Supports neuronal viability; mitigates inflammatory stress	Mechanistic neuroinflammation	[14,25,243]
Ischemia–reperfusion	Pathway branch choice; NAD⁺ augmentation	Stress → KYN branch → NAD⁺	NAD⁺ depletion when diverted; restoration rescues	Less oxidative injury with NAD⁺ repletion	Mechanistic/therapeutic modulation	[22,31,43]

 doi:10.20944/preprints202601.0822.v1

diversion away from quinolinate UMPS bypass completing NAD⁺ synthesis when canonical steps fail	UMPS (bypass), salvage enzymes	Engineered/alternative route → NAD⁺	antioxidant capacity Raises total NAD(H) when QPRT or steps are compromised	Enhances ETC throughput in designed systems	Engineering proof-of-principle	[244–246]
Quinolinate/NAM rise tracks mitochondrial work/biogenesis	Systemic KYNs NAD⁺ salvage	Workload/biogenesis → KYNs output	Correlated elevation of circulating quinolinate & nicotinamide with ETC demand	Links tissue respiratory programs to systemic KYNs tone	Integrative physiology;	[243,247,248]
Ubiquinol ($CoQH_2$) oxidation requirement beyond NAD⁺ regeneration	ETC Complex III/CoQ cycle	ETC constraint → metabolic outcome	NAD⁺ repletion alone insufficient if CoQ oxidation is limited	Governs tumor growth constraints; bioenergetic bottleneck	Mechanistic tumor bioenergetics	[85,217,218]
LKB1 programs & thioredoxin circuits sculpt NADH turnover	LKB1, TRX/thioredoxin	Kinase/antioxidant systems → NADH flux	Adjusts NADH oxidation and chromatin-linked NAD⁺ usage	Sets T-cell effector capacity	Mechanistic immune control	[249–251]

α-KG, alpha-ketoglutarate; $CoQH_2$, ubiquinol; ETC, electron transport chain; GPR35, G protein–coupled receptor 35; IDO, indoleamine 2,3-dioxygenase; IDO1, indoleamine 2,3-dioxygenase 1; IDH, isocitrate dehydrogenase; IFN, interferon; KAT, kynurenine aminotransferase; KYN, kynurenine; KYNA, kynurenic acid; LKB1, liver kinase B1; MAS, malate–aspartate shuttle; MCART1, mitochondrial carrier of NAD⁺ transporter 1; MDH2, malate dehydrogenase 2; ME1, malic enzyme 1; NAM, nicotinamide; NADS, NAD⁺ synthetase; NADH, nicotinamide adenine dinucleotide (reduced form); NADPH, nicotinamide adenine dinucleotide phosphate (reduced form); NMNAT, nicotinamide mononucleotide adenylyltransferase; NNT, nicotinamide nucleotide transhydrogenase; OAA, oxaloacetate; OXPHOS, oxidative phosphorylation; QA, quinolinic acid; QPRT, quinolinate phosphoribosyltransferase; ROS, reactive oxygen species; SDH, succinate dehydrogenase; SIRT, sirtuin; SLC25, solute carrier family 25; TCA, tricarboxylic acid cycle; TDO, tryptophan 2,3-dioxygenase; Trp, tryptophan; TRX, thioredoxin; UMPS, uridine monophosphate synthase.

3.2. Immunometabolic Integration

Immune activation tilts Trp fate toward the KYN axis, lowering substrate and generating metabolites that reprogram effector circuits [10,15,19]. KYN and allied ligands engage AhR, dampen T cell proliferation, and favor regulatory programs, shaping tolerance in infection, autoimmunity, and cancer [1,3,4,11,18]. Context matters. Inflammaging sustains this reflex, while serotonin–KYN balance and metabolic feedback refine outcomes [12,14,20]. KYN to Trp ratios index pathway load, and Rab4A dependent mTOR signaling links mitochondrial metabolism to KYN sensitivity [5,13].

Succinate links carbon flux to inflammatory licensing. In lipopolysaccharide challenged macrophages, accumulation of succinate stabilizes hypoxia-inducible factor 1 alpha (HIF-1α), boosts glycolysis, and elevates IL-1β transcription and release [2,10]. Mitochondrial control is pivotal. Inhibition or retuning of SDH rewires electron flow, sustains HIF-1α, and aggravates tissue injury, while SUCNR1 signaling extends succinate's reach to endothelium and epithelium, amplifying cytokines and vascular pathology [1,6,9,13,15]. Parallel cues converge. STING activation raises succinate and locks HIF-1α–dependent effector programs during infection; L-2-hydroxyglutarate similarly enforces the HIF-IL-1β axis [3,11,14].

Context shapes outcome. Proinflammatory cytokines further potentiate HIF-1α, embedding a feedforward loop, yet SDH also supports STAT3 driven IL-10, revealing countervailing anti-inflammatory circuitry within the same module [12,13,17]. Upstream metabolic governors, including SIRT6, adjust succinate levels and HIF linked glycolysis in pathogen challenged macrophages [18].

 doi:10.20944/preprints202601.0822.v1

In vascular and synovial beds, pharmacologic or nutraceutical inhibitors that blunt succinate accumulation or HIF-1α activation reduce IL-1β output, neovascularization, and plaque inflammation, illustrating therapeutic tractability across diseases characterized by immunometabolic stress [4,16,19,20,28,201,252]. Together these data position the succinate–HIF-1α axis as a tunable rheostat that integrates mitochondrial respiration with inflammatory effector commitment.

3-Hydroxykynurenine (3-HK) sits at a volatile intersection of metabolism and immunity, where its redox cycling can both ignite and quench oxidative chemistry. Autoxidation and dimerization generate ROS that deplete glutathione, derail the TCA cycle, and trigger apoptosis, yet context permits radical scavenging and neuroprotective outcomes [3–7]. In vascular, renal, and neuroinflammatory states, elevated 3-HK tracks with oxidative stress and endothelial dysfunction, positioning this metabolite as a sentinel of immunometabolic strain [1,5,6].

These redox swings feed signaling loops that tune inflammatory tone. ROS linked to 3-HK amplify IL-6 and IL-1–driven programs, prime monocytes through mTOR dependent circuits, and shape T cell activation thresholds and lineage decisions [2,8–12]. Feedback control is nuanced. Mitochondrial injury can proceed with or without early ROS surges, implying parallel mitochondria centered sensors and effector arms downstream of 3-HK [13]. Collectively, 3-HK orchestrates bidirectional crosstalk between metabolism and immunity, coupling Trp flux to ROS governed transcriptional and epigenetic checkpoints that determine tolerance versus tissue injury [1,4,7,10–12].

At the interface of Trp catabolism and the TCA cycle, a set of metabolic checkpoints governs whether immunity accelerates or brakes. Enzymes such as IDO1, TDO, and KMO gate substrate flow to KYN and downstream ligands that converge on AhR, adjusting effector programs, tolerance, and chronic inflammation [1–3]. This control integrates with organelle level routing of carbon and reducing equivalents, where cytosol–mitochondria handoffs shape glycolysis–TCA coupling and enforce redox thresholds for immune activation [8,9,11]. De novo NAD+ synthesis from KYN intermediates adds another lever, feeding respiratory capacity and feedback to transcriptional fate decisions in aging and cancer [6,12].

Checkpoint behavior is contextual. In T cells, Rab4A controlled endosomal traffic intersects with KYN sensitive mTOR signaling to couple mitophagy, nutrient transport, and lineage specification [4]. Tumors exploit depletion and signaling in parallel, creating an immunosuppressive niche that often resists single agent IDOs or TDO blockade, arguing for combinations that co target metabolic nodes and canonical immune checkpoints [2,5,13,15,18]. Microbial Trp products reinforce AhR dependent suppression in tumor associated macrophages, linking diet and microbiota to checkpoint tone [16]. Stress programs that arise when TCA flux is curtailed activate ATF4 and remodel amino acid and redox metabolism, thereby re indexing sensitivity to Trp pathway control [14]. Multi omic maps now resolve these modules in human macrophages and guide rational intervention across inflammatory disease and oncology [10,17,19].

3.3. Pathological Implications

From circuits to clinics, dysregulated Trp–KYN and TCA nodes shape disease trajectories across brain, vasculature, metabolism, and cancer. Imbalanced metabolites drive neurotoxicity, immune exhaustion, and cardiometabolic risk, while altered NAD^+ supply and ATF4 programs expose vulnerabilities [3–6,8–10,12–18]. Translational paths now pair pathway modulation with tumor bioenergetic targets and immune recalibration [6,12–14,16].

Excess QA and diminished KYNA form a pathogenic redox and excitotoxic dyad in neurodegeneration. QA engages NMDA receptors, drives mitochondrial ROS, and depresses respiratory capacity, creating a feedforward loop of bioenergetic failure and inflammation [2,5,16]. By contrast, KYNA buffers glutamatergic stress and restores antioxidant defenses, including Nrf2 signaling, yet is frequently reduced in Alzheimer's and Parkinson's disease [3,5,6,19]. Clinical and biomarker studies converge on elevated QA to KYNA ratios across aging and disease, linking this imbalance to tau and amyloid burden, neuronal dysfunction, and faster progression [1,7,11,17,49,53,253]. Therapeutically, redirecting flux away from QA and enhancing KYNA, for

 doi:10.20944/preprints202601.0822.v1

example with KMO inhibition or pathway modulation, offers a rational strategy to stabilize mitochondria and slow neurodegeneration [4,18,20].

Psychiatric disorders display a characteristic coupling of immune tone and bioenergetics, centered on a rerouting of Trp toward KYN metabolism [49,254,255]. Meta analyses and cohort studies reveal reduced Trp and KYN with imbalanced neurotoxic and neuroprotective metabolites, tracking mood, psychosis, and cognitive deficits [2–4,6]. Immune activation accelerates this shift, depresses serotonin, and favors QA, with state dependent oscillations across acute and remitted phases [10–12,18,19]. These molecular changes map onto mitochondrial and synaptic function, and show moderate blood–brain concordance for select metabolites that can index symptom burden and progression [13,16]. Mechanistically, KYN reprogramming may be compensatory or pathogenic, often both; therapeutic strategies now target enzymes and flux control while integrating microbiome sensitive modulators and trial readouts [1,5,7,14,15,256].

Tumors co-opt Trp catabolism to choreograph immune escape while fueling growth. IDO1 and TDO2 divert substrate toward KYN, which activates AhR, expands Tregs, and exhausts cytotoxic T cells; clinical experience shows that single-enzyme blockade often falters, underscoring redundant wiring and the need for multi-target strategies [1–4,6,12,15]. Beyond initiation, downstream nodes such as KMO and kynureninase (KYNU) shape metastatic behavior, stromal crosstalk, and chemoresistance, particularly in aggressive breast and renal cancers [5,7,8,14,16].

Therapeutic concepts increasingly pair immune checkpoint inhibitors with metabolic rewiring. KYNU depots deplete intratumoral KYN and synergize with programmed cell death protein 1 (PD-1) blockade, while small molecules like icariside I attenuate AhR signaling and restore effector function [9,10]. Remodeling the glutathione peroxidase 4 (GPX4)–KYNU axis or broader TME metabolism reprograms macrophage polarization and dismantles suppressive niches, offering tractable paths to overcome resistance [11,13,18–20].

Table 3. Clinical and Preclinical Patterns Connecting Kynurenine (KYN) Metabolism–TCA Crosstalk to Disease Phenotypes. Summary of disease-domain patterns linking KYN-pathway metabolites to mitochondrial phenotypes and clinical/functional readouts. Study type/size reflects the level of evidence stated in the text (meta-analyses/cohorts, biomarker studies, preclinical models, early clinical combination strategies) without inventing sample counts.

Indication (neurodegeneration/psychiatry/oncology)	Metabolite signature KYNA, QA, KYN, 3-hydroxykynurenine)	Mitochondrial phenotype	Clinical/functional readouts	Study type/size	References
Neurodegeneration	KYNA ↓, QA ↑; KYN context-dependent; 3-HK not primary in text	NMDA-driven ROS; depressed respiratory capacity; feed-forward bioenergetic failure and inflammation	Higher QA:KYNA ratios track tau/amyloid burden, neuronal dysfunction, faster progression	Clinical & biomarker studies; aging/disease cohorts; preclinical mechanistic work	[51,52,78]
Neurodegeneration (therapeutic angle)	Shift flux away from QA; raise KYNA (e.g., KMO modulation)	Mitochondrial stabilization; restored antioxidant defenses (incl. Nrf2 signaling)	Slower neurodegeneration trajectory; reduced excitotoxic stress	Preclinical + translational strategy proposals; early-phase targeting concepts	[3,8,205]
Psychiatry	Trp ↓, KYN ↓ (cohorts/meta-analyses); QA favored under immune activation; KYNA/KYN/QA show state-dependent oscillations; 3-HK not emphasized	Immune-bioenergetic coupling; mitochondrial/synaptic function shifts; serotonin depression when KYN metabolism is upshifted	Mood, psychosis, cognitive deficits; moderate blood–brain metabolite concordance indexing symptom burden/progression	Meta-analyses and multi-cohort studies; biomarker cohorts; mechanistic frameworks	[54,73,257]

 doi:10.20944/preprints202601.0822.v1

Psychiatry (therapeutic angle)	Enzyme/flux control targeting; microbiome-sensitive modulators	Rebalancing KYNs–TCA redox and neurotransmission coupling	Symptom modulation and progression tracking via peripheral KYNs panels	Translational strategies; trial-readout integration (sizes vary)	[49,50,61]
Oncology (tumor immune escape)	KYN ↑ via IDO1/TDO2 → AhR activation; downstream KMO/KYNU shape invasive traits; KYNA/QA context-specific	Bioenergetic rewiring supporting growth; TME-conditioned redox	Treg expansion, $CD8^+$ exhaustion; metastatic behavior, stromal crosstalk, chemoresistance	Clinical experience with IDOs/TDO blockade; preclinical tumor models; biomarker studies	[226,227,258]
Oncology (combination therapy)	KYN depletion (KYNU depots); AhR attenuation (e.g., small molecules)	Reprogrammed mitochondrial/immune metabolism; macrophage repolarization (e.g., GPX4–KYNU axis)	Synergy with PD-1 blockade; dismantling suppressive niches; overcoming resistance	Preclinical synergy studies; early translational combinations; emerging clinical strategies	[72,226,241]

3-HK, 3-hydroxykynurenine; AhR, aryl hydrocarbon receptor; $CD8^+$, cluster of differentiation 8 positive; GPX4, glutathione peroxidase 4; IDO1, indoleamine 2,3-dioxygenase 1; KMO, kynurenine 3-monooxygenase; KYN, kynurenine; KYNA, kynurenic acid; KYNU, kynureninase; Nrf2, nuclear factor erythroid 2–related factor 2; PD-1, programmed cell death protein 1; QA, quinolinic acid; ROS, reactive oxygen species; TCA, tricarboxylic acid cycle; TDO2, tryptophan 2,3-dioxygenase 2; TME, tumor microenvironment; Trp, tryptophan; Treg, regulatory T cell.,.

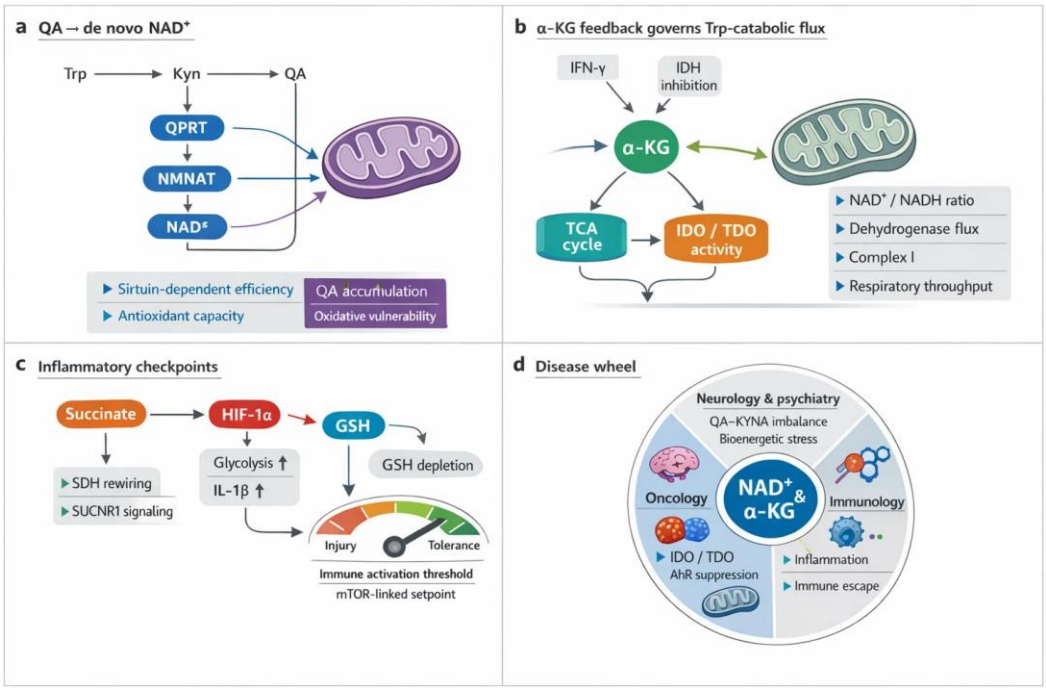

Figure 3. Bridging the Kynurenine (KYN) metabolism and the TCA cycle: NAD^+ biogenesis, α-ketoglutarate feedback, and inflammatory checkpoints. (A) Quinolinic acid (QA) → de novo NAD^+. Tryptophan (Trp) catabolism feeds QA into the QPRT–NMNAT–NADS axis to expand cellular and mitochondrial NAD(H) pools, thereby tuning matrix NAD^+/NADH ratios that control dehydrogenase flux, complex I–driven oxidation, and respiratory throughput. NAD^+ availability supports sirtuin-dependent mitochondrial efficiency and antioxidant capacity, whereas impaired QA→NAD^+ conversion promotes QA accumulation, NAD^+ depletion, and vulnerability to oxidative injury in inflammatory and ischemic settings. **(B)** α-Ketoglutarate (α-KG) as a flux governor. α-KG integrates carbon routing and redox context to condition IDO/TDO rate-setting and downstream KYN production, with immune cues (e.g., interferon-mediated IDH inhibition, macrophage polarization–linked

 doi:10.20944/preprints202601.0822.v1

"IDH break," and tumor microenvironment constraints) reshaping α-KG regeneration, NADPH buffering, and permissiveness for Trp-catabolic flux. **(C)** Checkpoint module: succinate/HIF-1α and 3-hydroxykynurenine (3-HK) ROS. Succinate accumulation stabilizes HIF-1α to amplify glycolysis and IL-1β programs, while SDH rewiring and SUCNR1 signaling extend inflammatory tone; in parallel, 3-HK redox cycling drives ROS–glutathione stress that modulates mTOR-linked activation thresholds and tissue injury versus tolerance. **(D)** Disease wheel. These coupled nodes map onto neurology and psychiatry (QA–KYNA imbalance, bioenergetic stress) and oncology (IDO/TDO–AhR immunosuppression and metabolic rewiring).

4. Analytical Strategies for Simultaneous Quantification

The combined measurement of the citric acid cycle (TCA) and KYN metabolic pathway in a single method has attracted significant interest in the fields of neurology, oncology, and mitochondrial biology [13,14,259]. While the two metabolic pathways are typically studied separately, combined studies are increasingly sought after [[63,260–262]. This allows for the investigation of interactions between pathways underlying disease phenotypes in a single method, without separate preparations, and by eliminating inter-assay variance. However, designing a single analytical method requires consideration of chromatographic incompatibilities, ionization, and polarity differences [263–265]. In addition, several orders of magnitude variations in biological samples for some metabolites must be taken into account, which weakens the usefulness of an already well-developed analytical method [266–268]. This section explains the fundamental challenges of the simultaneous measurement and presents practical engineering solutions. Finally, we would like to highlight the validation standards required in clinical research, similar to diagnostic applications, where the methods used must meet serious criteria, for which appropriate guidelines are available [269–271]

4.1. Rationale for Unified Measurement

The scientific and clinical promise of simultaneous quantification lies in minimizing fragmentation in experimental workflows [272–274]. Instead of separate assays for TCA intermediates and KYNs, a unified measurement allows for a simultaneous overview of cellular energetic processes and neuroactive metabolism [275–277]. Common measurement improves efficiency, reduces sample burden, and makes meaningful comparisons between groups more effective [278–280].

Metabolomic studies often struggle with limited availability. In cerebrospinal fluid (CSF), where lumbar punctures yield only a few hundred microliters, or in animal studies, where only a few microliters are available, distributing aliquots to multiple specialized assays reduces the measurement options, thereby compromising the results or the statistical power of the work [281–283]. Similarly, plasma samples collected in efficacy studies may be limited by ethical and logistical considerations, while tissue biopsies are often only available in milligram quantities [284–286]. When TCA intermediates and KYN derivatives are measured in separate analytical runs, each uses a portion of the already small amount of biological sample, which reduces measurement efficiency and may lead to the possibility of missing biologically important correlations [287–290]. Simultaneous measurements in single-run assays eliminate the need to split the sample volume into multiple aliquots, and metabolite relationships within it can be examined more reliably [267,288,291,292]. These measurements also allow the application of multivariate statistical models that integrate data collected from mitochondrial and KYN metabolites and increase the potential for cross-metabolic pathway analysis, allowing for more reliable quantification of ratios such as succinate/quinolinate ratios or citrate-KYNA correlations in psychiatric and neurological diseases. [13,14,231,242,293–298].

A major obstacle to reproducibility in biomarker research is interassay variability. Separate LC-MS methods, independently optimized for TCA intermediates and KYNs, differ in chromatographic stationary phases, gradient conditions, derivatization techniques, and ionization polarity [262,299–301]. Harmonized measurement reduces technical heterogeneity by incorporating both metabolic pathways into a single analytical measurement, ensuring that co-eluting matrix components and ion

 doi:10.20944/preprints202601.0822.v1

suppression phenomena are consistent across analytes [267,301–303]. This is particularly important for meta-analyses and longitudinal cohort integration, where cumulative error from multiple platforms can mask biologically significant differences [304–307]. Unified workflows also simplify QC procedures and validations, as pooled reference samples, system proficiency tests, and internal standards can be used globally [269,308–310]. This ultimately results in improved reproducibility, increased statistical reliability, and comparability between stronger studies—key requirements for moving beyond exploratory research to regulatory-level biomarker validation [311–313].

In addition to consistency within a single assay, standardized analytical workflows also facilitate inter-center comparability, allowing for standardization and the establishment of international cutoffs instead of results with diverse and high variance [71,314,315]. They are also characterized by long-term reproducibility and reliability [316–318]. When laboratories use identical chromatographic conditions, calibration strategies, and internal standard placements, the correction of batch-to-batch drift and instrument-specific biases becomes significantly more reliable, although in practice this is almost impossible due to the large variety of chromatographic systems, columns, and mass spectrometers available [319–322].

4.2. Chromatographic and Mass Spectrometric Challenges

Simultaneous detection of TCA intermediates and KYNs can be analytically challenging, if not impossible [262,289,323,324]. TCA acids are highly polar, have low molecular weight, break easily at low voltages, are poorly retained in reversed-phase systems, and are often measured in negative electrospray mode [262,325]. In contrast, KYNs exhibit different polarity, aromaticity, and proton affinity, and are typically measured in positive electrospray ionization (ESI) mode [66,289,326–328]. Reconciliation of these different physicochemical properties defines the fundamental challenge of chromatography and ionization [327,329–331].

TCA intermediates, such as citrate, α-ketoglutarate, and malate, are highly polar, low molecular weight organic acids that elute early on conventional C18 columns and exhibit poor retention [290,332,333]. Ion-pairing agents or hydrophilic interaction chromatography (HILIC) are often required for proper separation [334–337]. However, metabolites of KYN metabolism range from more neutral, aromatic amino acid derivatives (KYN, KYNA) to highly acidic, low molecular weight, simple molecular structures with few transitions (QA, picolinic acid), requiring a broader range of chromatographic selectivity [300,338–340]. Choosing a mobile phase that is capable of retaining both classes of molecules requires a balance between retention and ionization efficiency [264,341]. Formic acid is a common additive used for positive ion detection, while ammonium acetate or ammonium formate buffers at neutral-basic pH help negative mode detection by enhancing ionization [264,342,343]. Buffers with high ionic strength can suppress the electrospray response, especially for aromatic KYNs [327,344,345]. Consequently, hybrid strategies—slightly or slightly buffered aqueous phases with carefully screened organic modifiers—are used to retain acids without unduly compromising positive mode sensitivity [264,346–348]. Such trade-offs reflect the trade-off between chromatographic retention and MS compatibility [264,346,349].

The polarity of electrospray ionization fundamentally affects the quality of the signal, and some molecules only give signals in one polarity mode [327,350–352]. TCA cycle intermediates ionize best in the negative mode, forming stable deprotonated species [262,290,353]. KYNs, especially KYN and KYNA, favor the positive mode through protonation or ammonium adduct formation [66,247,354]. Trying to quantify both in a single run either forces a polarity switch within a gradient or the acceptance of one polarity, which can cause a decrease in sensitivity of up to several orders of magnitude for some analytes [265,355,356]. The polarity switch causes residence time losses when the analytes elute closely [265,357,358]. Furthermore, the ion source parameters—desolvation temperature, gas, and capillary voltage—should be set differently for acids and aromatics [359–362]. Adduct formation further complicates the process: sodium and potassium adducts are common for citrate and succinate, while ammonium adducts affect KYNs [363–365]. Without careful control, the diversity of ionic species reduces quantitative reproducibility [366–370]. Thus, the challenge is not

 doi:10.20944/preprints202601.0822.v1

only chromatographic but also electrochemical, requiring source-level design or the use of stable isotope-labeled internal standards to normalize for adduct heterogeneity [371–374].

P4 Dynamic range: mM vs nM–µM, saturation, and detector linearity (220)

Another critical difficulty arises from concentration differences. TCA intermediates such as lactate, pyruvate, citrate, malate and succinate often circulate in the plasma in the high micromolar and millimolar range, while downstream KYNs such as 3-hydroxykynurenine, xanthurenic acid, anthranilic acid, QA or picolinic acid are present in the nanomolar range [247,275,375–377]. This difference spans four to six orders of magnitude, exceeding the linear dynamic range of almost all detectors used in mass spectrometers [346,378,379]. Injecting samples to achieve adequate sensitivity for low amounts of KYNs carries the risk of saturating the signals of high amounts of TCA metabolites, leading to peak distortion and poor quantitation, while diluting samples to TCA concentrations below the detection limit of kynurenes can reduce detection limits [346,380,381]. Signal compression and ion suppression further exacerbate the problem when high concentrations of acids dominate the spray cloud [382–385]. These concentration dynamics require either double injections (concentrated and many-fold diluted) or special detector linearization approaches that carefully span the entire range [386–388]. Without such adaptations, single-run assays run the risk of erroneously measuring either low-abundance KYN metabolites or concentrated TCA intermediates [237,389].

4.3. Practical Solutions

Co-measurements with physicochemical and quantitative differences between TCA and KYN metabolites require considerable foresight and planning [66,390]. To solve this problem, advanced chromatographic approaches such as HILIC, mixed mode or multidimensional separations are available, but advanced use of the mass spectrometer is also essential, such as polarity switching and properly optimized ion source conditions [265,391–393]. The guiding principle is comprehensive metabolite coverage without sacrificing sensitivity or reproducibility.

Strong retention of polar acids provides better separation of TCA intermediates, while less polar KYNs can be adequately retained by selecting the appropriate eluent composition, gradients, column temperature, eluent composition, and pH. Mixed-mode columns, which combine ion-exchange and reversed-phase characteristics, offer another option, improving resolution across different chemical classes (e.g., ZIC-cHILIC), BEH Amide, BEH HILIC HILIC Silica, or Accucore HILIC) [66,279,394,395]. Even more precise, but more complex, are two-dimensional LC (2D-LC) systems, where an initial HILIC or ion-exchanger binds the highly polar acids, followed by reversed-phase separation of the aromatic kynurenes [396,397]. Although technically demanding, 2D-LC allows the analysis of both metabolite classes in a single workflow [398–400]. They also have the disadvantage of being complex, extremely error-prone and difficult to implement, especially in biological matrices [397,401]. A high degree of chromatographic and engineering expertise is required to design and operate such a complex system efficiently [402–404]. The piping, switching valves, and dead volume must be optimized to preserve peak shape and sensitivity [405]. Nevertheless, these approaches illustrate how chromatographic ingenuity can reduce polarity bias and expand assay coverage [334,406,407].

A practical compromise is to design two complementary LC-MS runs instead of forcing all analytes into a single chromatographic measurement [268,408,409]. For example, an optimized and validated run in negative mode for TCA intermediates and a second run in positive mode for KYNs allows for adequate sensitivity in both cases [71,262,410,411]. Although this doubles the run time, it can solve the problem of multiple sample preparation and sample volumes, and it also maintains quantitative reliability, but in return avoids retention or ionization compromises [287,401,410,412]. Hybrid approaches also exist: a single-run method that uses precisely timed polarity reversals at appropriate times in the gradient can measure both acidic and aromatic metabolites with acceptable reproducibility [263,413–416]. Advances in high-speed electronics optimization have reduced the time-dependent degradation of polarity reversal measurements, making single-run hybrids

 doi:10.20944/preprints202601.0822.v1

increasingly feasible [265,355,408]. The choice between two-run and single-run strategies depends on the scale of the study, throughput requirements, and instrumentation, with hybrid methods being preferred for exploratory studies and two-run strategies for large clinical cohorts where reproducibility overrides throughput [267,268,417–419].

Internal standards (IS) labeled with stable isotopes (D, C^{13}, N^{15}) are essential for reliable and reproducible mass spectrometry measurements [372,420,421]. They correct for matrix effects, ion suppression and adduct variability in both metabolite classes [420,422,423]. The choice of IS should be carefully considered due to their extremely high cost and availability [308,424]. Optimally, each metabolite to be measured would have its own stable isotope-labeled IS, but this would significantly increase the cost [421,425,426]. It is worth considering what the goal is, which metabolites can be combined under a common IS, incorporating them at the earliest possible step, ideally during sample extraction, compensates for losses during preparation and ensures normalization between runs [427–430]. For studies spanning a wide concentration range, multiple concentration-matched calibration curves recorded by IS prevent saturation in the high range while maintaining sensitivity for trace analytes [431–433]. Without this strategic use of isotopes, uniform workflows risk systematic bias in both chemical classes [428,434,435].

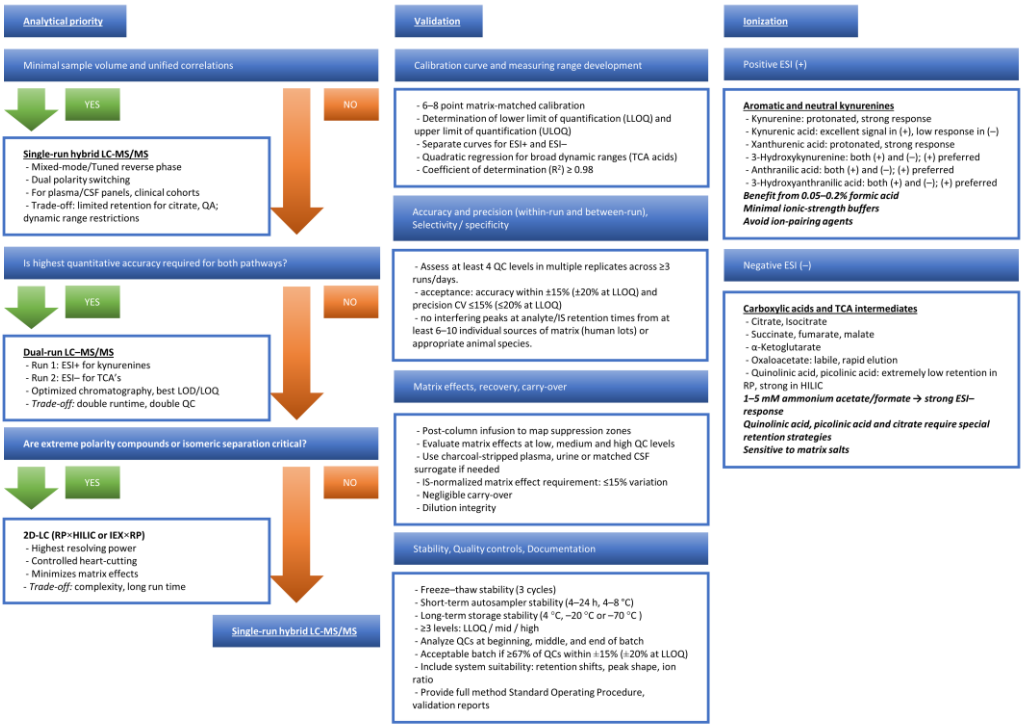

Figure 4. Decision Framework and Validation Pathways for LC–MS/MS Quantification of Kynurenine Pathway Metabolites and Tricarboxylic Acid Cycle (TCA) Intermediates. The figure summarizes a practical decision framework and validation roadmap for targeted LC–MS/MS quantification of kynurenine pathway metabolites alongside TCA intermediates. Method selection is driven by sample volume, polarity span, required quantitative rigor, and chromatographic feasibility, leading to three main options. Single-run hybrid LC–MS/MS (often mixed-mode) suits limited-volume clinical matrices (plasma, CSF) when unified conditions are needed, but can compromise retention and peak shape for highly polar organic acids. When accuracy and sensitivity must be maximized across both pathways, a dual-run strategy—typically ESI^+ for kynurenines and ESI^- for TCA acids—enables optimized chromatography and improved LLOQ/LOD, at the cost of longer runtime and expanded QC. For extreme polarity, isomeric overlap, or demanding resolution, 2D-LC (e.g., RP→HILIC or IEX→RP) provides orthogonality and separation power, but increases complexity. Validation emphasizes 6–8 point matrix-matched calibration, defined LLOQ/ULOQ, and accuracy/precision at ≥4 QC levels (≤15% deviation; ≤20% at LLOQ), alongside checks for interferences, retention-time stability, carryover, recovery, and matrix effects (e.g., post-

 doi:10.20944/preprints202601.0822.v1

column infusion). Ionization considerations are central: kynurenines favor ESI^+, whereas TCA acids require ESI^- and are matrix-sensitive; challenging analytes (e.g., quinolinic acid, citrate) often need tailored retention and suppression-mitigation via controlled buffers and mobile-phase consistency.

4.4. Validation and Clinical Feasibility

Rigorous validation is required for a simultaneous TCA-KYN metabolite assay to become a clinical or research method [262,288,408,436]. Guidelines governing mass spectrometry methods require reproducibility testing, both inter- and intraday, linearity, limit of detection, lower limit of quantification (LLQ) determination, carry-over, precision and accuracy, matrix effect, recovery, selectivity and stability testing [437–439].

An important step in validation is the linearity of the calibration curve, the determination of dynamic ranges, the measurement of matrix effects, and the stability of the samples [440–442]. The linearity range should be excellent (R2 > 0.98) from the nanomolar range to the millimolar range depending on the metabolite [408,443–445]. To calculate the matrix effect, a standard solution or different matrices need to be spiked for each matrix to be measured [446–449]. A mandatory element of stability studies is the performance of multiple freeze-thaw tests, and it is also important to test the stability of samples under different conditions (e.g., room temperature, 4 °C, -20 °C, -80 °C) [450–454]. Reproducibility is used to determine the differences between tests performed on the same day and on different days, which is an important basis for long-term QC [455–458]. Validations are accompanied by rigorous documentation, where changing any of the steps can cause critical differences in the results, so a validated system should not be modified without compelling reason, or only with caution and revalidation [459,460].

Several studies have shown that HILIC methods can be suitable for the analysis of both TCA and KYN metabolites with appropriate sensitivity and selectivity [406,415,461,462]. Methods using anion exchange stationary phase exploit the almost unlimited potential of buffers, which can be properly applied by a well-trained analyst [463–467]. Hybrid HILIC-AEX systems are promising for both clinical and research purposes, which can be used with high-resolution MS systems [279,468,469]. Although suitable assay KITs are not yet available on the market for a wide range of metabolites, especially for TCA and PK, their appearance in the future should be expected due to the high demand [308,470–472]. With the continuous optimization of diverse stationary phases, polarity switching protocols and isotope calibration, combined assays may soon provide robust, validated tools for integrative mitochondrial and immuno-metabolic diagnostics [263,473–476].

Table 5. LC-MS/MS bioanalytical validation criteria for the simultaneous measurement of kynurenines and TCA cycle metabolites.

Parameter	Acceptance Threshold	Notes / Mitigations	References
Calibration model	$R^2 \geq 0.98$; Back-calculated concentrations within ±15% (±20% at LLOQ)	Use matrix-matched standards; weighted (1/x or $1/x^2$) regression for wide dynamic ranges; verify linearity and curvature.	[477]
Linearity / Dynamic range	At least 6–8 calibration levels; deviation ≤15% (≤20% at LLOQ)	For TCA acids with steep response, consider quadratic fit; re-optimize injection volume to avoid saturation.	[478]
LLOQ / ULOQ	Signal ≥5× noise; precision ≤20%; accuracy 80–120%	Confirm LLOQ in actual matrix (plasma/CSF). Check for ion suppression at LLOQ.	[479]
Carryover	<20% of LLOQ signal and <5% of IS signal in blank after highest standard	Insert strong wash; consider needle wash with ACN/MeOH/water + 0.1% FA; extend gradient reequilibration.	[480]
Matrix effect (ME)	IS-normalized ME CV ≤15% across ≥6 donors	Perform post-column infusion; evaluate ME at low/mid/high QC; use isotopologues matched by polarity and retention.	[446,480,481]

 doi:10.20944/preprints202601.0822.v1

Extraction recovery	80–120% with CV ≤15%	Compare pre-spike vs post-spike; optimize precipitation solvent and pH; avoid ion-pairing agents in precipitant.	[446,482]
Precision—intra-day (repeatability)	CV ≤15% (≤20% at LLOQ)	Analyze ≥5 replicates each QC level; monitor retention shifts and ion ratio stability.	[479]
Precision—inter-day (reproducibility)	CV ≤15%	Include replicate QCs on ≥3 days; reinject archived QCs to detect long-term drift.	[478]
Accuracy	85–115% (80–120% at LLOQ)	Compare to spiked reference material; evaluate both absolute and IS-normalized values.	[477]
Short-term autosampler stability	≤15% change over 4–24 h at 4–8 °C	KYNs TCAs, may degrade—use immediate analysis or stabilizing additives.	[483]
Freeze–thaw stability	≤15% change after 3 cycles	Avoid repeated thawing; aliquot samples; confirm TCA acids stability separately.	[480]
Long-term stability (–70 °C)	≤15% deviation	Validate ≥1–3 months	[484]
Processed sample stability	≤15% after 6–12 h in autosampler	For unstable analytes use rapid acquisition.	[485]
System suitability	Retention time shift <0.2–0.3 min; IS area CV ≤10%; ion ratio within ±20%	Verify before each batch; monitor column pressure, peak shape, and polarity switching efficiency.	[486]
QC frequency per batch	≥3 levels (LQC/MQC/HQC); QCs at start, every 10–15 samples, and end	Large cohorts: insert pooled QC every 10–12 injections.	[479]
Batch acceptance criteria	≥67% of all QCs and ≥50% at each level must be within ±15% (±20% at LLOQ)	If failure: investigate ME shifts, IS suppression, column fouling, or calibration instability.	[478]
Inter-batch comparability	QC CV ≤15% across batches	Use pooled QC and IS-normalized drift correction.	[487]

[1] R^2: Coefficient of determination; LLOQ: lower limit of quantification; KYNs: kynurenines; TCA: tricarboxylic acid cycle; ULOQ: upper limit of quantification; CSF: cerebrospinal fluid; ACN: acetonitrile; MeOH: methanol; FA: formic acid; ME: matrix effect; IS: internal standard; QC: quality control; CV: coefficient of variation; LQC/MQC/HQC low/medium/high quality control;.

5. Discussion: Strengths, Limitations, and Future Perspectives

This section integrates mechanism with measurement. Strong signals emerge where high quality LC–MS workflows align with biology: KYN metabolite panels show diagnostic and prognostic promise, including KYNA in depression and cardiometabolic risk stratification [257,288,488]. Yet uncertainty persists. Static metabolite levels obscure flux and compartmentation, cell lines incompletely mirror tumors, and heterogeneous sampling blurs psychiatric associations [489,490]. Next steps should prioritize standardized protocols and reference materials, longitudinal and tissue matched cohorts, and fluxomics with stable isotopes to resolve directionality [491,492]. Improved annotation and pathway contextualization, combined with targeted validation and mechanistic interventions, will convert metabolite signatures into clinically actionable tools [493,494].

KYNA appears to choreograph mitochondrial resilience through a convergent receptor network [22]. Engagement of GPR35 preserves ATP under stress, tempers calcium influx, and restrains NLRP3 signaling, linking membrane cues to organelle protection in ischemia, infection, and metabolic inflammation [22,32]. Parallel signaling through the AhR modulates oxidative programs and inflammatory tone, with context specific outcomes across brain and cardiovascular systems [174,495]. At excitatory synapses, NMDA receptor antagonism by KYNA lowers excitotoxic drive and secondarily shields mitochondrial function [177,496]. $\alpha 7$ nicotinic receptor interactions remain debated, yet may contribute to immune–neuronal crosstalk in select settings [37,212]. Receptor

 doi:10.20944/preprints202601.0822.v1

crosstalk is likely, as GPR35 and AhR signals intersect calcium handling, bioenergetics, and transcriptional defenses, while gut derived KYNA can prime GPR35 positive myeloid cells or coordinate epithelial protection via combined AhR–GPR35 sensing [16,497]. Therapeutically, receptor selective modulation offers leverage to enhance mitochondrial robustness without broad immunosuppression [16,22].

Modern LC–MS has moved the KYN and TRY–NAD networks from piecemeal panels to near-complete coverage, enabling coordinated profiling across plasma, CSF, urine, peritoneal fluid, tissues, and even subcellular fractions [66,300]. Single-run or low-cost targeted assays quantify core KYN metabolites alongside central carbon nodes, while hybrid targeted–untargeted and solvent-switching workflows expand breadth without sacrificing precision [63,498]. Organelle-resolved strategies using chemical labeling now map compartmental metabolomes, a prerequisite for linking receptor cues to mitochondrial readouts in vivo [499,500]. Comparative cell-line and clinical applications illustrate scalability, drug screening utility, and disease stratification potential, including acute kidney injury and diabetes [501,502]. Limitations persist. Protocol heterogeneity, matrix effects, and incomplete annotation still blunt cross-study synthesis, motivating harmonized methods, reference materials, and improved pathway enrichment analytics [248,503]. The path forward integrates stable-isotope flux tracing with multi-organ, multi-compartment LC–MS to resolve directionality and translate signatures into actionable endpoints [504,505].

Coupling of the KYN metabolism to the TCA cycle provides a unifying scaffold for NAD^+ governance and redox control across tissues [14,50]. KYN flux supplies quinolinate for de novo NAD^+ and tunes mitochondrial function, intersecting with sirtuins, DNA repair, and stress programs [15,243]. Tissue context dictates outcome [14,506]. In liver ischemia–reperfusion, diversion from quinolinate depletes NAD^+, weakens antioxidant defenses, and heightens injury, whereas augmentation restores resilience [43,507]. Macrophages require KYN derived NAD^+ to maintain respiratory capacity and phagocytic competence, especially with aging [14,42]. Neurons and astrocytes similarly depend on KYN metabolites inputs to preserve viability and redox poise [45,225]. Kidney and brain exhibit disease specific deficits or sex dependent shifts in KYNs and NAD^+ pools, linking metabolic imbalance to dysfunction [508,509]. These nodes communicate with NADPH–glutathione circuits that relay mitochondrial workload to the endoplasmic reticulum, completing a cross organ redox axis [15,510]. Cancer exploits the same wiring to fuel growth and immune escape, emphasizing context precise intervention [227,241].

Generalization falters when biology and measurement drift by model and tissue. LC–MS workflows vary in extraction, ionization, and matrices, so results hinge on protocol and normalization choices; no single assay spans all key metabolites across compartments [511]. Biological context adds another filter [512]. Enzyme expression, receptor density, and circadian control reshape flux in organ specific ways, while inflammation rewires the same nodes differently across tissues [513]. Plasma signals often diverge from tumor or CNS readouts, and correlations between serum, CSF, urine, and viscera are imperfect, urging multi compartment designs with matrix specific validation [514]. Model choice matters. Disease stage, timing, and targeted enzyme alter outcomes in autoimmune and cancer settings, and cell line metabolism incompletely recapitulates in vivo states [515,516]. Standards are therefore essential. Anchored designs, reference materials, harmonized extraction, and data driven normalization should precede interpretation, enabling cross study synthesis and credible biomarker development [319,517].

Progress toward single-run LC–MS coverage of the KYN and Trp–NAD networks is real yet fragmented [64,248]. Panels quantifying 9–11 metabolites in CSF, plasma, urine, or peritoneal fluid prove feasibility, but validation remains matrix specific and inter-laboratory comparability is limited [66,288]. Methods for broader coverage or alternative separations extend analyte space while introducing longer run times, partial validation, or unresolved matrix effects [248,289]. Hybrid targeted–untargeted assays in large cohorts show precision, yet harmonized adoption and cross-site calibration are uncommon [63]. Cell-based workflows accelerate mechanism and screening but are not configured for clinical interchangeability [70,498]. The path forward is methodological

 doi:10.20944/preprints202601.0822.v1

convergence: clinical and laboratory standards institute (CLSI) C62-A–aligned development, isotopologue-rich internal standards, commutable multi-matrix calibrators, external quality assessment, and anchored normalization across batches and sites [289,300]. Reporting standards should include matrix-specific recovery, LLOQ, and carryover, plus retention-time locking and shared reference materials, so signatures translate across studies and into routine diagnostics [71,518].

Temporal and spatial resolution remain the weakest links in vivo. Most datasets provide static plasma or CSF snapshots that miss rapid fluxes and compartment shifts documented by disease meta-analyses and multi-compartment comparisons [519,520]. Maternal–fetal gradients and region-specific brain profiles illustrate strong spatial heterogeneity, yet longitudinal and organelle-resolved measurements are rare [521,522]. Cell-type time courses show inducible, phase-specific enzyme and metabolite waves, underscoring dynamics that bulk tissues blur [523,524]. Chronic KMO loss reshapes circulating metabolites without altering whole-body energetics, implying that acute transients, not steady states, drive phenotype [525]. Cross-kingdom exemplars point the way: subcellular fractionation and flux analysis resolve fast, compartment-locked control, often dictated by metabolite levels rather than enzyme abundance [526,527]. Physicochemical constraints and receptor transport further complicate KYNA partitioning, while KMO also governs mitochondrial morphology independent of catalysis [528,529]. Closing these blind spots will require synchronized sampling, stable-isotope fluxomics, spatial metabolomics, and organelle-targeted assays integrated across compartments and time.

A credible standardization roadmap rests on shared materials, shared methods, and shared language. First, anchor quantification with pooled multi-matrix reference materials, isotopologue-rich internal standards, and external proficiency testing to harmonize calibration and batch correction across sites [493,530]. Second, codify cross-lab standard operating procedures (SOPs) that cover preanalytics, extraction, chromatography, ionization, and QC frequency, drawing on best-practice tutorials and ultra-high-performance liquid chromatography (UHPLC)-high-resolution mass spectrometry (HRMS) guidance to minimize matrix effects and maximize metabolome coverage [531,532]. Third, mandate harmonized reporting: adopt community annotation levels, findable, accessible, interoperable, and reusable (FAIR) data deposition, and transparent identification criteria with library spectra, retention-time locking, and predictive models for MS1 features [322,533]. Open, referenceable workflows should be executable end-to-end and versioned in platforms such as MetaboAnalystR and Workflow4Metabolomics, with simulated and real benchmark datasets for software validation and interlaboratory comparability [534,535]. Finally, extend standardization to organelle-resolved assays using immunopurified mitochondria and absolute quantification, ensuring that pathway claims translate across compartments and cohorts [536,537].

Longitudinal, multi-layer cohorts can convert metabolomic snapshots into mechanistically anchored, prognostic readouts of mitochondrial health [538,539]. Population platforms such as translational metabolic cohort study (TMCS) and consortium of metabolomics studies (COMETS) already pair deep phenotyping with serial biospecimens, enabling stable-isotope substudies and genetic instruments to infer directionality between metabolite shifts and organelle function [538,540]. Coupling these frameworks to targeted mitochondrial phenotyping—multiplexed respiratory flux assays, immune-cell subtype profiling, and organelle-resolved metabolomics—links pathway panels to actionable defects in energy transfer, biogenesis, and redox control [475]. Prognostic models in sepsis, diabetic kidney disease, glioma, and mitochondrial disorders illustrate translational yield when pathway signatures are integrated with outcomes and imaging [541,542].

Genomic and microbiome layers further de-risk translation by prioritizing causal metabolites, resolving ancestry-specific effects, and exposing host–microbe axes that shape mitochondrial phenotypes [543,544]. Systems proteomics in liver and cross-species maps of mitochondrial gene function provide mechanistic scaffolds to interpret cohort signals and nominate interventions [545,546]. The immediate agenda is practical: harmonize preanalytics, embed reference materials, schedule repeated sampling, and co-capture mitochondrial function with metabolomics at scale [547].

 doi:10.20944/preprints202601.0822.v1

Such integrated phenotyping will upgrade risk prediction, clarify therapeutic targets, and shorten the path from discovery to clinic [475,548].

Medicinal chemistry around KYNA is poised to pivot from blunt modulation to receptor precise control [549]. Decades of structure–activity work already yielded high affinity glycine site antagonists at NMDA receptors and clarified competitive versus noncompetitive mechanisms, setting a template for selective central nervous system probes [223,549]. Parallel advances nominate GPR35 as a mitochondrial-proximal target for ischemic protection and inflammasome control, motivating small molecules with tuned efficacy and residence at this GPCR [16,22]. AhR active KYN scaffolds expand the chemical space for immunometabolic intervention, while a critical appraisal of purported $\alpha 7$ nicotinic activity focuses prioritization on validated targets [226,550]. Next steps should embrace biased agonism: leverage GPCR structural insights, cryptic allosteric pockets, and pathway selective screening to favor mitochondrial calcium restraint and anti inflammatory outputs over broad immunosuppression [551,552]. Integration with enzyme directed KYN-pathway modulators will enable orthogonal control of flux and signaling, improving therapeutic index in neurodegeneration and oncology [92,553].

A coherent strategy emerges when chemistry, receptor pharmacology, and mitochondrial biology are integrated [22]. Decades of structure–activity relationship (SAR) around KYNA yielded potent, glycine site selective NMDA antagonists and clarified mixed competitive and noncompetitive mechanisms, furnishing precise probes for circuit protection [37,554]. In parallel, GPR35 has surfaced as a tractable target linking receptor activation to ATP preservation and inflammasome restraint, motivating mitochondria facing agonists with tuned residence and efficacy [22,92]. Trace KYN scaffolds that potently engage the AhR broaden the repertoire for immunometabolic control [96,258]. Equally important, disputed $\alpha 7$ nicotinic activity reframes prioritization toward validated targets and cleaner selectivity profiles [37]. Next generation design should explicitly exploit biased agonism: leverage GPCR structural insights, cryptic allosteric pockets, and pathway selective assays to favor calcium sparing, anti-inflammatory, and pro resilience signaling while minimizing immunosuppression and dysmetabolism [96,555]. Such receptor selective and bias engineered ligands, layered with pathway modulators, offer a systems level route to organelle protection and disease modification [22,556].

6. Conclusions

This review converges on a simple logic with wide reach: KYN metabolic flux, receptor signaling, and TCA cycle control co-determine mitochondrial resilience, redox poise, and immune tone. The authors integrate receptor biology with NAD+ economics and analytics, showing how KYNA–GPR35, AhR, and NMDA interfaces can be read alongside unified LC–MS panels [14,557]. The take-home message is pragmatic. Mechanism and measurement must travel together to turn associative metabolomics into causal, intervention-ready biology. Three priorities emerge. First, clinically validated, harmonized assays that quantify KYN and TCA intermediates in single runs across matrices, with isotope-labeled standards and cross-lab QC. Second, causal trials that pair receptor-selective ligands or enzyme modulators with mitochondrial endpoints such as ATP preservation, $\Delta\Psi m$ stability, and mitophagy readouts. Third, longitudinal, compartment-aware cohorts linking pathway state to outcomes in neurology, psychiatry, cardiometabolic disease, and oncology [49]. These steps will de-risk translation, refine patient selection, and enable adaptive designs that use pathway ratios as eligibility and pharmacodynamic markers [61,64]. The authors' comprehensive synthesis underscores a tractable path from circuits to clinics: receptor-selective KYNA analogs, de novo NAD+ support, and standardized analytics. Uncertainties remain around temporal dynamics, tissue specificity, and receptor–mitochondria causality in vivo [227]. Future work should integrate isotope tracing, organelle profiling, and receptor bias pharmacology within harmonized workflows. With these elements aligned, mechanistic precision can mature into durable therapies and decision-grade biomarkers.

 doi:10.20944/preprints202601.0822.v1

Author Contributions: Conceptualization, M.T.; methodology, L.J., Z.G., and M.T.; software, L.J., Z.G., and M.T.; validation, L.J., Z.G., and M.T..; formal analysis, L.J., Z.G., and M.T.; investigation, L.J., Z.G., and M.T.; resources, L.J., Z.G., and M.T.; data curation, L.J., Z.G., and M.T.; writing—original draft preparation, L.J., Z.G., and M.T.; writing—review and editing, L.J., Z.G., M.T., and L.V.; visualization, L.J., Z.G., and M.T.; supervision, M.T. and L.V.; project administration, M.T. and L.V.; funding acquisition, M.T. and L.V. All authors have read and agreed to the published version of the manuscript.

Funding: This work was supported by the National Research, Development, and Innovation Office—NKFIH K138125, SZTE SZAOK-KKA No: 2022/5S729, SZTE SZAOK-KKA SZGYA No: 2023/5S775, the HUN-REN Hungarian Research Network and University of Szeged Open Access Fund 8317.

Acknowledgments: The graphical abstract was created using biorender.com.

Conflicts of Interest: The authors declare no conflicts of interest.

Abbreviations

The following abbreviations are used in this manuscript:

α7nAChR	Nicotinic acetylcholine receptors containing α7 subunits
AhR	aryl hydrocarbon receptor
AKT	protein kinase B
AMPK	AMP-activated protein kinase
ATP	adenosine triphosphate
ATPIF1	ATP synthase inhibitory factor 1
BNIP3	BCL2 interacting protein 3
cAMP	cyclic adenosine monophosphate
CD98	cluster of differentiation 98
CLSI	clinical and laboratory standards institute
COMETS	consortium of metabolomics studies
CSF	cerebrospinal fluid
ERK	extracellular signal-regulated kinase
FAIR	findable, accessible, interoperable, and reusable
GPR35	G protein–coupled receptor 35
GPX4	glutathione peroxidase 4
HIF-1α	hypoxia-inducible factor 1 alpha
HILIC	hydrophilic interaction liquid chromatography
HRMS	high-resolution mass spectrometry
IDO	indoleamine 2,3-dioxygenase
IDO1	indoleamine 2,3-dioxygenase 1
IDO2	indoleamine 2,3-dioxygenase 2
KATs	kynurenine aminotransferases
KMO	kynurenine 3-monooxygenase
KYN	kynurenine
KYNA	kynurenic acid
KYNU	kynureninase
LC–MS	liquid chromatography–mass spectrometry
LLOQ	lower limit of quantitation
MCART1	mitochondrial carrier transporting NAD+
MDH2	malate dehydrogenase 2
mPTP	mitochondrial permeability transition pore
NAD^+	nicotinamide adenine dinucleotide (oxidized form)
NADH	nicotinamide adenine dinucleotide (reduced form)
NADPH	nicotinamide adenine dinucleotide phosphate (reduced form)
NF-κB	nuclear factor kappa-light-chain-enhancer of activated b cells
NMDA	N-methyl-D-aspartate

 doi:10.20944/preprints202601.0822.v1

NMD-R	N-methyl-D-aspartate receptor
NRF1	nuclear respiratory factor 1
NRF2	nuclear factor erythroid 2–related factor 2
PD-1	programmed cell death protein 1
PI3K	phosphoinositide 3-kinase
QC	quality control
QA	quinolinic acid
Rho	ras homolog family protein
ROS	reactive oxygen species
SAR	structure–activity relationship
SDH	succinate dehydrogenase
SOP	standard operating procedure
TCA	tricarboxylic acid
TDO	tryptophan 2,3-dioxygenase
TMCS	translational metabolic cohort study
Trp	tryptophan
UHPLC	ultra-high-performance liquid chromatography

References

1. Liu, B.H.; Xu, C.Z.; Liu, Y.; Lu, Z.L.; Fu, T.L.; Li, G.R.; Deng, Y.; Luo, G.Q.; Ding, S.; Li, N.; et al. Mitochondrial quality control in human health and disease. *Mil Med Res* **2024**, *11*, 32, doi:10.1186/s40779-024-00536-5.
2. Chakrabarty, R.P.; Chandel, N.S. Mitochondria as Signaling Organelles Control Mammalian Stem Cell Fate. *Cell Stem Cell* **2021**, *28*, 394-408, doi:10.1016/j.stem.2021.02.011.
3. Esteras, N.; Abramov, A.Y. Nrf2 as a regulator of mitochondrial function: Energy metabolism and beyond. *Free Radic Biol Med* **2022**, *189*, 136-153, doi:10.1016/j.freeradbiomed.2022.07.013.
4. Hu, S.; Feng, J.; Wang, M.; Wufuer, R.; Liu, K.; Zhang, Z.; Zhang, Y. Nrf1 is an indispensable redox-determining factor for mitochondrial homeostasis by integrating multi-hierarchical regulatory networks. *Redox Biol* **2022**, *57*, 102470, doi:10.1016/j.redox.2022.102470.
5. Ježek, P.; Holendová, B.; Garlid, K.D.; Jabůrek, M. Mitochondrial Uncoupling Proteins: Subtle Regulators of Cellular Redox Signaling. *Antioxid Redox Signal* **2018**, *29*, 667-714, doi:10.1089/ars.2017.7225.
6. Echtay, K.S.; Roussel, D.; St-Pierre, J.; Jekabsons, M.B.; Cadenas, S.; Stuart, J.A.; Harper, J.A.; Roebuck, S.J.; Morrison, A.; Pickering, S.; et al. Superoxide activates mitochondrial uncoupling proteins. *Nature* **2002**, *415*, 96-99, doi:10.1038/415096a.
7. Ma, K.; Chen, G.; Li, W.; Kepp, O.; Zhu, Y.; Chen, Q. Mitophagy, Mitochondrial Homeostasis, and Cell Fate. *Front Cell Dev Biol* **2020**, *8*, 467, doi:10.3389/fcell.2020.00467.
8. Tanaka, M.; Szatmári, I.; Vécsei, L. Quinoline Quest: Kynurenic Acid Strategies for Next-Generation Therapeutics via Rational Drug Design. *Pharmaceuticals (Basel)* **2025**, *18*, doi:10.3390/ph18050607.
9. Tan, D.Q.; Suda, T. Reactive Oxygen Species and Mitochondrial Homeostasis as Regulators of Stem Cell Fate and Function. *Antioxid Redox Signal* **2018**, *29*, 149-168, doi:10.1089/ars.2017.7273.
10. Tanaka, M. Neurogenesis and Neuroinflammation in Dialogue: Mapping Gaps, Modulating Microglia, Rewiring Aging. *Cells* **2026**, *15*, 78, doi:https://doi.org/10.3390/cells15010078.
11. Murakami, S.; Kusano, Y.; Okazaki, K.; Akaike, T.; Motohashi, H. NRF2 signalling in cytoprotection and metabolism. *Br J Pharmacol* **2023**, doi:10.1111/bph.16246.
12. Ryoo, I.G.; Kwak, M.K. Regulatory crosstalk between the oxidative stress-related transcription factor Nfe2l2/Nrf2 and mitochondria. *Toxicol Appl Pharmacol* **2018**, *359*, 24-33, doi:10.1016/j.taap.2018.09.014.
13. Juhász, L.; Spisák, K.; Szolnoki, B.Z.; Nászai, A.; Szabó, Á.; Rutai, A.; Tallósy, S.P.; Szabó, A.; Toldi, J.; Tanaka, M.; et al. The Power Struggle: Kynurenine Pathway Enzyme Knockouts and Brain Mitochondrial Respiration. *J Neurochem* **2025**, *169*, e70075, doi:10.1111/jnc.70075.
14. Castro-Portuguez, R.; Sutphin, G.L. Kynurenine pathway, NAD(+) synthesis, and mitochondrial function: Targeting tryptophan metabolism to promote longevity and healthspan. *Exp Gerontol* **2020**, *132*, 110841, doi:10.1016/j.exger.2020.110841.

 doi:10.20944/preprints202601.0822.v1

15. González Esquivel, D.; Ramírez-Ortega, D.; Pineda, B.; Castro, N.; Ríos, C.; Pérez de la Cruz, V. Kynurenine pathway metabolites and enzymes involved in redox reactions. *Neuropharmacology* **2017**, *112*, 331-345, doi:10.1016/j.neuropharm.2016.03.013.
16. Agudelo, L.Z.; Ferreira, D.M.S.; Cervenka, I.; Bryzgalova, G.; Dadvar, S.; Jannig, P.R.; Pettersson-Klein, A.T.; Lakshmikanth, T.; Sustarsic, E.G.; Porsmyr-Palmertz, M.; et al. Kynurenic Acid and Gpr35 Regulate Adipose Tissue Energy Homeostasis and Inflammation. *Cell Metab* **2018**, *27*, 378-392.e375, doi:10.1016/j.cmet.2018.01.004.
17. Zhen, D.; Liu, J.; Zhang, X.D.; Song, Z. Kynurenic Acid Acts as a Signaling Molecule Regulating Energy Expenditure and Is Closely Associated With Metabolic Diseases. *Front Endocrinol (Lausanne)* **2022**, *13*, 847611, doi:10.3389/fendo.2022.847611.
18. Sánchez Chapul, L.; Pérez de la Cruz, G.; Ramos Chávez, L.A.; Valencia León, J.F.; Torres Beltrán, J.; Estrada Camarena, E.; Carillo Mora, P.; Ramírez Ortega, D.; Baños Vázquez, J.U.; Martínez Nava, G.; et al. Characterization of Redox Environment and Tryptophan Catabolism through Kynurenine Pathway in Military Divers' and Swimmers' Serum Samples. *Antioxidants (Basel)* **2022**, *11*, doi:10.3390/antiox11071223.
19. Guidetti, P.; Amori, L.; Sapko, M.T.; Okuno, E.; Schwarcz, R. Mitochondrial aspartate aminotransferase: a third kynurenate-producing enzyme in the mammalian brain. *J Neurochem* **2007**, *102*, 103-111, doi:10.1111/j.1471-4159.2007.04556.x.
20. Wyckelsma, V.L.; Lindkvist, W.; Venckunas, T.; Brazaitis, M.; Kamandulis, S.; Pääsuke, M.; Ereline, J.; Westerblad, H.; Andersson, D.C. Kynurenine aminotransferase isoforms display fiber-type specific expression in young and old human skeletal muscle. *Exp Gerontol* **2020**, *134*, 110880, doi:10.1016/j.exger.2020.110880.
21. Szabó, Á.G., Z.; Spekker, E.; Martos, D.; Szűcs, M.; Fejes-Szabó, A.; Fehér, Á.; Takeda, K.; Ozaki, K.; Inoue, H.; et al. Behavioral Balance in Tryptophan Turmoil: Regional Metabolic Rewiring in Kynurenine Aminotransferase II Knockout Mice. *Cells* **2025**, *2025*, 1711.
22. Wyant, G.A.; Yu, W.; Doulamis, I.P.; Nomoto, R.S.; Saeed, M.Y.; Duignan, T.; McCully, J.D.; Kaelin, W.G., Jr. Mitochondrial remodeling and ischemic protection by G protein-coupled receptor 35 agonists. *Science* **2022**, *377*, 621-629, doi:10.1126/science.abm1638.
23. Zhao, M.; Wang, Y.; Li, L.; Liu, S.; Wang, C.; Yuan, Y.; Yang, G.; Chen, Y.; Cheng, J.; Lu, Y.; et al. Mitochondrial ROS promote mitochondrial dysfunction and inflammation in ischemic acute kidney injury by disrupting TFAM-mediated mtDNA maintenance. *Theranostics* **2021**, *11*, 1845-1863, doi:10.7150/thno.50905.
24. Lin, Q.; Li, S.; Jiang, N.; Shao, X.; Zhang, M.; Jin, H.; Zhang, Z.; Shen, J.; Zhou, Y.; Zhou, W.; et al. PINK1-parkin pathway of mitophagy protects against contrast-induced acute kidney injury via decreasing mitochondrial ROS and NLRP3 inflammasome activation. *Redox Biol* **2019**, *26*, 101254, doi:10.1016/j.redox.2019.101254.
25. Braidy, N.; Liu, Y. NAD+ therapy in age-related degenerative disorders: A benefit/risk analysis. *Exp Gerontol* **2020**, *132*, 110831, doi:10.1016/j.exger.2020.110831.
26. Tanaka, M.; Tóth, F.; Polyák, H.; Szabó, Á.; Mándi, Y.; Vécsei, L. Immune Influencers in Action: Metabolites and Enzymes of the Tryptophan-Kynurenine Metabolic Pathway. *Biomedicines* **2021**, *9*, doi:10.3390/biomedicines9070734.
27. Tanaka, M.; Battaglia, S. Dualistic Dynamics in Neuropsychiatry: From Monoaminergic Modulators to Multiscale Biomarker Maps. *Biomedicines* **2025**, *13*, doi:10.3390/biomedicines13061456.
28. Figueiredo Godoy, A.C.; Frota, F.F.; Araújo, L.P.; Valenti, V.E.; Pereira, E.; Detregiachi, C.R.P.; Galhardi, C.M.; Caracio, F.C.; Haber, R.S.A.; Fornari Laurindo, L.; et al. Neuroinflammation and Natural Antidepressants: Balancing Fire with Flora. *Biomedicines* **2025**, *13*, doi:10.3390/biomedicines13051129.
29. Barbalho, S.M.; Laurindo, L.F.; de Oliveira Zanuso, B.; da Silva, R.M.S.; Gallerani Caglioni, L.; Nunes Junqueira de Moraes, V.B.F.; Fornari Laurindo, L.; Dogani Rodrigues, V.; da Silva Camarinha Oliveira, J.; Beluce, M.E.; et al. AdipoRon's Impact on Alzheimer's Disease-A Systematic Review and Meta-Analysis. *Int J Mol Sci* **2025**, *26*, doi:10.3390/ijms26020484.
30. Tanaka, M.; Szabó, Á.; Vécsei, L. Redefining Roles: A Paradigm Shift in Tryptophan-Kynurenine Metabolism for Innovative Clinical Applications. *Int J Mol Sci* **2024**, *25*, doi:10.3390/ijms252312767.

 doi:10.20944/preprints202601.0822.v1

31. Gáspár, R.; Nógrádi-Halmi, D.; Demján, V.; Diószegi, P.; Igaz, N.; Vincze, A.; Pipicz, M.; Kiricsi, M.; Vécsei, L.; Csont, T. Kynurenic acid protects against ischemia/reperfusion injury by modulating apoptosis in cardiomyocytes. *Apoptosis* **2024**, *29*, 1483-1498, doi:10.1007/s10495-024-02004-w.
32. Sun, T.; Xie, R.; He, H.; Xie, Q.; Zhao, X.; Kang, G.; Cheng, C.; Yin, W.; Cong, J.; Li, J.; et al. Kynurenic acid ameliorates NLRP3 inflammasome activation by blocking calcium mobilization via GPR35. *Front Immunol* **2022**, *13*, 1019365, doi:10.3389/fimmu.2022.1019365.
33. Zheng, X.; Hu, M.; Zang, X.; Fan, Q.; Liu, Y.; Che, Y.; Guan, X.; Hou, Y.; Wang, G.; Hao, H. Kynurenic acid/GPR35 axis restricts NLRP3 inflammasome activation and exacerbates colitis in mice with social stress. *Brain Behav Immun* **2019**, *79*, 244-255, doi:10.1016/j.bbi.2019.02.009.
34. Wirthgen, E.; Hoeflich, A.; Rebl, A.; Günther, J. Kynurenic Acid: The Janus-Faced Role of an Immunomodulatory Tryptophan Metabolite and Its Link to Pathological Conditions. *Front Immunol* **2017**, *8*, 1957, doi:10.3389/fimmu.2017.01957.
35. Grishanova, A.Y.; Perepechaeva, M.L. Kynurenic Acid/AhR Signaling at the Junction of Inflammation and Cardiovascular Diseases. *Int J Mol Sci* **2024**, *25*, doi:10.3390/ijms25136933.
36. Stone, T.W.; Stoy, N.; Darlington, L.G. An expanding range of targets for kynurenine metabolites of tryptophan. *Trends Pharmacol Sci* **2013**, *34*, 136-143, doi:10.1016/j.tips.2012.09.006.
37. Stone, T.W. Does kynurenic acid act on nicotinic receptors? An assessment of the evidence. *J Neurochem* **2020**, *152*, 627-649, doi:10.1111/jnc.14907.
38. Oka, S.; Ota, R.; Shima, M.; Yamashita, A.; Sugiura, T. GPR35 is a novel lysophosphatidic acid receptor. *Biochem Biophys Res Commun* **2010**, *395*, 232-237, doi:10.1016/j.bbrc.2010.03.169.
39. Deng, H.; Hu, H.; Fang, Y. Multiple tyrosine metabolites are GPR35 agonists. *Sci Rep* **2012**, *2*, 373, doi:10.1038/srep00373.
40. Badawy, A.A. Kynurenine Pathway of Tryptophan Metabolism: Regulatory and Functional Aspects. *Int J Tryptophan Res* **2017**, *10*, 1178646917691938, doi:10.1177/1178646917691938.
41. Sas, K.; Szabó, E.; Vécsei, L. Mitochondria, Oxidative Stress and the Kynurenine System, with a Focus on Ageing and Neuroprotection. *Molecules* **2018**, *23*, doi:10.3390/molecules23010191.
42. Minhas, P.S.; Liu, L.; Moon, P.K.; Joshi, A.U.; Dove, C.; Mhatre, S.; Contrepois, K.; Wang, Q.; Lee, B.A.; Coronado, M.; et al. Macrophage de novo NAD(+) synthesis specifies immune function in aging and inflammation. *Nat Immunol* **2019**, *20*, 50-63, doi:10.1038/s41590-018-0255-3.
43. Xu, B.; Zhang, P.; Tang, X.; Wang, S.; Shen, J.; Zheng, Y.; Gao, C.; Mi, P.; Zhang, C.; Qu, H.; et al. Metabolic Rewiring of Kynurenine Pathway during Hepatic Ischemia-Reperfusion Injury Exacerbates Liver Damage by Impairing NAD Homeostasis. *Adv Sci (Weinh)* **2022**, *9*, e2204697, doi:10.1002/advs.202204697.
44. Yang, Y.; Borel, T.; de Azambuja, F.; Johnson, D.; Sorrentino, J.P.; Udokwu, C.; Davis, I.; Liu, A.; Altman, R.A. Diflunisal Derivatives as Modulators of ACMS Decarboxylase Targeting the Tryptophan-Kynurenine Pathway. *J Med Chem* **2021**, *64*, 797-811, doi:10.1021/acs.jmedchem.0c01762.
45. Braidy, N.; Guillemin, G.J.; Grant, R. Effects of Kynurenine Pathway Inhibition on NAD Metabolism and Cell Viability in Human Primary Astrocytes and Neurons. *Int J Tryptophan Res* **2011**, *4*, 29-37, doi:10.4137/ijtr.S7052.
46. Xue, C.; Li, G.; Zheng, Q.; Gu, X.; Shi, Q.; Su, Y.; Chu, Q.; Yuan, X.; Bao, Z.; Lu, J.; et al. Tryptophan metabolism in health and disease. *Cell Metab* **2023**, *35*, 1304-1326, doi:10.1016/j.cmet.2023.06.004.
47. Stone, T.W.; Williams, R.O. Modulation of T cells by tryptophan metabolites in the kynurenine pathway. *Trends Pharmacol Sci* **2023**, *44*, 442-456, doi:10.1016/j.tips.2023.04.006.
48. Lu, Z.; Zhang, C.; Zhang, J.; Su, W.; Wang, G.; Wang, Z. The Kynurenine Pathway and Indole Pathway in Tryptophan Metabolism Influence Tumor Progression. *Cancer Med* **2025**, *14*, e70703, doi:10.1002/cam4.70703.
49. Tanaka, M.; Vécsei, L. From Microbial Switches to Metabolic Sensors: Rewiring the Gut-Brain Kynurenine Circuit. *Biomedicines* **2025**, *13*, doi:10.3390/biomedicines13082020.
50. Savitz, J. The kynurenine pathway: a finger in every pie. *Mol Psychiatry* **2020**, *25*, 131-147, doi:10.1038/s41380-019-0414-4.
51. Mor, A.; Tankiewicz-Kwedlo, A.; Krupa, A.; Pawlak, D. Role of Kynurenine Pathway in Oxidative Stress during Neurodegenerative Disorders. *Cells* **2021**, *10*, doi:10.3390/cells10071603.

52. Pathak, S.; Nadar, R.; Kim, S.; Liu, K.; Govindarajulu, M.; Cook, P.; Watts Alexander, C.S.; Dhanasekaran, M.; Moore, T. The Influence of Kynurenine Metabolites on Neurodegenerative Pathologies. *Int J Mol Sci* **2024**, *25*, doi:10.3390/ijms25020853.
53. Tanaka, M.; Battaglia, S. From Biomarkers to Behavior: Mapping the Neuroimmune Web of Pain, Mood, and Memory. *Biomedicines* **2025**, *13*, doi:10.3390/biomedicines13092226.
54. Strasser, B.; Becker, K.; Fuchs, D.; Gostner, J.M. Kynurenine pathway metabolism and immune activation: Peripheral measurements in psychiatric and co-morbid conditions. *Neuropharmacology* **2017**, *112*, 286-296, doi:10.1016/j.neuropharm.2016.02.030.
55. Tanaka, M. Special Issue "Translating Molecular Psychiatry: From Biomarkers to Personalized Therapies". *Int J Mol Sci* **2025**, *26*, doi:10.3390/ijms262010238.
56. Tanaka, M. Beyond the boundaries: Transitioning from categorical to dimensional paradigms in mental health diagnostics. *Adv Clin Exp Med* **2024**, *33*, 1295-1301, doi:10.17219/acem/197425.
57. Liloia, D.; Zamfira, D.A.; Tanaka, M.; Manuello, J.; Crocetta, A.; Keller, R.; Cozzolino, M.; Duca, S.; Cauda, F.; Costa, T. Disentangling the role of gray matter volume and concentration in autism spectrum disorder: A meta-analytic investigation of 25 years of voxel-based morphometry research. *Neurosci Biobehav Rev* **2024**, *164*, 105791, doi:10.1016/j.neubiorev.2024.105791.
58. Wang, Q.; Liu, D.; Song, P.; Zou, M.H. Tryptophan-kynurenine pathway is dysregulated in inflammation, and immune activation. *Front Biosci (Landmark Ed)* **2015**, *20*, 1116-1143, doi:10.2741/4363.
59. Baumgartner, R.; Forteza, M.J.; Ketelhuth, D.F.J. The interplay between cytokines and the Kynurenine pathway in inflammation and atherosclerosis. *Cytokine* **2019**, *122*, 154148, doi:10.1016/j.cyto.2017.09.004.
60. Kozieł, K.; Urbanska, E.M. Kynurenine Pathway in Diabetes Mellitus-Novel Pharmacological Target? *Cells* **2023**, *12*, doi:10.3390/cells12030460.
61. Pires, A.S.; Sundaram, G.; Heng, B.; Krishnamurthy, S.; Brew, B.J.; Guillemin, G.J. Recent advances in clinical trials targeting the kynurenine pathway. *Pharmacol Ther* **2022**, *236*, 108055, doi:10.1016/j.pharmthera.2021.108055.
62. Sforzini, L.; Nettis, M.A.; Mondelli, V.; Pariante, C.M. Inflammation in cancer and depression: a starring role for the kynurenine pathway. *Psychopharmacology (Berl)* **2019**, *236*, 2997-3011, doi:10.1007/s00213-019-05200-8.
63. Eggertsen, P.P.; Hansen, J.; Andersen, M.L.; Nielsen, J.F.; Olsen, R.K.J.; Palmfeldt, J. Simultaneous measurement of kynurenine metabolites and explorative metabolomics using liquid chromatography-mass spectrometry: A novel accurate method applied to serum and plasma samples from a large healthy cohort. *J Pharm Biomed Anal* **2023**, *227*, 115304, doi:10.1016/j.jpba.2023.115304.
64. Hossen, M.M.; Fleiss, B.; Zakaria, R. The current state in liquid chromatography-mass spectrometry methods for quantifying kynurenine pathway metabolites in biological samples: a systematic review. *Crit Rev Clin Lab Sci* **2025**, *62*, 437-453, doi:10.1080/10408363.2025.2495160.
65. Gomez-Gomez, A.; Olesti, E.; Montero-San-Martin, B.; Soldevila, A.; Deschamps, T.; Pizarro, N.; de la Torre, R.; Pozo, O.J. Determination of up to twenty carboxylic acid containing compounds in clinically relevant matrices by o-benzylhydroxylamine derivatization and liquid chromatography-tandem mass spectrometry. *J Pharm Biomed Anal* **2022**, *208*, 114450, doi:10.1016/j.jpba.2021.114450.
66. Sadok, I.; Jędruchniewicz, K.; Rawicz-Pruszyński, K.; Staniszewska, M. UHPLC-ESI-MS/MS Quantification of Relevant Substrates and Metabolites of the Kynurenine Pathway Present in Serum and Peritoneal Fluid from Gastric Cancer Patients-Method Development and Validation. *Int J Mol Sci* **2021**, *22*, doi:10.3390/ijms22136972.
67. Panuwet, P.; Hunter, R.E., Jr.; D'Souza, P.E.; Chen, X.; Radford, S.A.; Cohen, J.R.; Marder, M.E.; Kartavenka, K.; Ryan, P.B.; Barr, D.B. Biological Matrix Effects in Quantitative Tandem Mass Spectrometry-Based Analytical Methods: Advancing Biomonitoring. *Crit Rev Anal Chem* **2016**, *46*, 93-105, doi:10.1080/10408347.2014.980775.
68. Whiley, L.; Nye, L.C.; Grant, I.; Andreas, N.; Chappell, K.E.; Sarafian, M.H.; Misra, R.; Plumb, R.S.; Lewis, M.R.; Nicholson, J.K.; et al. Ultrahigh-Performance Liquid Chromatography Tandem Mass Spectrometry with Electrospray Ionization Quantification of Tryptophan Metabolites and Markers of Gut Health in

 doi:10.20944/preprints202601.0822.v1

Serum and Plasma-Application to Clinical and Epidemiology Cohorts. *Anal Chem* **2019**, *91*, 5207-5216, doi:10.1021/acs.analchem.8b05884.

69. Chawdhury, A.; Shamsi, S.A.; Miller, A.; Liu, A. Capillary electrochromatography-mass spectrometry of kynurenine pathway metabolites. *J Chromatogr A* **2021**, *1651*, 462294, doi:10.1016/j.chroma.2021.462294.
70. Sadok, I.; Rachwał, K.; Staniszewska, M. Simultaneous Quantification of Selected Kynurenines Analyzed by Liquid Chromatography-Mass Spectrometry in Medium Collected from Cancer Cell Cultures. *J Vis Exp* **2020**, doi:10.3791/61031.
71. Khetarpal, V.; Herbst, T.; Akhtar, S.; LaFayette, A.; Miller, D.; Farnham, J.; Steege, T.; Miao, Z.; Marks, B.; Ledvina, A.; et al. Validation of LC-MS/MS methods for quantitative analysis of kynurenine pathway metabolites in human plasma and cerebrospinal fluid. *Bioanalysis* **2023**, *15*, 637-651, doi:10.4155/bio-2023-0016.
72. Huang, N.; Winans, T.; Wyman, B.; Oaks, Z.; Faludi, T.; Choudhary, G.; Lai, Z.W.; Lewis, J.; Beckford, M.; Duarte, M.; et al. Rab4A-directed endosome traffic shapes pro-inflammatory mitochondrial metabolism in T cells via mitophagy, CD98 expression, and kynurenine-sensitive mTOR activation. *Nat Commun* **2024**, *15*, 2598, doi:10.1038/s41467-024-46441-2.
73. Ou, W.; Chen, Y.; Ju, Y.; Ma, M.; Qin, Y.; Bi, Y.; Liao, M.; Liu, B.; Liu, J.; Zhang, Y.; et al. The kynurenine pathway in major depressive disorder under different disease states: A systematic review and meta-analysis. *J Affect Disord* **2023**, *339*, 624-632, doi:10.1016/j.jad.2023.07.078.
74. Cristina, B.; Veronica, R.; Silvia, A.; Andrea, G.; Sara, C.; Luca, P.; Nicoletta, B.; M, C.B.; Silvio, B.; Fabio, T. Identification and characterization of the kynurenine pathway in the pond snail Lymnaea stagnalis. *Sci Rep* **2022**, *12*, 15617, doi:10.1038/s41598-022-19652-0.
75. Schwarcz, R.; Stone, T.W. The kynurenine pathway and the brain: Challenges, controversies and promises. *Neuropharmacology* **2017**, *112*, 237-247, doi:10.1016/j.neuropharm.2016.08.003.
76. Sadok, I.; Staniszewska, M. Electrochemical Determination of Kynurenine Pathway Metabolites-Challenges and Perspectives. *Sensors (Basel)* **2021**, *21*, doi:10.3390/s21217152.
77. Mrštná, K.; Krčmová, L.K.; Švec, F. Advances in kynurenine analysis. *Clin Chim Acta* **2023**, *547*, 117441, doi:10.1016/j.cca.2023.117441.
78. Tanaka, M.; Battaglia, S.; Liloia, D. Navigating Neurodegeneration: Integrating Biomarkers, Neuroinflammation, and Imaging in Parkinson's, Alzheimer's, and Motor Neuron Disorders. *Biomedicines* **2025**, *13*, doi:10.3390/biomedicines13051045.
79. Tanaka, M. From Serendipity to Precision: Integrating AI, Multi-Omics, and Human-Specific Models for Personalized Neuropsychiatric Care. *Biomedicines* **2025**, *13*, doi:10.3390/biomedicines13010167.
80. da Rocha, A.L.; Pinto, A.P.; de Sousa Neto, I.V.; Muñoz, V.R.; Marafon, B.B.; da Silva, L.; Pauli, J.R.; Cintra, D.E.; Ropelle, E.R.; Simabuco, F.M.; et al. Exhaustive exercise abolishes REV-ERB-α circadian rhythm and shifts the kynurenine pathway to a neurotoxic profile in mice. *J Physiol* **2025**, *603*, 3923-3944, doi:10.1113/jp288290.
81. O'Leary, K.M.; Slezak, T.; Kossiakoff, A.A. Conformation-specific synthetic intrabodies modulate mTOR signaling with subcellular spatial resolution. *Proc Natl Acad Sci U S A* **2025**, *122*, e2424679122, doi:10.1073/pnas.2424679122.
82. Bader, J.M.; Albrecht, V.; Mann, M. MS-Based Proteomics of Body Fluids: The End of the Beginning. *Mol Cell Proteomics* **2023**, *22*, 100577, doi:10.1016/j.mcpro.2023.100577.
83. Chen, W.; Zhao, H.; Li, Y. Mitochondrial dynamics in health and disease: mechanisms and potential targets. *Signal Transduct Target Ther* **2023**, *8*, 333, doi:10.1038/s41392-023-01547-9.
84. Rischke, S.; Hahnefeld, L.; Burla, B.; Behrens, F.; Gurke, R.; Garrett, T.J. Small molecule biomarker discovery: Proposed workflow for LC-MS-based clinical research projects. *J Mass Spectrom Adv Clin Lab* **2023**, *28*, 47-55, doi:10.1016/j.jmsacl.2023.02.003.
85. Lee, J.; Yesilkanal, A.E.; Wynne, J.P.; Frankenberger, C.; Liu, J.; Yan, J.; Elbaz, M.; Rabe, D.C.; Rustandy, F.D.; Tiwari, P.; et al. Effective breast cancer combination therapy targeting BACH1 and mitochondrial metabolism. *Nature* **2019**, *568*, 254-258, doi:10.1038/s41586-019-1005-x.

86. Schneditz, G.; Elias, J.E.; Pagano, E.; Zaeem Cader, M.; Saveljeva, S.; Long, K.; Mukhopadhyay, S.; Arasteh, M.; Lawley, T.D.; Dougan, G.; et al. GPR35 promotes glycolysis, proliferation, and oncogenic signaling by engaging with the sodium potassium pump. *Sci Signal* **2019**, *12*, doi:10.1126/scisignal.aau9048.
87. Elias, J.E.; Debela, M.; Sewell, G.W.; Stopforth, R.J.; Partl, H.; Heissbauer, S.; Holland, L.M.; Karlsen, T.H.; Kaser, A.; Kaneider, N.C. GPR35 prevents osmotic stress induced cell damage. *Commun Biol* **2025**, *8*, 478, doi:10.1038/s42003-025-07848-9.
88. Wu, Y.; Zhang, P.; Fan, H.; Zhang, C.; Yu, P.; Liang, X.; Chen, Y. GPR35 acts a dual role and therapeutic target in inflammation. *Frontiers in Immunology* **2023**, *14*, 1254446.
89. Lin, L.C.; Quon, T.; Engberg, S.; Mackenzie, A.E.; Tobin, A.B.; Milligan, G. G Protein-Coupled Receptor GPR35 Suppresses Lipid Accumulation in Hepatocytes. *ACS Pharmacol Transl Sci* **2021**, *4*, 1835-1848, doi:10.1021/acsptsci.1c00224.
90. Wei, X.; Yin, F.; Wu, M.; Xie, Q.; Zhao, X.; Zhu, C.; Xie, R.; Chen, C.; Liu, M.; Wang, X. G protein-coupled receptor 35 attenuates nonalcoholic steatohepatitis by reprogramming cholesterol homeostasis in hepatocytes. *Acta pharmaceutica Sinica B* **2023**, *13*, 1128-1144.
91. Nam, S.-Y.; Park, S.-J.; Im, D.-S. Protective effect of lodoxamide on hepatic steatosis through GPR35. *Cellular Signalling* **2019**, *53*, 190-200.
92. Nesci, S. GPR35, ally of the anti-ischemic ATPIF1-ATP synthase interaction. *Trends Pharmacol Sci* **2022**, *43*, 891-893, doi:10.1016/j.tips.2022.09.003.
93. Sharmin, O.; Abir, A.H.; Potol, A.; Alam, M.; Banik, J.; Rahman, A.; Tarannum, N.; Wadud, R.; Habib, Z.F.; Rahman, M. Activation of GPR35 protects against cerebral ischemia by recruiting monocyte-derived macrophages. *Sci Rep* **2020**, *10*, 9400, doi:10.1038/s41598-020-66417-8.
94. Boleij, A.; Fathi, P.; Dalton, W.; Park, B.; Wu, X.; Huso, D.; Allen, J.; Besharati, S.; Anders, R.A.; Housseau, F.; et al. G-protein coupled receptor 35 (GPR35) regulates the colonic epithelial cell response to enterotoxigenic Bacteroides fragilis. *Commun Biol* **2021**, *4*, 585, doi:10.1038/s42003-021-02014-3.
95. Chen, K.; He, L.; Li, Y.; Li, X.; Qiu, C.; Pei, H.; Yang, D. Inhibition of GPR35 Preserves Mitochondrial Function After Myocardial Infarction by Targeting Calpain 1/2. *J Cardiovasc Pharmacol* **2020**, *75*, 556-563, doi:10.1097/fjc.0000000000000819.
96. Milligan, G. GPR35: from enigma to therapeutic target. *Trends Pharmacol Sci* **2023**, *44*, 263-273, doi:10.1016/j.tips.2023.03.001.
97. Cheng, L.; Wu, H.; Cai, X.; Zhang, Y.; Yu, S.; Hou, Y.; Yin, Z.; Yan, Q.; Wang, Q.; Sun, T.; et al. A Gpr35-tuned gut microbe-brain metabolic axis regulates depressive-like behavior. *Cell Host Microbe* **2024**, *32*, 227-243.e226, doi:10.1016/j.chom.2023.12.009.
98. Tanaka, M.; He, Z.; Han, S.; Battaglia, S. Editorial: Noninvasive brain stimulation: a promising approach to study and improve emotion regulation. *Front Behav Neurosci* **2025**, *19*, 1633936, doi:10.3389/fnbeh.2025.1633936.
99. Wu, Y.; Zhang, P.; Fan, H.; Zhang, C.; Yu, P.; Liang, X.; Chen, Y. GPR35 acts a dual role and therapeutic target in inflammation. *Front Immunol* **2023**, *14*, 1254446, doi:10.3389/fimmu.2023.1254446.
100. Mackenzie, A.E.; Lappin, J.E.; Taylor, D.L.; Nicklin, S.A.; Milligan, G. GPR35 as a Novel Therapeutic Target. *Front Endocrinol (Lausanne)* **2011**, *2*, 68, doi:10.3389/fendo.2011.00068.
101. Stone, T.W.; Darlington, L.G.; Badawy, A.A.-B.; Williams, R.O. The complex world of kynurenic acid: reflections on biological issues and therapeutic strategy. *International Journal of Molecular Sciences* **2024**, *25*, 9040.
102. Brust, T.F.; Conley, J.M.; Watts, V.J. Gα(i/o)-coupled receptor-mediated sensitization of adenylyl cyclase: 40 years later. *Eur J Pharmacol* **2015**, *763*, 223-232, doi:10.1016/j.ejphar.2015.05.014.
103. Dhillon, A.S.; Pollock, C.; Steen, H.; Shaw, P.E.; Mischak, H.; Kolch, W. Cyclic AMP-dependent kinase regulates Raf-1 kinase mainly by phosphorylation of serine 259. *Mol Cell Biol* **2002**, *22*, 3237-3246, doi:10.1128/mcb.22.10.3237-3246.2002.
104. Zhang, L.; Shi, G. Gq-Coupled Receptors in Autoimmunity. *J Immunol Res* **2016**, *2016*, 3969023, doi:10.1155/2016/3969023.

105. Takkar, S.; Sharma, G.; Kaushal, J.B.; Abdullah, K.M.; Batra, S.K.; Siddiqui, J.A. From orphan to oncogene: The role of GPR35 in cancer and immune modulation. *Cytokine Growth Factor Rev* **2024**, *77*, 56-66, doi:10.1016/j.cytogfr.2024.03.004.
106. Poźniak, O.; Sitarz, R.; Sitarz, M.Z.; Kowalczuk, D.; Słoń, E.; Dudzińska, E. Utilization of AhR and GPR35 Receptor Ligands as Superfoods in Cancer Prevention for Individuals with IBD. *Int J Mol Sci* **2025**, *26*, doi:10.3390/ijms26189160.
107. Nógrádi-Halmi, D.; Erdélyi-Furka, B.; Csóré, D.; Plechl, É.; Igaz, N.; Juhász, L.; Poles, M.Z.; Nógrádi, B.; Patai, R.; Polgár, T.F.; et al. Kynurenic Acid Protects Against Myocardial Ischemia/Reperfusion Injury by Activating GPR35 Receptors and Preserving Mitochondrial Structure and Function. *Biomolecules* **2025**, *15*, doi:10.3390/biom15101481.
108. García-Trevijano, E.R.; Ortiz-Zapater, E.; Gimeno, A.; Viña, J.R.; Zaragozá, R. Calpains, the proteases of two faces controlling the epithelial homeostasis in mammary gland. *Front Cell Dev Biol* **2023**, *11*, 1249317, doi:10.3389/fcell.2023.1249317.
109. Hernando, V.; Inserte, J.; Sartório, C.L.; Parra, V.M.; Poncelas-Nozal, M.; Garcia-Dorado, D. Calpain translocation and activation as pharmacological targets during myocardial ischemia/reperfusion. *J Mol Cell Cardiol* **2010**, *49*, 271-279, doi:10.1016/j.yjmcc.2010.02.024.
110. Chen, Q.; Lesnefsky, E.J. Heart mitochondria and calpain 1: Location, function, and targets. *Biochim Biophys Acta* **2015**, *1852*, 2372-2378, doi:10.1016/j.bbadis.2015.08.004.
111. Chen, M.; Won, D.J.; Krajewski, S.; Gottlieb, R.A. Calpain and mitochondria in ischemia/reperfusion injury. *J Biol Chem* **2002**, *277*, 29181-29186, doi:10.1074/jbc.M204951200.
112. Zheng, D.; Cao, T.; Zhang, L.L.; Fan, G.C.; Qiu, J.; Peng, T.Q. Targeted inhibition of calpain in mitochondria alleviates oxidative stress-induced myocardial injury. *Acta Pharmacol Sin* **2021**, *42*, 909-920, doi:10.1038/s41401-020-00526-y.
113. Ni, R.; Zheng, D.; Xiong, S.; Hill, D.J.; Sun, T.; Gardiner, R.B.; Fan, G.C.; Lu, Y.; Abel, E.D.; Greer, P.A.; et al. Mitochondrial Calpain-1 Disrupts ATP Synthase and Induces Superoxide Generation in Type 1 Diabetic Hearts: A Novel Mechanism Contributing to Diabetic Cardiomyopathy. *Diabetes* **2016**, *65*, 255-268, doi:10.2337/db15-0963.
114. Jenkins, L.; Alvarez-Curto, E.; Campbell, K.; de Munnik, S.; Canals, M.; Schlyer, S.; Milligan, G. Agonist activation of the G protein-coupled receptor GPR35 involves transmembrane domain III and is transduced via $G\alpha_{13}$ and β-arrestin-2. *Br J Pharmacol* **2011**, *162*, 733-748, doi:10.1111/j.1476-5381.2010.01082.x.
115. Domínguez-Zorita, S.; Romero-Carramiñana, I.; Santacatterina, F.; Esparza-Moltó, P.B.; Simó, C.; Del-Arco, A.; Núñez de Arenas, C.; Saiz, J.; Barbas, C.; Cuezva, J.M. IF1 ablation prevents ATP synthase oligomerization, enhances mitochondrial ATP turnover and promotes an adenosine-mediated pro-inflammatory phenotype. *Cell Death Dis* **2023**, *14*, 413, doi:10.1038/s41419-023-05957-z.
116. Warnsmann, V.; Marschall, L.M.; Osiewacz, H.D. Impaired F(1)F(o)-ATP-Synthase Dimerization Leads to the Induction of Cyclophilin D-Mediated Autophagy-Dependent Cell Death and Accelerated Aging. *Cells* **2021**, *10*, doi:10.3390/cells10040757.
117. Domínguez-Zorita, S.; Romero-Carramiñana, I.; Cuezva, J.M.; Esparza-Moltó, P.B. The ATPase Inhibitory Factor 1 is a Tissue-Specific Physiological Regulator of the Structure and Function of Mitochondrial ATP Synthase: A Closer Look Into Neuronal Function. *Front Physiol* **2022**, *13*, 868820, doi:10.3389/fphys.2022.868820.
118. Nikolaou, P.E.; Lambrinidis, G.; Georgiou, M.; Karagiannis, D.; Efentakis, P.; Bessis-Lazarou, P.; Founta, K.; Kampoukos, S.; Konstantin, V.; Palmeira, C.M.; et al. Hydrolytic Activity of Mitochondrial F(1)F(O)-ATP Synthase as a Target for Myocardial Ischemia-Reperfusion Injury: Discovery and In Vitro and In Vivo Evaluation of Novel Inhibitors. *J Med Chem* **2023**, *66*, 15115-15140, doi:10.1021/acs.jmedchem.3c01048.
119. Mnatsakanyan, N.; Jonas, E.A. The new role of F(1)F(o) ATP synthase in mitochondria-mediated neurodegeneration and neuroprotection. *Exp Neurol* **2020**, *332*, 113400, doi:10.1016/j.expneurol.2020.113400.
120. Acin-Perez, R.; Benincá, C.; Fernandez Del Rio, L.; Shu, C.; Baghdasarian, S.; Zanette, V.; Gerle, C.; Jiko, C.; Khairallah, R.; Khan, S.; et al. Inhibition of ATP synthase reverse activity restores energy homeostasis in mitochondrial pathologies. *Embo j* **2023**, *42*, e111699, doi:10.15252/embj.2022111699.

 doi:10.20944/preprints202601.0822.v1

121. Pan, Y.; Ji, N.; Jiang, L.; Zhou, Y.; Feng, X.; Li, J.; Zeng, X.; Wang, J.; Shen, Y.Q.; Chen, Q. GPCRs identified on mitochondrial membranes: New therapeutic targets for diseases. *J Pharm Anal* **2025**, *15*, 101178, doi:10.1016/j.jpha.2024.101178.
122. García-Bermúdez, J.; Cuezva, J.M. The ATPase Inhibitory Factor 1 (IF1): A master regulator of energy metabolism and of cell survival. *Biochim Biophys Acta* **2016**, *1857*, 1167-1182, doi:10.1016/j.bbabio.2016.02.004.
123. Kaim, G.; Dimroth, P. ATP synthesis by F-type ATP synthase is obligatorily dependent on the transmembrane voltage. *Embo j* **1999**, *18*, 4118-4127, doi:10.1093/emboj/18.15.4118.
124. Dimroth, P.; Kaim, G.; Matthey, U. Crucial role of the membrane potential for ATP synthesis by F(1)F(o) ATP synthases. *J Exp Biol* **2000**, *203*, 51-59, doi:10.1242/jeb.203.1.51.
125. Zorova, L.D.; Popkov, V.A.; Plotnikov, E.Y.; Silachev, D.N.; Pevzner, I.B.; Jankauskas, S.S.; Babenko, V.A.; Zorov, S.D.; Balakireva, A.V.; Juhaszova, M.; et al. Mitochondrial membrane potential. *Anal Biochem* **2018**, *552*, 50-59, doi:10.1016/j.ab.2017.07.009.
126. Gottlieb, E.; Armour, S.M.; Harris, M.H.; Thompson, C.B. Mitochondrial membrane potential regulates matrix configuration and cytochrome c release during apoptosis. *Cell Death Differ* **2003**, *10*, 709-717, doi:10.1038/sj.cdd.4401231.
127. Zamzami, N.; Marchetti, P.; Castedo, M.; Zanin, C.; Vayssière, J.L.; Petit, P.X.; Kroemer, G. Reduction in mitochondrial potential constitutes an early irreversible step of programmed lymphocyte death in vivo. *J Exp Med* **1995**, *181*, 1661-1672, doi:10.1084/jem.181.5.1661.
128. Chen, K.; He, L.; Li, Y.; Li, X.; Qiu, C.; Pei, H.; Yang, D. Inhibition of GPR35 preserves mitochondrial function after myocardial infarction by targeting calpain 1/2. *Journal of Cardiovascular Pharmacology* **2020**, *75*, 556-563.
129. Dadvar, S.; Ferreira, D.M.S.; Cervenka, I.; Ruas, J.L. The weight of nutrients: kynurenine metabolites in obesity and exercise. *J Intern Med* **2018**, *284*, 519-533, doi:10.1111/joim.12830.
130. Jung, T.W.; Park, J.; Sun, J.L.; Ahn, S.H.; Abd El-Aty, A.M.; Hacimuftuoglu, A.; Kim, H.C.; Shim, J.H.; Shin, S.; Jeong, J.H. Administration of kynurenic acid reduces hyperlipidemia-induced inflammation and insulin resistance in skeletal muscle and adipocytes. *Mol Cell Endocrinol* **2020**, *518*, 110928, doi:10.1016/j.mce.2020.110928.
131. Mándi, Y.; Endrész, V.; Mosolygó, T.; Burián, K.; Lantos, I.; Fülöp, F.; Szatmári, I.; Lőrinczi, B.; Balog, A.; Vécsei, L. The Opposite Effects of Kynurenic Acid and Different Kynurenic Acid Analogs on Tumor Necrosis Factor-α (TNF-α) Production and Tumor Necrosis Factor-Stimulated Gene-6 (TSG-6) Expression. *Front Immunol* **2019**, *10*, 1406, doi:10.3389/fimmu.2019.01406.
132. Fallarini, S.; Magliulo, L.; Paoletti, T.; de Lalla, C.; Lombardi, G. Expression of functional GPR35 in human iNKT cells. *Biochem Biophys Res Commun* **2010**, *398*, 420-425, doi:10.1016/j.bbrc.2010.06.091.
133. Richter, C.A.; Tillitt, D.E.; Hannink, M. Regulation of subcellular localization of the aryl hydrocarbon receptor (AhR). *Arch Biochem Biophys* **2001**, *389*, 207-217, doi:10.1006/abbi.2001.2339.
134. Kewley, R.J.; Whitelaw, M.L.; Chapman-Smith, A. The mammalian basic helix-loop-helix/PAS family of transcriptional regulators. *Int J Biochem Cell Biol* **2004**, *36*, 189-204, doi:10.1016/s1357-2725(03)00211-5.
135. Sorg, O. AhR signalling and dioxin toxicity. *Toxicol Lett* **2014**, *230*, 225-233, doi:10.1016/j.toxlet.2013.10.039.
136. Corre, S.; Tardif, N.; Mouchet, N.; Leclair, H.M.; Boussemart, L.; Gautron, A.; Bachelot, L.; Perrot, A.; Soshilov, A.; Rogiers, A.; et al. Sustained activation of the Aryl hydrocarbon Receptor transcription factor promotes resistance to BRAF-inhibitors in melanoma. *Nat Commun* **2018**, *9*, 4775, doi:10.1038/s41467-018-06951-2.
137. Dai, S.; Qu, L.; Li, J.; Zhang, Y.; Jiang, L.; Wei, H.; Guo, M.; Chen, X.; Chen, Y. Structural insight into the ligand binding mechanism of aryl hydrocarbon receptor. *Nat Commun* **2022**, *13*, 6234, doi:10.1038/s41467-022-33858-w.
138. Polonio, C.M.; McHale, K.A.; Sherr, D.H.; Rubenstein, D.; Quintana, F.J. The aryl hydrocarbon receptor: a rehabilitated target for therapeutic immune modulation. *Nat Rev Drug Discov* **2025**, *24*, 610-630, doi:10.1038/s41573-025-01172-x.

 doi:10.20944/preprints202601.0822.v1

139. Heo, M.J.; Suh, J.H.; Lee, S.H.; Poulsen, K.L.; An, Y.A.; Moorthy, B.; Hartig, S.M.; Moore, D.D.; Kim, K.H. Aryl hydrocarbon receptor maintains hepatic mitochondrial homeostasis in mice. *Mol Metab* **2023**, *72*, 101717, doi:10.1016/j.molmet.2023.101717.
140. Bahman, F.; Choudhry, K.; Al-Rashed, F.; Al-Mulla, F.; Sindhu, S.; Ahmad, R. Aryl hydrocarbon receptor: current perspectives on key signaling partners and immunoregulatory role in inflammatory diseases. *Front Immunol* **2024**, *15*, 1421346, doi:10.3389/fimmu.2024.1421346.
141. Nebert, D.W.; Karp, C.L. Endogenous functions of the aryl hydrocarbon receptor (AHR): intersection of cytochrome P450 1 (CYP1)-metabolized eicosanoids and AHR biology. *J Biol Chem* **2008**, *283*, 36061-36065, doi:10.1074/jbc.R800053200.
142. Gutiérrez-Vázquez, C.; Quintana, F.J. Regulation of the Immune Response by the Aryl Hydrocarbon Receptor. *Immunity* **2018**, *48*, 19-33, doi:10.1016/j.immuni.2017.12.012.
143. Rothhammer, V.; Quintana, F.J. The aryl hydrocarbon receptor: an environmental sensor integrating immune responses in health and disease. *Nat Rev Immunol* **2019**, *19*, 184-197, doi:10.1038/s41577-019-0125-8.
144. Nacarino-Palma, A.; González-Rico, F.J.; Rejano-Gordillo, C.M.; Ordiales-Talavero, A.; Merino, J.M.; Fernández-Salguero, P.M. The aryl hydrocarbon receptor promotes differentiation during mouse preimplantational embryo development. *Stem Cell Reports* **2021**, *16*, 2351-2363, doi:10.1016/j.stemcr.2021.08.002.
145. DiNatale, B.C.; Murray, I.A.; Schroeder, J.C.; Flaveny, C.A.; Lahoti, T.S.; Laurenzana, E.M.; Omiecinski, C.J.; Perdew, G.H. Kynurenic acid is a potent endogenous aryl hydrocarbon receptor ligand that synergistically induces interleukin-6 in the presence of inflammatory signaling. *Toxicol Sci* **2010**, *115*, 89-97, doi:10.1093/toxsci/kfq024.
146. Moroni, F.; Cozzi, A.; Sili, M.; Mannaioni, G. Kynurenic acid: a metabolite with multiple actions and multiple targets in brain and periphery. *J Neural Transm (Vienna)* **2012**, *119*, 133-139, doi:10.1007/s00702-011-0763-x.
147. Wu, X.; Wei, J.; Ran, W.; Liu, D.; Yi, Y.; Gong, M.; Liu, X.; Gong, Q.; Li, H.; Gao, J. The Gut Microbiota-Xanthurenic Acid-Aromatic Hydrocarbon Receptor Axis Mediates the Anticolitic Effects of Trilobatin. *Adv Sci (Weinh)* **2025**, *12*, e2412234, doi:10.1002/advs.202412234.
148. Ashrafi, G.; Schwarz, T.L. The pathways of mitophagy for quality control and clearance of mitochondria. *Cell Death Differ* **2013**, *20*, 31-42, doi:10.1038/cdd.2012.81.
149. Youle, R.J.; Narendra, D.P. Mechanisms of mitophagy. *Nat Rev Mol Cell Biol* **2011**, *12*, 9-14, doi:10.1038/nrm3028.
150. Wang, S.; Long, H.; Hou, L.; Feng, B.; Ma, Z.; Wu, Y.; Zeng, Y.; Cai, J.; Zhang, D.W.; Zhao, G. The mitophagy pathway and its implications in human diseases. *Signal Transduct Target Ther* **2023**, *8*, 304, doi:10.1038/s41392-023-01503-7.
151. Palikaras, K.; Tavernarakis, N. Mitophagy in neurodegeneration and aging. *Front Genet* **2012**, *3*, 297, doi:10.3389/fgene.2012.00297.
152. Hamacher-Brady, A.; Brady, N.R. Mitophagy programs: mechanisms and physiological implications of mitochondrial targeting by autophagy. *Cell Mol Life Sci* **2016**, *73*, 775-795, doi:10.1007/s00018-015-2087-8.
153. Picca, A.; Faitg, J.; Auwerx, J.; Ferrucci, L.; D'Amico, D. Mitophagy in human health, ageing and disease. *Nat Metab* **2023**, *5*, 2047-2061, doi:10.1038/s42255-023-00930-8.
154. Peng, X.; Wang, K.; Zhang, C.; Bao, J.P.; Vlf, C.; Gao, J.W.; Zhou, Z.M.; Wu, X.T. The mitochondrial antioxidant SS-31 attenuated lipopolysaccharide-induced apoptosis and pyroptosis of nucleus pulposus cells via scavenging mitochondrial ROS and maintaining the stability of mitochondrial dynamics. *Free Radic Res* **2021**, *55*, 1080-1093, doi:10.1080/10715762.2021.2018426.
155. Cao, J.; Bao, Q.; Hao, H. Indole-3-Carboxaldehyde Alleviates LPS-Induced Intestinal Inflammation by Inhibiting ROS Production and NLRP3 Inflammasome Activation. *Antioxidants (Basel)* **2024**, *13*, doi:10.3390/antiox13091107.
156. Ma, M.; Guo, J.; Su, X.; Ma, B.; Wang, X.; Wangshao, M.; Zhong, K.; Wang, Y.; Yang, G.; Han, Y. Aryl hydrocarbon receptor (AhR) alleviates the LPS-induced inflammatory responses in IPEC-J2 cells by activating PINK1/Parkin-mediated mitophagy. *Inflamm Res* **2025**, *74*, 98, doi:10.1007/s00011-025-02063-y.

157. Lanis, J.M.; Alexeev, E.E.; Curtis, V.F.; Kitzenberg, D.A.; Kao, D.J.; Battista, K.D.; Gerich, M.E.; Glover, L.E.; Kominsky, D.J.; Colgan, S.P. Tryptophan metabolite activation of the aryl hydrocarbon receptor regulates IL-10 receptor expression on intestinal epithelia. *Mucosal Immunol* **2017**, *10*, 1133-1144, doi:10.1038/mi.2016.133.
158. Tanaka, M. Parkinson's Disease: Bridging Gaps, Building Biomarkers, and Reimagining Clinical Translation. *Cells* **2025**, *14*, doi:10.3390/cells14151161.
159. Li, Y.; Zheng, W.; Lu, Y.; Zheng, Y.; Pan, L.; Wu, X.; Yuan, Y.; Shen, Z.; Ma, S.; Zhang, X.; et al. BNIP3L/NIX-mediated mitophagy: molecular mechanisms and implications for human disease. *Cell Death Dis* **2021**, *13*, 14, doi:10.1038/s41419-021-04469-y.
160. Ding, W.X.; Yin, X.M. Mitophagy: mechanisms, pathophysiological roles, and analysis. *Biol Chem* **2012**, *393*, 547-564, doi:10.1515/hsz-2012-0119.
161. Antico, O.; Thompson, P.W.; Hertz, N.T.; Muqit, M.M.K.; Parton, L.E. Targeting mitophagy in neurodegenerative diseases. *Nat Rev Drug Discov* **2025**, *24*, 276-299, doi:10.1038/s41573-024-01105-0.
162. Palikaras, K.; Lionaki, E.; Tavernarakis, N. Mechanisms of mitophagy in cellular homeostasis, physiology and pathology. *Nat Cell Biol* **2018**, *20*, 1013-1022, doi:10.1038/s41556-018-0176-2.
163. Onishi, M.; Yamano, K.; Sato, M.; Matsuda, N.; Okamoto, K. Molecular mechanisms and physiological functions of mitophagy. *Embo j* **2021**, *40*, e104705, doi:10.15252/embj.2020104705.
164. Birgisdottir Å, B.; Lamark, T.; Johansen, T. The LIR motif—crucial for selective autophagy. *J Cell Sci* **2013**, *126*, 3237-3247, doi:10.1242/jcs.126128.
165. Zong, Y.; Li, H.; Liao, P.; Chen, L.; Pan, Y.; Zheng, Y.; Zhang, C.; Liu, D.; Zheng, M.; Gao, J. Mitochondrial dysfunction: mechanisms and advances in therapy. *Signal Transduct Target Ther* **2024**, *9*, 124, doi:10.1038/s41392-024-01839-8.
166. Murphy, M.P.; Hartley, R.C. Mitochondria as a therapeutic target for common pathologies. *Nat Rev Drug Discov* **2018**, *17*, 865-886, doi:10.1038/nrd.2018.174.
167. Kalogeris, T.; Bao, Y.; Korthuis, R.J. Mitochondrial reactive oxygen species: a double edged sword in ischemia/reperfusion vs preconditioning. *Redox Biol* **2014**, *2*, 702-714, doi:10.1016/j.redox.2014.05.006.
168. Senft, A.P.; Dalton, T.P.; Nebert, D.W.; Genter, M.B.; Puga, A.; Hutchinson, R.J.; Kerzee, J.K.; Uno, S.; Shertzer, H.G. Mitochondrial reactive oxygen production is dependent on the aromatic hydrocarbon receptor. *Free Radic Biol Med* **2002**, *33*, 1268-1278, doi:10.1016/s0891-5849(02)01014-6.
169. Onishi, M.; Okamoto, K. Mitochondrial clearance: mechanisms and roles in cellular fitness. *FEBS Lett* **2021**, *595*, 1239-1263, doi:10.1002/1873-3468.14060.
170. Garza-Lombó, C.; Pappa, A.; Panayiotidis, M.I.; Franco, R. Redox homeostasis, oxidative stress and mitophagy. *Mitochondrion* **2020**, *51*, 105-117, doi:10.1016/j.mito.2020.01.002.
171. Huang, Y.; Zhang, J.; Tao, Y.; Ji, C.; Aniagu, S.; Jiang, Y.; Chen, T. AHR/ROS-mediated mitochondria apoptosis contributes to benzo[a]pyrene-induced heart defects and the protective effects of resveratrol. *Toxicology* **2021**, *462*, 152965, doi:10.1016/j.tox.2021.152965.
172. Wang, X.; Li, S.; Liu, L.; Jian, Z.; Cui, T.; Yang, Y.; Guo, S.; Yi, X.; Wang, G.; Li, C.; et al. Role of the aryl hydrocarbon receptor signaling pathway in promoting mitochondrial biogenesis against oxidative damage in human melanocytes. *J Dermatol Sci* **2019**, *96*, 33-41, doi:10.1016/j.jdermsci.2019.09.001.
173. Chen, J.; Zhang, M.; Zou, H.; Aniagu, S.; Jiang, Y.; Chen, T. PM2.5 induces mitochondrial dysfunction via AHR-mediated cyp1a1 overexpression during zebrafish heart development. *Toxicology* **2023**, *487*, 153466, doi:10.1016/j.tox.2023.153466.
174. Ren, R.; Fang, Y.; Sherchan, P.; Lu, Q.; Lenahan, C.; Zhang, J.H.; Zhang, J.; Tang, J. Kynurenine/Aryl Hydrocarbon Receptor Modulates Mitochondria-Mediated Oxidative Stress and Neuronal Apoptosis in Experimental Intracerebral Hemorrhage. *Antioxid Redox Signal* **2022**, *37*, 1111-1129, doi:10.1089/ars.2021.0215.
175. Majláth, Z.; Török, N.; Toldi, J.; Vécsei, L. Memantine and Kynurenic Acid: Current Neuropharmacological Aspects. *Curr Neuropharmacol* **2016**, *14*, 200-209, doi:10.2174/1570159x14666151113123221.
176. Oliver, M.W.; Kessler, M.; Larson, J.; Schottler, F.; Lynch, G. Glycine site associated with the NMDA receptor modulates long-term potentiation. *Synapse* **1990**, *5*, 265-270, doi:10.1002/syn.890050403.

177. Birch, P.J.; Grossman, C.J.; Hayes, A.G. Kynurenic acid antagonises responses to NMDA via an action at the strychnine-insensitive glycine receptor. *Eur J Pharmacol* **1988**, *154*, 85-87, doi:10.1016/0014-2999(88)90367-6.
178. Poles, M.Z.; Nászai, A.; Gulácsi, L.; Czakó, B.L.; Gál, K.G.; Glenz, R.J.; Dookhun, D.; Rutai, A.; Tallósy, S.P.; Szabó, A.; et al. Kynurenic Acid and Its Synthetic Derivatives Protect Against Sepsis-Associated Neutrophil Activation and Brain Mitochondrial Dysfunction in Rats. *Front Immunol* **2021**, *12*, 717157, doi:10.3389/fimmu.2021.717157.
179. Kaszaki, J.; Erces, D.; Varga, G.; Szabó, A.; Vécsei, L.; Boros, M. Kynurenines and intestinal neurotransmission: the role of N-methyl-D-aspartate receptors. *J Neural Transm (Vienna)* **2012**, *119*, 211-223, doi:10.1007/s00702-011-0658-x.
180. Hansen, K.B.; Yi, F.; Perszyk, R.E.; Menniti, F.S.; Traynelis, S.F. NMDA Receptors in the Central Nervous System. *Methods Mol Biol* **2017**, *1677*, 1-80, doi:10.1007/978-1-4939-7321-7_1.
181. Mony, L.; Paoletti, P. Mechanisms of NMDA receptor regulation. *Curr Opin Neurobiol* **2023**, *83*, 102815, doi:10.1016/j.conb.2023.102815.
182. Hunter, D.R.; Haworth, R.A. The Ca2+-induced membrane transition in mitochondria. I. The protective mechanisms. *Arch Biochem Biophys* **1979**, *195*, 453-459, doi:10.1016/0003-9861(79)90371-0.
183. Nászai, A.; Terhes, E.; Kaszaki, J.; Boros, M.; Juhász, L. Ca((2+))N It Be Measured? Detection of Extramitochondrial Calcium Movement With High-Resolution FluoRespirometry. *Sci Rep* **2019**, *9*, 19229, doi:10.1038/s41598-019-55618-5.
184. Mira, R.G.; Cerpa, W. Building a Bridge Between NMDAR-Mediated Excitotoxicity and Mitochondrial Dysfunction in Chronic and Acute Diseases. *Cell Mol Neurobiol* **2021**, *41*, 1413-1430, doi:10.1007/s10571-020-00924-0.
185. Halestrap, A.P. What is the mitochondrial permeability transition pore? *J Mol Cell Cardiol* **2009**, *46*, 821-831, doi:10.1016/j.yjmcc.2009.02.021.
186. Bonora, M.; Giorgi, C.; Pinton, P. Molecular mechanisms and consequences of mitochondrial permeability transition. *Nat Rev Mol Cell Biol* **2022**, *23*, 266-285, doi:10.1038/s41580-021-00433-y.
187. Endlicher, R.; Drahota, Z.; Štefková, K.; Červinková, Z.; Kučera, O. The Mitochondrial Permeability Transition Pore-Current Knowledge of Its Structure, Function, and Regulation, and Optimized Methods for Evaluating Its Functional State. *Cells* **2023**, *12*, doi:10.3390/cells12091273.
188. Baev, A.Y.; Vinokurov, A.Y.; Potapova, E.V.; Dunaev, A.V.; Angelova, P.R.; Abramov, A.Y. Mitochondrial Permeability Transition, Cell Death and Neurodegeneration. *Cells* **2024**, *13*, doi:10.3390/cells13070648.
189. Riley, J.S.; Tait, S.W. Mitochondrial DNA in inflammation and immunity. *EMBO Rep* **2020**, *21*, e49799, doi:10.15252/embr.201949799.
190. Patrushev, M.; Kasymov, V.; Patrusheva, V.; Ushakova, T.; Gogvadze, V.; Gaziev, A. Mitochondrial permeability transition triggers the release of mtDNA fragments. *Cell Mol Life Sci* **2004**, *61*, 3100-3103, doi:10.1007/s00018-004-4424-1.
191. Zhang, G.; Wei, H.; Zhao, A.; Yan, X.; Zhang, X.; Gan, J.; Guo, M.; Wang, J.; Zhang, F.; Jiang, Y.; et al. Mitochondrial DNA leakage: underlying mechanisms and therapeutic implications in neurological disorders. *J Neuroinflammation* **2025**, *22*, 34, doi:10.1186/s12974-025-03363-0.
192. Lee, D.Y.; Lee, K.S.; Lee, H.J.; Noh, Y.H.; Kim, D.H.; Lee, J.Y.; Cho, S.H.; Yoon, O.J.; Lee, W.B.; Kim, K.Y.; et al. Kynurenic acid attenuates MPP(+)-induced dopaminergic neuronal cell death via a Bax-mediated mitochondrial pathway. *Eur J Cell Biol* **2008**, *87*, 389-397, doi:10.1016/j.ejcb.2008.03.003.
193. Szabo, M.; Lajkó, N.; Dulka, K.; Szatmári, I.; Fülöp, F.; Mihály, A.; Vécsei, L.; Gulya, K. Kynurenic Acid and Its Analog SZR104 Exhibit Strong Antiinflammatory Effects and Alter the Intracellular Distribution and Methylation Patterns of H3 Histones in Immunochallenged Microglia-Enriched Cultures of Newborn Rat Brains. *Int J Mol Sci* **2022**, *23*, doi:10.3390/ijms23031079.
194. Nesterov, S.V.; Skorobogatova, Y.A.; Panteleeva, A.A.; Pavlik, L.L.; Mikheeva, I.B.; Yaguzhinsky, L.S.; Nartsissov, Y.R. NMDA and GABA receptor presence in rat heart mitochondria. *Chem Biol Interact* **2018**, *291*, 40-46, doi:10.1016/j.cbi.2018.06.004.
195. Korde, A.S.; Maragos, W.F. Identification of an N-methyl-D-aspartate receptor in isolated nervous system mitochondria. *J Biol Chem* **2012**, *287*, 35192-35200, doi:10.1074/jbc.M111.322032.

196. Korde, A.S.; Maragos, W.F. Mitochondrial N-methyl-d-aspartate receptor activation enhances bioenergetics by calcium-dependent and -Independent mechanisms. *Mitochondrion* **2021**, *59*, 76-82, doi:10.1016/j.mito.2021.04.011.
197. Gingrich, J.R.; Pelkey, K.A.; Fam, S.R.; Huang, Y.; Petralia, R.S.; Wenthold, R.J.; Salter, M.W. Unique domain anchoring of Src to synaptic NMDA receptors via the mitochondrial protein NADH dehydrogenase subunit 2. *Proc Natl Acad Sci U S A* **2004**, *101*, 6237-6242, doi:10.1073/pnas.0401413101.
198. Scanlon, D.P.; Bah, A.; Krzeminski, M.; Zhang, W.; Leduc-Pessah, H.L.; Dong, Y.N.; Forman-Kay, J.D.; Salter, M.W. An evolutionary switch in ND2 enables Src kinase regulation of NMDA receptors. *Nat Commun* **2017**, *8*, 15220, doi:10.1038/ncomms15220.
199. Salter, M.W.; Kalia, L.V. Src kinases: a hub for NMDA receptor regulation. *Nat Rev Neurosci* **2004**, *5*, 317-328, doi:10.1038/nrn1368.
200. Szabó, Á.; Galla, Z.; Spekker, E.; Szűcs, M.; Martos, D.; Takeda, K.; Ozaki, K.; Inoue, H.; Yamamoto, S.; Toldi, J.; et al. Oxidative and Excitatory Neurotoxic Stresses in CRISPR/Cas9-Induced Kynurenine Aminotransferase Knockout Mice: A Novel Model for Despair-Based Depression and Post-Traumatic Stress Disorder. *Front Biosci (Landmark Ed)* **2025**, *30*, 25706, doi:10.31083/fbl25706.
201. Barbalho, S.M.; Leme Boaro, B.; da Silva Camarinha Oliveira, J.; Patočka, J.; Barbalho Lamas, C.; Tanaka, M.; Laurindo, L.F. Molecular Mechanisms Underlying Neuroinflammation Intervention with Medicinal Plants: A Critical and Narrative Review of the Current Literature. *Pharmaceuticals (Basel)* **2025**, *18*, doi:10.3390/ph18010133.
202. de Lima, E.P.; Tanaka, M.; Lamas, C.B.; Quesada, K.; Detregiachi, C.R.P.; Araújo, A.C.; Guiguer, E.L.; Catharin, V.; de Castro, M.V.M.; Junior, E.B.; et al. Vascular Impairment, Muscle Atrophy, and Cognitive Decline: Critical Age-Related Conditions. *Biomedicines* **2024**, *12*, doi:10.3390/biomedicines12092096.
203. Tanaka, M.; Vécsei, L. Revolutionizing our understanding of Parkinson's disease: Dr. Heinz Reichmann's pioneering research and future research direction. *J Neural Transm (Vienna)* **2024**, *131*, 1367-1387, doi:10.1007/s00702-024-02812-z.
204. Vécsei, L.; Szalárdy, L.; Fülöp, F.; Toldi, J. Kynurenines in the CNS: recent advances and new questions. *Nat Rev Drug Discov* **2013**, *12*, 64-82, doi:10.1038/nrd3793.
205. Fujigaki, H.; Yamamoto, Y.; Saito, K. L-Tryptophan-kynurenine pathway enzymes are therapeutic target for neuropsychiatric diseases: Focus on cell type differences. *Neuropharmacology* **2017**, *112*, 264-274, doi:10.1016/j.neuropharm.2016.01.011.
206. Tan, L.; Yu, J.T.; Tan, L. The kynurenine pathway in neurodegenerative diseases: mechanistic and therapeutic considerations. *J Neurol Sci* **2012**, *323*, 1-8, doi:10.1016/j.jns.2012.08.005.
207. Németh, H.; Toldi, J.; Vécsei, L. Kynurenines, Parkinson's disease and other neurodegenerative disorders: preclinical and clinical studies. *J Neural Transm Suppl* **2006**, 285-304, doi:10.1007/978-3-211-45295-0_45.
208. Ostapiuk, A.; Urbanska, E.M. Kynurenic acid in neurodegenerative disorders-unique neuroprotection or double-edged sword? *CNS Neurosci Ther* **2022**, *28*, 19-35, doi:10.1111/cns.13768.
209. Gergalova, G.; Lykhmus, O.; Kalashnyk, O.; Koval, L.; Chernyshov, V.; Kryukova, E.; Tsetlin, V.; Komisarenko, S.; Skok, M. Mitochondria express α7 nicotinic acetylcholine receptors to regulate Ca2+ accumulation and cytochrome c release: study on isolated mitochondria. *PLoS One* **2012**, *7*, e31361, doi:10.1371/journal.pone.0031361.
210. Kalashnyk, O.; Lykhmus, O.; Uspenska, K.; Izmailov, M.; Komisarenko, S.; Skok, M. Mitochondrial α7 nicotinic acetylcholine receptors are displaced from complexes with VDAC1 to form complexes with Bax upon apoptosis induction. *Int J Biochem Cell Biol* **2020**, *129*, 105879, doi:10.1016/j.biocel.2020.105879.
211. Gergalova, G.; Lykhmus, O.; Komisarenko, S.; Skok, M. α7 nicotinic acetylcholine receptors control cytochrome c release from isolated mitochondria through kinase-mediated pathways. *Int J Biochem Cell Biol* **2014**, *49*, 26-31, doi:10.1016/j.biocel.2014.01.001.
212. Abraham, S.M.; Suresh, S.; Komal, P. Targeting Neuronal Alpha7 Nicotinic Acetylcholine Receptor Upregulation in Age-Related Neurological Disorders. *Cell Mol Neurobiol* **2025**, *45*, 70, doi:10.1007/s10571-025-01586-6.
213. Papke, R.L.; Horenstein, N.A. Therapeutic Targeting of α7 Nicotinic Acetylcholine Receptors. *Pharmacol Rev* **2021**, *73*, 1118-1149, doi:10.1124/pharmrev.120.000097.

 doi:10.20944/preprints202601.0822.v1

214. Wu, L.; Shen, F.; Lin, L.; Zhang, X.; Bruce, I.C.; Xia, Q. The neuroprotection conferred by activating the mitochondrial ATP-sensitive K+ channel is mediated by inhibiting the mitochondrial permeability transition pore. *Neurosci Lett* **2006**, *402*, 184-189, doi:10.1016/j.neulet.2006.04.001.
215. Schultz, J.E.; Qian, Y.Z.; Gross, G.J.; Kukreja, R.C. The ischemia-selective KATP channel antagonist, 5-hydroxydecanoate, blocks ischemic preconditioning in the rat heart. *J Mol Cell Cardiol* **1997**, *29*, 1055-1060, doi:10.1006/jmcc.1996.0358.
216. Chen, Z.; Jiao, Y.; Zhang, Y.; Wang, Q.; Wu, W.; Zheng, J.; Li, J. G-Protein Coupled Receptor 35 Induces Intervertebral Disc Degeneration by Mediating the Influx of Calcium Ions and Upregulating Reactive Oxygen Species. *Oxid Med Cell Longev* **2022**, *2022*, 5469220, doi:10.1155/2022/5469220.
217. Hirst, J. Mitochondrial complex I. *Annu Rev Biochem* **2013**, *82*, 551-575, doi:10.1146/annurev-biochem-070511-103700.
218. Bleier, L.; Dröse, S. Superoxide generation by complex III: from mechanistic rationales to functional consequences. *Biochim Biophys Acta* **2013**, *1827*, 1320-1331, doi:10.1016/j.bbabio.2012.12.002.
219. Okoye, C.N.; Koren, S.A.; Wojtovich, A.P. Mitochondrial complex I ROS production and redox signaling in hypoxia. *Redox Biol* **2023**, *67*, 102926, doi:10.1016/j.redox.2023.102926.
220. Lugo-Huitrón, R.; Blanco-Ayala, T.; Ugalde-Muñiz, P.; Carrillo-Mora, P.; Pedraza-Chaverrí, J.; Silva-Adaya, D.; Maldonado, P.D.; Torres, I.; Pinzón, E.; Ortiz-Islas, E.; et al. On the antioxidant properties of kynurenic acid: free radical scavenging activity and inhibition of oxidative stress. *Neurotoxicol Teratol* **2011**, *33*, 538-547, doi:10.1016/j.ntt.2011.07.002.
221. Tappenden, D.M.; Lynn, S.G.; Crawford, R.B.; Lee, K.; Vengellur, A.; Kaminski, N.E.; Thomas, R.S.; LaPres, J.J. The aryl hydrocarbon receptor interacts with ATP5α1, a subunit of the ATP synthase complex, and modulates mitochondrial function. *Toxicol Appl Pharmacol* **2011**, *254*, 299-310, doi:10.1016/j.taap.2011.05.004.
222. Brinkmann, V.; Ale-Agha, N.; Haendeler, J.; Ventura, N. The Aryl Hydrocarbon Receptor (AhR) in the Aging Process: Another Puzzling Role for This Highly Conserved Transcription Factor. *Front Physiol* **2019**, *10*, 1561, doi:10.3389/fphys.2019.01561.
223. Alkondon, M.; Pereira, E.F.; Yu, P.; Arruda, E.Z.; Almeida, L.E.; Guidetti, P.; Fawcett, W.P.; Sapko, M.T.; Randall, W.R.; Schwarcz, R.; et al. Targeted deletion of the kynurenine aminotransferase ii gene reveals a critical role of endogenous kynurenic acid in the regulation of synaptic transmission via alpha7 nicotinic receptors in the hippocampus. *J Neurosci* **2004**, *24*, 4635-4648, doi:10.1523/jneurosci.5631-03.2004.
224. Mugayar, A.A.; da Silva Guimarães, G.; de Oliveira, P.H.T.; Miranda, R.L.; Dos Santos, A.A. Apoptosis in the neuroprotective effect of α7 nicotinic receptor in neurodegenerative models. *J Neurosci Res* **2023**, *101*, 1795-1802, doi:10.1002/jnr.25239.
225. Braidy, N.; Grant, R.; Brew, B.J.; Adams, S.; Jayasena, T.; Guillemin, G.J. Effects of Kynurenine Pathway Metabolites on Intracellular NAD Synthesis and Cell Death in Human Primary Astrocytes and Neurons. *Int J Tryptophan Res* **2009**, *2*, 61-69, doi:10.4137/ijtr.s2318.
226. Cheong, J.E.; Sun, L. Targeting the IDO1/TDO2-KYN-AhR Pathway for Cancer Immunotherapy—Challenges and Opportunities. *Trends Pharmacol Sci* **2018**, *39*, 307-325, doi:10.1016/j.tips.2017.11.007.
227. Gouasmi, R.; Ferraro-Peyret, C.; Nancey, S.; Coste, I.; Renno, T.; Chaveroux, C.; Aznar, N.; Ansieau, S. The Kynurenine Pathway and Cancer: Why Keep It Simple When You Can Make It Complicated. *Cancers (Basel)* **2022**, *14*, doi:10.3390/cancers14112793.
228. Luongo, T.S.; Eller, J.M.; Lu, M.J.; Niere, M.; Raith, F.; Perry, C.; Bornstein, M.R.; Oliphint, P.; Wang, L.; McReynolds, M.R.; et al. SLC25A51 is a mammalian mitochondrial NAD(+) transporter. *Nature* **2020**, *588*, 174-179, doi:10.1038/s41586-020-2741-7.
229. Kory, N.; Uit de Bos, J.; van der Rijt, S.; Jankovic, N.; Güra, M.; Arp, N.; Pena, I.A.; Prakash, G.; Chan, S.H.; Kunchok, T.; et al. MCART1/SLC25A51 is required for mitochondrial NAD transport. *Sci Adv* **2020**, *6*, doi:10.1126/sciadv.abe5310.
230. Girardi, E.; Agrimi, G.; Goldmann, U.; Fiume, G.; Lindinger, S.; Sedlyarov, V.; Srndic, I.; Gürtl, B.; Agerer, B.; Kartnig, F.; et al. Epistasis-driven identification of SLC25A51 as a regulator of human mitochondrial NAD import. *Nat Commun* **2020**, *11*, 6145, doi:10.1038/s41467-020-19871-x.
231. Martínez-Reyes, I.; Chandel, N.S. Mitochondrial TCA cycle metabolites control physiology and disease. *Nat Commun* **2020**, *11*, 102, doi:10.1038/s41467-019-13668-3.

232. Ronchi, J.A.; Francisco, A.; Passos, L.A.; Figueira, T.R.; Castilho, R.F. The Contribution of Nicotinamide Nucleotide Transhydrogenase to Peroxide Detoxification Is Dependent on the Respiratory State and Counterbalanced by Other Sources of NADPH in Liver Mitochondria. *J Biol Chem* **2016**, *291*, 20173-20187, doi:10.1074/jbc.M116.730473.
233. Ronchi, J.A.; Figueira, T.R.; Ravagnani, F.G.; Oliveira, H.C.; Vercesi, A.E.; Castilho, R.F. A spontaneous mutation in the nicotinamide nucleotide transhydrogenase gene of C57BL/6J mice results in mitochondrial redox abnormalities. *Free Radic Biol Med* **2013**, *63*, 446-456, doi:10.1016/j.freeradbiomed.2013.05.049.
234. Fisher-Wellman, K.H.; Lin, C.T.; Ryan, T.E.; Reese, L.R.; Gilliam, L.A.; Cathey, B.L.; Lark, D.S.; Smith, C.D.; Muoio, D.M.; Neufer, P.D. Pyruvate dehydrogenase complex and nicotinamide nucleotide transhydrogenase constitute an energy-consuming redox circuit. *Biochem J* **2015**, *467*, 271-280, doi:10.1042/bj20141447.
235. Simmen, F.A.; Alhallak, I.; Simmen, R.C.M. Malic enzyme 1 (ME1) in the biology of cancer: it is not just intermediary metabolism. *J Mol Endocrinol* **2020**, *65*, R77-r90, doi:10.1530/jme-20-0176.
236. Ying, M.; You, D.; Zhu, X.; Cai, L.; Zeng, S.; Hu, X. Lactate and glutamine support NADPH generation in cancer cells under glucose deprived conditions. *Redox Biol* **2021**, *46*, 102065, doi:10.1016/j.redox.2021.102065.
237. Hernandez-Baixauli, J.; Abasolo, N.; Palacios-Jordan, H.; Foguet-Romero, E.; Suñol, D.; Galofré, M.; Caimari, A.; Baselga-Escudero, L.; Del Bas, J.M.; Mulero, M. Imbalances in TCA, Short Fatty Acids and One-Carbon Metabolisms as Important Features of Homeostatic Disruption Evidenced by a Multi-Omics Integrative Approach of LPS-Induced Chronic Inflammation in Male Wistar Rats. *Int J Mol Sci* **2022**, *23*, doi:10.3390/ijms23052563.
238. Hart, M.L.; Quon, E.; Vigil, A.B.G.; Engstrom, I.A.; Newsom, O.J.; Davidsen, K.; Hoellerbauer, P.; Carlisle, S.M.; Sullivan, L.B. Mitochondrial redox adaptations enable alternative aspartate synthesis in SDH-deficient cells. *Elife* **2023**, *12*, doi:10.7554/eLife.78654.
239. Lussey-Lepoutre, C.; Hollinshead, K.E.; Ludwig, C.; Menara, M.; Morin, A.; Castro-Vega, L.J.; Parker, S.J.; Janin, M.; Martinelli, C.; Ottolenghi, C.; et al. Loss of succinate dehydrogenase activity results in dependency on pyruvate carboxylation for cellular anabolism. *Nat Commun* **2015**, *6*, 8784, doi:10.1038/ncomms9784.
240. Esteban-Amo, M.J.; Jiménez-Cuadrado, P.; Serrano-Lorenzo, P.; de la Fuente, M.; Simarro, M. Succinate Dehydrogenase and Human Disease: Novel Insights into a Well-Known Enzyme. *Biomedicines* **2024**, *12*, doi:10.3390/biomedicines12092050.
241. Wan, J.; Cheng, C.; Hu, J.; Huang, H.; Han, Q.; Jie, Z.; Zou, Q.; Shi, J.H.; Yu, X. De novo NAD(+) synthesis contributes to CD8(+) T cell metabolic fitness and antitumor function. *Cell Rep* **2023**, *42*, 113518, doi:10.1016/j.celrep.2023.113518.
242. Sadeghdoust, M.; Das, A.; Kaushik, D.K. Fueling neurodegeneration: metabolic insights into microglia functions. *J Neuroinflammation* **2024**, *21*, 300, doi:10.1186/s12974-024-03296-0.
243. Moffett, J.R.; Arun, P.; Puthillathu, N.; Vengilote, R.; Ives, J.A.; Badawy, A.A.; Namboodiri, A.M. Quinolinate as a Marker for Kynurenine Metabolite Formation and the Unresolved Question of NAD(+) Synthesis During Inflammation and Infection. *Front Immunol* **2020**, *11*, 31, doi:10.3389/fimmu.2020.00031.
244. McReynolds, M.R.; Wang, W.; Holleran, L.M.; Hanna-Rose, W. Uridine monophosphate synthetase enables eukaryotic de novo NAD(+) biosynthesis from quinolinic acid. *J Biol Chem* **2017**, *292*, 11147-11153, doi:10.1074/jbc.C117.795344.
245. Ding, Y.; Li, X.; Horsman, G.P.; Li, P.; Wang, M.; Li, J.; Zhang, Z.; Liu, W.; Wu, B.; Tao, Y.; et al. Construction of an Alternative NAD(+) De Novo Biosynthesis Pathway. *Adv Sci (Weinh)* **2021**, *8*, 2004632, doi:10.1002/advs.202004632.
246. Zhu, S.; Zhang, R.; Yao, L.; Lin, Z.; Li, Y.; Li, S.; Wu, L. De novo NAD(+) synthesis is ineffective for NAD(+) supply in axenically cultured Caenorhabditis elegans. *Commun Biol* **2025**, *8*, 545, doi:10.1038/s42003-025-07984-2.
247. Trepci, A.; Imbeault, S.; Wyckelsma, V.L.; Westerblad, H.; Hermansson, S.; Andersson, D.C.; Piehl, F.; Venckunas, T.; Brazaitis, M.; Kamandulis, S.; et al. Quantification of Plasma Kynurenine Metabolites Following One Bout of Sprint Interval Exercise. *Int J Tryptophan Res* **2020**, *13*, 1178646920978241, doi:10.1177/1178646920978241.

 doi:10.20944/preprints202601.0822.v1

248. Wu, P.; Wang, W.; Huang, C.; Sun, L.; Wu, X.; Xu, L.; Xiao, P. A rapid and reliable targeted LC-MS/MS method for quantitative analysis of the Tryptophan-NAD metabolic network disturbances in tissues and blood of sleep deprivation mice. *Anal Chim Acta* **2024**, *1328*, 343125, doi:10.1016/j.aca.2024.343125.
249. Baixauli, F.; Piletic, K.; Puleston, D.J.; Villa, M.; Field, C.S.; Flachsmann, L.J.; Quintana, A.; Rana, N.; Edwards-Hicks, J.; Matsushita, M.; et al. An LKB1-mitochondria axis controls T(H)17 effector function. *Nature* **2022**, *610*, 555-561, doi:10.1038/s41586-022-05264-1.
250. Muri, J.; Heer, S.; Matsushita, M.; Pohlmeier, L.; Tortola, L.; Fuhrer, T.; Conrad, M.; Zamboni, N.; Kisielow, J.; Kopf, M. The thioredoxin-1 system is essential for fueling DNA synthesis during T-cell metabolic reprogramming and proliferation. *Nat Commun* **2018**, *9*, 1851, doi:10.1038/s41467-018-04274-w.
251. Lee, S.; Kim, S.M.; Lee, R.T. Thioredoxin and thioredoxin target proteins: from molecular mechanisms to functional significance. *Antioxid Redox Signal* **2013**, *18*, 1165-1207, doi:10.1089/ars.2011.4322.
252. Nunes, Y.C.; Mendes, N.M.; Pereira de Lima, E.; Chehadi, A.C.; Lamas, C.B.; Haber, J.F.S.; Dos Santos Bueno, M.; Araújo, A.C.; Catharin, V.C.S.; Detregiachi, C.R.P.; et al. Curcumin: A Golden Approach to Healthy Aging: A Systematic Review of the Evidence. *Nutrients* **2024**, *16*, doi:10.3390/nu16162721.
253. de Lima, E.P.; Laurindo, L.F.; Catharin, V.C.S.; Direito, R.; Tanaka, M.; Jasmin Santos German, I.; Lamas, C.B.; Guiguer, E.L.; Araújo, A.C.; Fiorini, A.M.R.; et al. Polyphenols, Alkaloids, and Terpenoids Against Neurodegeneration: Evaluating the Neuroprotective Effects of Phytocompounds Through a Comprehensive Review of the Current Evidence. *Metabolites* **2025**, *15*, doi:10.3390/metabo15020124.
254. Martos, D.; Lőrinczi, B.; Szatmári, I.; Vécsei, L.; Tanaka, M. Decoupling Behavioral Domains via Kynurenic Acid Analog Optimization: Implications for Schizophrenia and Parkinson's Disease Therapeutics. *Cells* **2025**, *14*, doi:10.3390/cells14130973.
255. Tanaka, M. From Monoamines to Systems Psychiatry: Rewiring Depression Science and Care (1960s–2025). *Biomedicines* **2026**, *14*, 35, doi:https://doi.org/10.3390/biomedicines14010035.
256. Chehadi, A.C.P.d.L., E.; Detregiachi, C.R.P.; Santos de Argollo Haber, R.; Catharin, V.M.C.S.; Fornari Laurindo, L.; Engracia Valenti, V.; Machado Galhardi, C.; Tanaka, M.; Maria Barbalho, S. Harnessing Dietary Tryptophan: Bridging the Gap Between Neurobiology and Psychiatry in Depression Management. *International Journal of Molecular Sciences* **2026**, *27*, 465, doi:https://doi.org/10.3390/ijms27010465.
257. Ogyu, K.; Kubo, K.; Noda, Y.; Iwata, Y.; Tsugawa, S.; Omura, Y.; Wada, M.; Tarumi, R.; Plitman, E.; Moriguchi, S.; et al. Kynurenine pathway in depression: A systematic review and meta-analysis. *Neurosci Biobehav Rev* **2018**, *90*, 16-25, doi:10.1016/j.neubiorev.2018.03.023.
258. Seok, S.H.; Ma, Z.X.; Feltenberger, J.B.; Chen, H.; Chen, H.; Scarlett, C.; Lin, Z.; Satyshur, K.A.; Cortopassi, M.; Jefcoate, C.R.; et al. Trace derivatives of kynurenine potently activate the aryl hydrocarbon receptor (AHR). *J Biol Chem* **2018**, *293*, 1994-2005, doi:10.1074/jbc.RA117.000631.
259. Palzkill, V.R.; Thome, T.; Murillo, A.L.; Khattri, R.B.; Ryan, T.E. Increasing plasma L-kynurenine impairs mitochondrial oxidative phosphorylation prior to the development of atrophy in murine skeletal muscle: A pilot study. *Front Physiol* **2022**, *13*, 992413, doi:10.3389/fphys.2022.992413.
260. Galla, Z.; Rajda, C.; Rácz, G.; Grecsó, N.; Baráth, Á.; Vécsei, L.; Bereczki, C.; Monostori, P. Simultaneous determination of 30 neurologically and metabolically important molecules: A sensitive and selective way to measure tyrosine and tryptophan pathway metabolites and other biomarkers in human serum and cerebrospinal fluid. *Journal of Chromatography A* **2021**, *1635*, 461775.
261. Galla, Z.; Rácz, G.; Grecsó, N.; Baráth, Á.; Kósa, M.; Bereczki, C.; Monostori, P. Improved LC-MS/MS method for the determination of 42 neurologically and metabolically important molecules in urine. *J Chromatogr B Analyt Technol Biomed Life Sci* **2021**, *1179*, 122846, doi:10.1016/j.jchromb.2021.122846.
262. Al Kadhi, O.; Melchini, A.; Mithen, R.; Saha, S. Development of a LC-MS/MS Method for the Simultaneous Detection of Tricarboxylic Acid Cycle Intermediates in a Range of Biological Matrices. *J Anal Methods Chem* **2017**, *2017*, 5391832, doi:10.1155/2017/5391832.
263. Le, A.; Mak, J.; Cowan, T.M. Metabolic profiling by reversed-phase/ion-exchange mass spectrometry. *J Chromatogr B Analyt Technol Biomed Life Sci* **2020**, *1143*, 122072, doi:10.1016/j.jchromb.2020.122072.
264. Cajka, T.; Hricko, J.; Rudl Kulhava, L.; Paucova, M.; Novakova, M.; Kuda, O. Optimization of Mobile Phase Modifiers for Fast LC-MS-Based Untargeted Metabolomics and Lipidomics. *Int J Mol Sci* **2023**, *24*, doi:10.3390/ijms24031987.

265. Carlsson, H.; Vaivade, A.; Emami Khoonsari, P.; Burman, J.; Kultima, K. Evaluation of polarity switching for untargeted lipidomics using liquid chromatography coupled to high resolution mass spectrometry. *J Chromatogr B Analyt Technol Biomed Life Sci* **2022**, *1195*, 123200, doi:10.1016/j.jchromb.2022.123200.
266. Ren, J.L.; Zhang, A.H.; Kong, L.; Wang, X.J. Advances in mass spectrometry-based metabolomics for investigation of metabolites. *RSC Adv* **2018**, *8*, 22335-22350, doi:10.1039/c8ra01574k.
267. Zhang, L.; Zheng, J.; Johnson, M.; Mandal, R.; Cruz, M.; Martínez-Huélamo, M.; Andres-Lacueva, C.; Wishart, D.S. A Comprehensive LC-MS Metabolomics Assay for Quantitative Analysis of Serum and Plasma. *Metabolites* **2024**, *14*, doi:10.3390/metabo14110622.
268. Lee, H.J.; Kremer, D.M.; Sajjakulnukit, P.; Zhang, L.; Lyssiotis, C.A. A large-scale analysis of targeted metabolomics data from heterogeneous biological samples provides insights into metabolite dynamics. *Metabolomics* **2019**, *15*, 103, doi:10.1007/s11306-019-1564-8.
269. Broadhurst, D.; Goodacre, R.; Reinke, S.N.; Kuligowski, J.; Wilson, I.D.; Lewis, M.R.; Dunn, W.B. Guidelines and considerations for the use of system suitability and quality control samples in mass spectrometry assays applied in untargeted clinical metabolomic studies. *Metabolomics* **2018**, *14*, 72, doi:10.1007/s11306-018-1367-3.
270. Jenkins, R.; Duggan, J.X.; Aubry, A.F.; Zeng, J.; Lee, J.W.; Cojocaru, L.; Dufield, D.; Garofolo, F.; Kaur, S.; Schultz, G.A.; et al. Recommendations for validation of LC-MS/MS bioanalytical methods for protein biotherapeutics. *Aaps j* **2015**, *17*, 1-16, doi:10.1208/s12248-014-9685-5.
271. .
272. Thomas, S.N.; French, D.; Jannetto, P.J.; Rappold, B.A.; Clarke, W.A. Liquid chromatography-tandem mass spectrometry for clinical diagnostics. *Nat Rev Methods Primers* **2022**, *2*, 96, doi:10.1038/s43586-022-00175-x.
273. Holbrook, J.H.; Kemper, G.E.; Hummon, A.B. Quantitative mass spectrometry imaging: therapeutics & biomolecules. *Chem Commun (Camb)* **2024**, *60*, 2137-2151, doi:10.1039/d3cc05988j.
274. Thorsteinsdóttir, U.A.; Thorsteinsdóttir, M. Design of experiments for development and optimization of a liquid chromatography coupled to tandem mass spectrometry bioanalytical assay. *J Mass Spectrom* **2021**, *56*, e4727, doi:10.1002/jms.4727.
275. Pocivavsek, A.; Schwarcz, R.; Erhardt, S. Neuroactive Kynurenines as Pharmacological Targets: New Experimental Tools and Exciting Therapeutic Opportunities. *Pharmacol Rev* **2024**, *76*, 978-1008, doi:10.1124/pharmrev.124.000239.
276. Kurhaluk, N. Tricarboxylic Acid Cycle Intermediates and Individual Ageing. *Biomolecules* **2024**, *14*, doi:10.3390/biom14030260.
277. Kurhaluk, N. Tricarboxylic acid cycle intermediates and individual ageing. *Biomolecules* **2024**, *14*, 260.
278. Tang, Y.; Wang, S.; Zhang, W.; Yang, R.; Yu, X.; Wang, X.; Mu, H.; Li, H.; Ji, F.; Chen, W. A single-run, rapid polarity switching method for simultaneous quantification of cardiovascular disease-related metabolites using liquid chromatography–tandem mass spectrometry. *International Journal of Mass Spectrometry* **2021**, *461*, 116500.
279. Nakatani, K.; Izumi, Y.; Takahashi, M.; Bamba, T. Unified-Hydrophilic-Interaction/Anion-Exchange Liquid Chromatography Mass Spectrometry (Unified-HILIC/AEX/MS): A Single-Run Method for Comprehensive and Simultaneous Analysis of Polar Metabolome. *Anal Chem* **2022**, *94*, 16877-16886, doi:10.1021/acs.analchem.2c03986.
280. Quan, S.; Zhao, S.; Li, L. Study of Metabolite Detectability in Simultaneous Profiling of Amine/Phenol and Hydroxyl Submetabolomes by Analyzing a Mixture of Two Separately Dansyl-Labeled Samples. *Metabolites* **2025**, *15*, doi:10.3390/metabo15080496.
281. Huan, T.; Xian, J.W.; Leung, W.N.; Li, L.; Chan, C.W. Cerebrospinal Fluid Metabolomics After Natural Product Treatment in an Experimental Model of Cerebral Ischemia. *Omics* **2016**, *20*, 670-680, doi:10.1089/omi.2016.0112.
282. Yan, J.; Kuzhiumparambil, U.; Bandodkar, S.; Dale, R.C.; Fu, S. Cerebrospinal fluid metabolomics: detection of neuroinflammation in human central nervous system disease. *Clin Transl Immunology* **2021**, *10*, e1318, doi:10.1002/cti2.1318.
283. Carlsson, H.; Abujrais, S.; Herman, S.; Khoonsari, P.E.; Åkerfeldt, T.; Svenningsson, A.; Burman, J.; Kultima, K. Targeted metabolomics of CSF in healthy individuals and patients with secondary progressive multiple

 doi:10.20944/preprints202601.0822.v1

sclerosis using high-resolution mass spectrometry. *Metabolomics* **2020**, *16*, 26, doi:10.1007/s11306-020-1648-5.

284. Saoi, M.; Britz-McKibbin, P. New Advances in Tissue Metabolomics: A Review. *Metabolites* **2021**, *11*, doi:10.3390/metabo11100672.
285. Unsihuay, D.; Phipps, W.S.; Paulovich, A.G.; Chapman, J.R.; Ducret, A.; Eberlin, L.S.; Spraggins, J.M.; Goodwin, R.J.A. Tissue Mass Spectrometry: How Solid Is Our Future? *Clin Chem* **2023**, *69*, 676-683, doi:10.1093/clinchem/hvad061.
286. Harstad, E.; Andaya, R.; Couch, J.; Ding, X.; Liang, X.; Liederer, B.M.; Messick, K.; Nguyen, T.; Schweiger, M.; Tarrant, J.; et al. Balancing Blood Sample Volume with 3Rs: Implementation and Best Practices for Small Molecule Toxicokinetic Assessments in Rats. *Ilar j* **2016**, *57*, 157-165, doi:10.1093/ilar/ilw023.
287. Jeppesen, M.J.; Powers, R. Multiplatform untargeted metabolomics. *Magn Reson Chem* **2023**, *61*, 628-653, doi:10.1002/mrc.5350.
288. Patel, V.D.; Shamsi, S.A.; Miller, A.; Liu, A.; Powell, M. Simultaneous separation and detection of nine kynurenine pathway metabolites by reversed-phase liquid chromatography-mass spectrometry: Quantitation of inflammation in human cerebrospinal fluid and plasma. *Anal Chim Acta* **2023**, *1278*, 341659, doi:10.1016/j.aca.2023.341659.
289. Abusoglu, S.; Eryavuz Onmaz, D.; Abusoglu, G.; Humeyra Yerlikaya, F.; Unlu, A. Measurement of kynurenine pathway metabolites by tandem mass spectrometry. *J Mass Spectrom Adv Clin Lab* **2023**, *28*, 114-121, doi:10.1016/j.jmsacl.2023.04.003.
290. Rathod, R.; Gajera, B.; Nazir, K.; Wallenius, J.; Velagapudi, V. Simultaneous Measurement of Tricarboxylic Acid Cycle Intermediates in Different Biological Matrices Using Liquid Chromatography-Tandem Mass Spectrometry; Quantitation and Comparison of TCA Cycle Intermediates in Human Serum, Plasma, Kasumi-1 Cell and Murine Liver Tissue. *Metabolites* **2020**, *10*, doi:10.3390/metabo10030103.
291. Ivanisevic, J.; Want, E.J. From Samples to Insights into Metabolism: Uncovering Biologically Relevant Information in LC-HRMS Metabolomics Data. *Metabolites* **2019**, *9*, doi:10.3390/metabo9120308.
292. Wei, R.; Li, G.; Seymour, A.B. Multiplexed, quantitative, and targeted metabolite profiling by LC-MS/MRM. *Methods Mol Biol* **2014**, *1198*, 171-199, doi:10.1007/978-1-4939-1258-2_12.
293. Pukoli, D.; Vécsei, L. Kynurenines and Mitochondrial Disturbances in Multiple Sclerosis. *Int J Mol Sci* **2025**, *26*, doi:10.3390/ijms26115098.
294. Gomez-Gomez, A.; Aguilera, P.; Langohr, K.; Casals, G.; Pavon, C.; Marcos, J.; To-Figueras, J.; Pozo, O.J. Evaluation of Metabolic Changes in Acute Intermittent Porphyria Patients by Targeted Metabolomics. *Int J Mol Sci* **2022**, *23*, doi:10.3390/ijms23063219.
295. Hestad, K.; Alexander, J.; Rootwelt, H.; Aaseth, J.O. The Role of Tryptophan Dysmetabolism and Quinolinic Acid in Depressive and Neurodegenerative Diseases. *Biomolecules* **2022**, *12*, doi:10.3390/biom12070998.
296. Myint, A.M.; Halaris, A. Imbalances in Kynurenines as Potential Biomarkers in the Diagnosis and Treatment of Psychiatric Disorders. *Front Psychiatry* **2022**, *13*, 913303, doi:10.3389/fpsyt.2022.913303.
297. Boyd, A.; Boccara, F.; Meynard, J.L.; Ichou, F.; Bastard, J.P.; Fellahi, S.; Samri, A.; Sauce, D.; Haddour, N.; Autran, B.; et al. Serum Tryptophan-Derived Quinolinate and Indole-3-Acetate Are Associated With Carotid Intima-Media Thickness and its Evolution in HIV-Infected Treated Adults. *Open Forum Infect Dis* **2019**, *6*, ofz516, doi:10.1093/ofid/ofz516.
298. Zhang, Y.M.; Qi, Y.B.; Gao, Y.N.; Chen, W.G.; Zhou, T.; Zang, Y.; Li, J. Astrocyte metabolism and signaling pathways in the CNS. *Front Neurosci* **2023**, *17*, 1217451, doi:10.3389/fnins.2023.1217451.
299. Harrieder, E.M.; Kretschmer, F.; Böcker, S.; Witting, M. Current state-of-the-art of separation methods used in LC-MS based metabolomics and lipidomics. *J Chromatogr B Analyt Technol Biomed Life Sci* **2022**, *1188*, 123069, doi:10.1016/j.jchromb.2021.123069.
300. Fuertig, R.; Ceci, A.; Camus, S.M.; Bezard, E.; Luippold, A.H.; Hengerer, B. LC-MS/MS-based quantification of kynurenine metabolites, tryptophan, monoamines and neopterin in plasma, cerebrospinal fluid and brain. *Bioanalysis* **2016**, *8*, 1903-1917, doi:10.4155/bio-2016-0111.
301. Walvekar, A.; Rashida, Z.; Maddali, H.; Laxman, S. A versatile LC-MS/MS approach for comprehensive, quantitative analysis of central metabolic pathways. *Wellcome Open Res* **2018**, *3*, 122, doi:10.12688/wellcomeopenres.14832.1.

302. Iqbal, K.; Intemann, T.; Börnhorst, C.; Zhang, J.; Aleksandrova, K. Approaches for harmonization of biomarker data from multiple studies: a narrative methodological review. *AJE Advances: Research in Epidemiology* **2025**, *1*, uuaf005.
303. Ivanovová, E.; Piskláková, B.; Dobešová, D.; Janečková, H.; Foltenová, H.; Kvasnička, A.; Prídavok, M.; Bouchalová, K.; de Sousa, J.; Friedecký, D. Wide metabolite coverage LC-MS/MS assay for the diagnosis of inherited metabolic disorders in urine. *Talanta* **2024**, *271*, 125699, doi:10.1016/j.talanta.2024.125699.
304. Roth, H.E.; Powers, R. Meta-Analysis Reveals Both the Promises and the Challenges of Clinical Metabolomics. *Cancers (Basel)* **2022**, *14*, doi:10.3390/cancers14163992.
305. Sloan, A.; Cheng, C.; Rosner, B.; Ziegler, R.G.; Smith-Warner, S.A.; Wang, M. A repeated measures approach to pooled and calibrated biomarker data. *Biometrics* **2023**, *79*, 1485-1495, doi:10.1111/biom.13618.
306. Rhee, E.P.; Waikar, S.S.; Rebholz, C.M.; Zheng, Z.; Perichon, R.; Clish, C.B.; Evans, A.M.; Avila, J.; Denburg, M.R.; Anderson, A.H.; et al. Variability of Two Metabolomic Platforms in CKD. *Clin J Am Soc Nephrol* **2019**, *14*, 40-48, doi:10.2215/cjn.07070618.
307. Liu, C.; Debnath, N.; Mosoyan, G.; Chauhan, K.; Vasquez-Rios, G.; Soudant, C.; Menez, S.; Parikh, C.R.; Coca, S.G. Systematic Review and Meta-Analysis of Plasma and Urine Biomarkers for CKD Outcomes. *J Am Soc Nephrol* **2022**, *33*, 1657-1672, doi:10.1681/asn.2022010098.
308. Lippa, K.A.; Aristizabal-Henao, J.J.; Beger, R.D.; Bowden, J.A.; Broeckling, C.; Beecher, C.; Clay Davis, W.; Dunn, W.B.; Flores, R.; Goodacre, R.; et al. Reference materials for MS-based untargeted metabolomics and lipidomics: a review by the metabolomics quality assurance and quality control consortium (mQACC). *Metabolomics* **2022**, *18*, 24, doi:10.1007/s11306-021-01848-6.
309. Rehder, C.; Bean, L.J.H.; Bick, D.; Chao, E.; Chung, W.; Das, S.; O'Daniel, J.; Rehm, H.; Shashi, V.; Vincent, L.M. Next-generation sequencing for constitutional variants in the clinical laboratory, 2021 revision: a technical standard of the American College of Medical Genetics and Genomics (ACMG). *Genet Med* **2021**, *23*, 1399-1415, doi:10.1038/s41436-021-01139-4.
310. Broeckling, C.D.; Beger, R.D.; Cheng, L.L.; Cumeras, R.; Cuthbertson, D.J.; Dasari, S.; Davis, W.C.; Dunn, W.B.; Evans, A.M.; Fernández-Ochoa, A.; et al. Current Practices in LC-MS Untargeted Metabolomics: A Scoping Review on the Use of Pooled Quality Control Samples. *Anal Chem* **2023**, *95*, 18645-18654, doi:10.1021/acs.analchem.3c02924.
311. Ou, F.S.; Michiels, S.; Shyr, Y.; Adjei, A.A.; Oberg, A.L. Biomarker Discovery and Validation: Statistical Considerations. *J Thorac Oncol* **2021**, *16*, 537-545, doi:10.1016/j.jtho.2021.01.1616.
312. Mattsson-Carlgren, N.; Palmqvist, S.; Blennow, K.; Hansson, O. Publisher Correction: Increasing the reproducibility of fluid biomarker studies in neurodegenerative studies. *Nat Commun* **2021**, *12*, 196, doi:10.1038/s41467-020-20693-0.
313. Chau, C.H.; Rixe, O.; McLeod, H.; Figg, W.D. Validation of analytic methods for biomarkers used in drug development. *Clin Cancer Res* **2008**, *14*, 5967-5976, doi:10.1158/1078-0432.Ccr-07-4535.
314. Saito, K.; Goda, R.; Arai, K.; Asahina, K.; Kawabata, M.; Uchiyama, H.; Andou, T.; Shimizu, H.; Takahara, K.; Kakehi, M.; et al. Interlaboratory evaluation of LC-MS-based biomarker assays. *Bioanalysis* **2024**, *16*, 389-402, doi:10.4155/bio-2023-0173.
315. Jia, Z.; Qiu, Q.; He, R.; Zhou, T.; Chen, L. Identification of Metabolite Interference Is Necessary for Accurate LC-MS Targeted Metabolomics Analysis. *Anal Chem* **2023**, *95*, 7985-7992, doi:10.1021/acs.analchem.3c00804.
316. Addona, T.A.; Abbatiello, S.E.; Schilling, B.; Skates, S.J.; Mani, D.R.; Bunk, D.M.; Spiegelman, C.H.; Zimmerman, L.J.; Ham, A.J.; Keshishian, H.; et al. Multi-site assessment of the precision and reproducibility of multiple reaction monitoring-based measurements of proteins in plasma. *Nat Biotechnol* **2009**, *27*, 633-641, doi:10.1038/nbt.1546.
317. Thompson, J.W.; Adams, K.J.; Adamski, J.; Asad, Y.; Borts, D.; Bowden, J.A.; Byram, G.; Dang, V.; Dunn, W.B.; Fernandez, F.; et al. International Ring Trial of a High Resolution Targeted Metabolomics and Lipidomics Platform for Serum and Plasma Analysis. *Anal Chem* **2019**, *91*, 14407-14416, doi:10.1021/acs.analchem.9b02908.
318. Fernández-Metzler, C.; Ackermann, B.; Garofolo, F.; Arnold, M.E.; DeSilva, B.; Gu, H.; Laterza, O.; Mao, Y.; Rose, M.; Vazvaei-Smith, F.; et al. Biomarker Assay Validation by Mass Spectrometry. *Aaps j* **2022**, *24*, 66, doi:10.1208/s12248-022-00707-z.

 doi:10.20944/preprints202601.0822.v1

319. Brunius, C.; Shi, L.; Landberg, R. Large-scale untargeted LC-MS metabolomics data correction using between-batch feature alignment and cluster-based within-batch signal intensity drift correction. *Metabolomics* **2016**, *12*, 173, doi:10.1007/s11306-016-1124-4.
320. Wehrens, R.; Hageman, J.A.; van Eeuwijk, F.; Kooke, R.; Flood, P.J.; Wijnker, E.; Keurentjes, J.J.; Lommen, A.; van Eekelen, H.D.; Hall, R.D.; et al. Improved batch correction in untargeted MS-based metabolomics. *Metabolomics* **2016**, *12*, 88, doi:10.1007/s11306-016-1015-8.
321. Malinka, F.; Zareie, A.; Prochazka, J.; Sedlacek, R.; Novosadova, V. Batch alignment via retention orders for preprocessing large-scale multi-batch LC-MS experiments. *Bioinformatics* **2022**, *38*, 3759-3767, doi:10.1093/bioinformatics/btac407.
322. Yao, Y.; Zhang, H.; Tu, L.; Yu, T.; Chen, B.; Huang, P.; Hu, Y.; Luan, T. Normalization Approach by a Reference Material to Improve LC-MS-Based Metabolomic Data Comparability of Multibatch Samples. *Anal Chem* **2023**, *95*, 1309-1317, doi:10.1021/acs.analchem.2c04188.
323. Siegel, D.; Permentier, H.; Reijngoud, D.J.; Bischoff, R. Chemical and technical challenges in the analysis of central carbon metabolites by liquid-chromatography mass spectrometry. *J Chromatogr B Analyt Technol Biomed Life Sci* **2014**, *966*, 21-33, doi:10.1016/j.jchromb.2013.11.022.
324. Jankech, T.; Gerhardtova, I.; Majerova, P.; Piestansky, J.; Jampilek, J.; Kovac, A. Derivatization of carboxylic groups prior to their LC analysis—A review. *Anal Chim Acta* **2024**, *1300*, 342435, doi:10.1016/j.aca.2024.342435.
325. Lu, W.; Clasquin, M.F.; Melamud, E.; Amador-Noguez, D.; Caudy, A.A.; Rabinowitz, J.D. Metabolomic analysis via reversed-phase ion-pairing liquid chromatography coupled to a stand alone orbitrap mass spectrometer. *Anal Chem* **2010**, *82*, 3212-3221, doi:10.1021/ac902837x.
326. Vazquez, S.; Truscott, R.J.; O'Hair, R.A.; Weimann, A.; Sheil, M.M. A study of kynurenine fragmentation using electrospray tandem mass spectrometry. *J Am Soc Mass Spectrom* **2001**, *12*, 786-794, doi:10.1016/s1044-0305(01)00255-0.
327. Kiontke, A.; Oliveira-Birkmeier, A.; Opitz, A.; Birkemeyer, C. Electrospray Ionization Efficiency Is Dependent on Different Molecular Descriptors with Respect to Solvent pH and Instrumental Configuration. *PLoS One* **2016**, *11*, e0167502, doi:10.1371/journal.pone.0167502.
328. Steckel, A.; Schlosser, G. An Organic Chemist's Guide to Electrospray Mass Spectrometric Structure Elucidation. *Molecules* **2019**, *24*, doi:10.3390/molecules24030611.
329. Liigand, J.; Laaniste, A.; Kruve, A. pH Effects on Electrospray Ionization Efficiency. *J Am Soc Mass Spectrom* **2017**, *28*, 461-469, doi:10.1007/s13361-016-1563-1.
330. Hermans, J.; Ongay, S.; Markov, V.; Bischoff, R. Physicochemical Parameters Affecting the Electrospray Ionization Efficiency of Amino Acids after Acylation. *Anal Chem* **2017**, *89*, 9159-9166, doi:10.1021/acs.analchem.7b01899.
331. Ngere, J.B.; Ebrahimi, K.H.; Williams, R.; Pires, E.; Walsby-Tickle, J.; McCullagh, J.S.O. Ion-Exchange Chromatography Coupled to Mass Spectrometry in Life Science, Environmental, and Medical Research. *Anal Chem* **2023**, *95*, 152-166, doi:10.1021/acs.analchem.2c04298.
332. Jang, C.; Chen, L.; Rabinowitz, J.D. Metabolomics and Isotope Tracing. *Cell* **2018**, *173*, 822-837, doi:10.1016/j.cell.2018.03.055.
333. Wang, G.; Kakumanu, R.; Amer, B. Reversed phase LC-MS analysis of organic acids involved in the tricarboxylic acid cycle. **2025**.
334. Ovbude, S.T.; Sharmeen, S.; Kyei, I.; Olupathage, H.; Jones, J.; Bell, R.J.; Powers, R.; Hage, D.S. Applications of chromatographic methods in metabolomics: A review. *J Chromatogr B Analyt Technol Biomed Life Sci* **2024**, *1239*, 124124, doi:10.1016/j.jchromb.2024.124124.
335. Keefer, J.F.; Schuster, S.M. Separation of citric acid cycle intermediates by high-performance liquid chromatography with ion pairing. *J Chromatogr* **1986**, *383*, 297-305, doi:10.1016/s0378-4347(00)83475-1.
336. Tang, D.Q.; Zou, L.; Yin, X.X.; Ong, C.N. HILIC-MS for metabolomics: An attractive and complementary approach to RPLC-MS. *Mass spectrometry reviews* **2016**, *35*, 574-600.
337. Schwaiger, M.; Schoeny, H.; El Abiead, Y.; Hermann, G.; Rampler, E.; Koellensperger, G. Merging metabolomics and lipidomics into one analytical run. *Analyst* **2018**, *144*, 220-229, doi:10.1039/c8an01219a.

338. Hiefner, J.; Rische, J.; Bunders, M.J.; Worthmann, A. A liquid chromatography-tandem mass spectrometry based method for the quantification of adenosine nucleotides and NAD precursors and products in various biological samples. *Front Immunol* **2023**, *14*, 1250762, doi:10.3389/fimmu.2023.1250762.
339. Meinitzer, A.; Tomaschitz, A.; Pilz, S.; Truber, M.; Zechner, G.; Gaksch, M.; Prietl, B.; Treiber, G.; Schwarz, M.; Baranyi, A. Development of a liquid chromatography-mass spectrometry method for the determination of the neurotoxic quinolinic acid in human serum. *Clin Chim Acta* **2014**, *436*, 268-272, doi:10.1016/j.cca.2014.06.010.
340. Tömösi, F.; Kecskeméti, G.; Cseh, E.K.; Szabó, E.; Rajda, C.; Kormány, R.; Szabó, Z.; Vécsei, L.; Janáky, T. A validated UHPLC-MS method for tryptophan metabolites: Application in the diagnosis of multiple sclerosis. *J Pharm Biomed Anal* **2020**, *185*, 113246, doi:10.1016/j.jpba.2020.113246.
341. Brookhart, A.; Arora, M.; McCullagh, M.; Wilson, I.D.; Plumb, R.S.; Vissers, J.P.; Tanna, N. Understanding mobile phase buffer composition and chemical structure effects on electrospray ionization mass spectrometry response. *J Chromatogr A* **2023**, *1696*, 463966, doi:10.1016/j.chroma.2023.463966.
342. Nshanian, M.; Lakshmanan, R.; Chen, H.; Ogorzalek Loo, R.R.; Loo, J.A. Enhancing Sensitivity of Liquid Chromatography-Mass Spectrometry of Peptides and Proteins Using Supercharging Agents. *Int J Mass Spectrom* **2018**, *427*, 157-164, doi:10.1016/j.ijms.2017.12.006.
343. Walter, T.H.; Blaze, M.T.M.; Boissel, C. Electrospray ionization mass spectrometry ion suppression/enhancement caused by column bleed for three mixed-mode reversed-phase/anion-exchange high-performance liquid chromatography columns. *Rapid Commun Mass Spectrom* **2021**, *35*, e9098, doi:10.1002/rcm.9098.
344. Sterling, H.J.; Batchelor, J.D.; Wemmer, D.E.; Williams, E.R. Effects of buffer loading for electrospray ionization mass spectrometry of a noncovalent protein complex that requires high concentrations of essential salts. *J Am Soc Mass Spectrom* **2010**, *21*, 1045-1049, doi:10.1016/j.jasms.2010.02.003.
345. Zheng, J.J.; Lynch, E.D.; Unger, S.E. Comparison of SPE and fast LC to eliminate mass spectrometric matrix effects from microsomal incubation products. *J Pharm Biomed Anal* **2002**, *28*, 279-285, doi:10.1016/s0731-7085(01)00562-3.
346. Rakusanova, S.; Cajka, T. Tips and tricks for LC–MS-based metabolomics and lipidomics analysis. *TrAC Trends in Analytical Chemistry* **2024**, *180*, 117940.
347. Silvester, S. Mobile phase pH and organic modifier in reversed-phase LC-ESI-MS bioanalytical methods: assessment of sensitivity, chromatography and correlation of retention time with in silico logD predictions. *Bioanalysis* **2013**, *5*, 2753-2770, doi:10.4155/bio.13.250.
348. Liigand, J.; de Vries, R.; Cuyckens, F. Optimization of flow splitting and make-up flow conditions in liquid chromatography/electrospray ionization mass spectrometry. *Rapid Commun Mass Spectrom* **2019**, *33*, 314-322, doi:10.1002/rcm.8352.
349. Heinisch, S.; Rocca, J. Effect of mobile phase composition, pH and buffer type on the retention of ionizable compounds in reversed-phase liquid chromatography: application to method development. *Journal of Chromatography A* **2004**, *1048*, 183-193.
350. Liigand, P.; Kaupmees, K.; Haav, K.; Liigand, J.; Leito, I.; Girod, M.; Antoine, R.; Kruve, A. Think Negative: Finding the Best Electrospray Ionization/MS Mode for Your Analyte. *Anal Chem* **2017**, *89*, 5665-5668, doi:10.1021/acs.analchem.7b00096.
351. Henriksen, T.; Juhler, R.K.; Svensmark, B.; Cech, N.B. The relative influences of acidity and polarity on responsiveness of small organic molecules to analysis with negative ion electrospray ionization mass spectrometry (ESI-MS). *J Am Soc Mass Spectrom* **2005**, *16*, 446-455, doi:10.1016/j.jasms.2004.11.021.
352. Venter, P. The Effects of Solvation Enthalpy, Surface Tension, and Conductivity of Common Additives on Positive Electrospray Ionization in Selected Pharmaceuticals. *Molecules* **2025**, *30*, doi:10.3390/molecules30091885.
353. Han, J.; Gagnon, S.; Eckle, T.; Borchers, C.H. Metabolomic analysis of key central carbon metabolism carboxylic acids as their 3-nitrophenylhydrazones by UPLC/ESI-MS. *Electrophoresis* **2013**, *34*, 2891-2900, doi:10.1002/elps.201200601.

354. Huang, Y.; Louie, A.; Yang, Q.; Massenkoff, N.; Xu, C.; Hunt, P.W.; Gee, W. A simple LC-MS/MS method for determination of kynurenine and tryptophan concentrations in human plasma from HIV-infected patients. *Bioanalysis* **2013**, *5*, 1397-1407, doi:10.4155/bio.13.74.
355. Breitkopf, S.B.; Ricoult, S.J.H.; Yuan, M.; Xu, Y.; Peake, D.A.; Manning, B.D.; Asara, J.M. A relative quantitative positive/negative ion switching method for untargeted lipidomics via high resolution LC-MS/MS from any biological source. *Metabolomics* **2017**, *13*, doi:10.1007/s11306-016-1157-8.
356. Cai, R.; Mikkilä, J.; Bengs, A.; Koirala, M.; Mikkilä, J.; Holm, S.; Juuti, P.; Meder, M.; Partovi, F.; Shcherbinin, A.; et al. Extending the Range of Detectable Trace Species with the Fast Polarity Switching of Chemical Ionization Orbitrap Mass Spectrometry. *Anal Chem* **2024**, *96*, 8604-8612, doi:10.1021/acs.analchem.4c00650.
357. Yuan, M.; Breitkopf, S.B.; Yang, X.; Asara, J.M. A positive/negative ion-switching, targeted mass spectrometry-based metabolomics platform for bodily fluids, cells, and fresh and fixed tissue. *Nat Protoc* **2012**, *7*, 872-881, doi:10.1038/nprot.2012.024.
358. Kluger, B.; Bueschl, C.; Neumann, N.; Stückler, R.; Doppler, M.; Chassy, A.W.; Waterhouse, A.L.; Rechthaler, J.; Kampleitner, N.; Thallinger, G.G.; et al. Untargeted profiling of tracer-derived metabolites using stable isotopic labeling and fast polarity-switching LC-ESI-HRMS. *Anal Chem* **2014**, *86*, 11533-11537, doi:10.1021/ac503290j.
359. Zherebker, A.; Kostyukevich, Y.; Kononikhin, A.; Roznyatovsky, V.A.; Popov, I.; Grishin, Y.K.; Perminova, I.V.; Nikolaev, E. High desolvation temperature facilitates the ESI-source H/D exchange at non-labile sites of hydroxybenzoic acids and aromatic amino acids. *Analyst* **2016**, *141*, 2426-2434, doi:10.1039/c5an02676h.
360. Paíga, P.; Silva, L.M.; Delerue-Matos, C. Optimization of the Ion Source-Mass Spectrometry Parameters in Non-Steroidal Anti-Inflammatory and Analgesic Pharmaceuticals Analysis by a Design of Experiments Approach. *J Am Soc Mass Spectrom* **2016**, *27*, 1703-1714, doi:10.1007/s13361-016-1459-0.
361. Pedro, L.; Van Voorhis, W.C.; Quinn, R.J. Optimization of Electrospray Ionization by Statistical Design of Experiments and Response Surface Methodology: Protein-Ligand Equilibrium Dissociation Constant Determinations. *J Am Soc Mass Spectrom* **2016**, *27*, 1520-1530, doi:10.1007/s13361-016-1417-x.
362. Prothmann, J.; Molins-Delgado, D.; Braune, A.; Sandahl, M.; Turner, C.; Spégel, P. Examining functional group-dependent effects on the ionization of lignin monomers using supercritical fluid chromatography/electrospray ionization mass spectrometry. *Anal Bioanal Chem* **2024**, *416*, 4007-4014, doi:10.1007/s00216-024-05358-x.
363. Kruve, A.; Kaupmees, K. Adduct Formation in ESI/MS by Mobile Phase Additives. *J Am Soc Mass Spectrom* **2017**, *28*, 887-894, doi:10.1007/s13361-017-1626-y.
364. Flick, T.G.; Merenbloom, S.I.; Williams, E.R. Anion effects on sodium ion and acid molecule adduction to protein ions in electrospray ionization mass spectrometry. *J Am Soc Mass Spectrom* **2011**, *22*, 1968-1977, doi:10.1007/s13361-011-0218-5.
365. Carnevale Neto, F.; Pascua, V.; Raftery, D. Formation of sodium cluster ions complicates liquid chromatography-mass spectrometry metabolomics analyses. *Rapid Commun Mass Spectrom* **2021**, *35*, e9175, doi:10.1002/rcm.9175.
366. Mortier, K.A.; Zhang, G.F.; van Peteghem, C.H.; Lambert, W.E. Adduct formation in quantitative bioanalysis: effect of ionization conditions on paclitaxel. *J Am Soc Mass Spectrom* **2004**, *15*, 585-592, doi:10.1016/j.jasms.2003.12.013.
367. Stricker, T.; Bonner, R.; Lisacek, F.; Hopfgartner, G. Adduct annotation in liquid chromatography/high-resolution mass spectrometry to enhance compound identification. *Anal Bioanal Chem* **2021**, *413*, 503-517, doi:10.1007/s00216-020-03019-3.
368. Birdsall, R.E.; Gilar, M.; Shion, H.; Yu, Y.Q.; Chen, W. Reduction of metal adducts in oligonucleotide mass spectra in ion-pair reversed-phase chromatography/mass spectrometry analysis. *Rapid Commun Mass Spectrom* **2016**, *30*, 1667-1679, doi:10.1002/rcm.7596.
369. Erngren, I.; Nestor, M.; Pettersson, C.; Hedeland, M. Improved Sensitivity in Hydrophilic Interaction Liquid Chromatography-Electrospray-Mass Spectrometry after Removal of Sodium and Potassium Ions from Biological Samples. *Metabolites* **2021**, *11*, doi:10.3390/metabo11030170.
370. Nash, W.J.; Ngere, J.B.; Najdekr, L.; Dunn, W.B. Characterization of Electrospray Ionization Complexity in Untargeted Metabolomic Studies. *Anal Chem* **2024**, *96*, 10935-10942, doi:10.1021/acs.analchem.4c00966.

371. Erngren, I.; Haglöf, J.; Engskog, M.K.R.; Nestor, M.; Hedeland, M.; Arvidsson, T.; Pettersson, C. Adduct formation in electrospray ionisation-mass spectrometry with hydrophilic interaction liquid chromatography is strongly affected by the inorganic ion concentration of the samples. *J Chromatogr A* **2019**, *1600*, 174-182, doi:10.1016/j.chroma.2019.04.049.
372. Stokvis, E.; Rosing, H.; Beijnen, J.H. Stable isotopically labeled internal standards in quantitative bioanalysis using liquid chromatography/mass spectrometry: necessity or not? *Rapid Commun Mass Spectrom* **2005**, *19*, 401-407, doi:10.1002/rcm.1790.
373. Kapoore, R.V.; Vaidyanathan, S. Towards quantitative mass spectrometry-based metabolomics in microbial and mammalian systems. *Philos Trans A Math Phys Eng Sci* **2016**, *374*, doi:10.1098/rsta.2015.0363.
374. Liigand, P.; Liigand, J.; Kaupmees, K.; Kruve, A. 30 Years of research on ESI/MS response: Trends, contradictions and applications. *Anal Chim Acta* **2021**, *1152*, 238117, doi:10.1016/j.aca.2020.11.049.
375. Chen, F.; Willenbockel, H.F.; Cordes, T. Mapping the Metabolic Niche of Citrate Metabolism and SLC13A5. *Metabolites* **2023**, *13*, doi:10.3390/metabo13030331.
376. Dankel, S.N.; Kalleklev, T.L.; Tungland, S.L.; Stafsnes, M.H.; Bruheim, P.; Aloysius, T.A.; Lindquist, C.; Skorve, J.; Nygård, O.K.; Madsen, L.; et al. Changes in Plasma Pyruvate and TCA Cycle Metabolites upon Increased Hepatic Fatty Acid Oxidation and Ketogenesis in Male Wistar Rats. *Int J Mol Sci* **2023**, *24*, doi:10.3390/ijms242115536.
377. Stone, T.W.; Darlington, L.G.; Badawy, A.A.; Williams, R.O. The Complex World of Kynurenic Acid: Reflections on Biological Issues and Therapeutic Strategy. *Int J Mol Sci* **2024**, *25*, doi:10.3390/ijms25169040.
378. Tang, K.; Page, J.S.; Smith, R.D. Charge competition and the linear dynamic range of detection in electrospray ionization mass spectrometry. *J Am Soc Mass Spectrom* **2004**, *15*, 1416-1423, doi:10.1016/j.jasms.2004.04.034.
379. Bruin, M.A.C.; Rosing, H.; Lucas, L.; Wang, J.; Huitema, A.D.R.; Schinkel, A.H.; Beijnen, J.H. Development and validation of an LC-MS/MS method with a broad linear dynamic range for the quantification of tivozanib in human and mouse plasma, mouse tissue homogenates, and culture medium. *J Chromatogr B Analyt Technol Biomed Life Sci* **2019**, *1125*, 121723, doi:10.1016/j.jchromb.2019.121723.
380. Liu, X.; Ser, Z.; Locasale, J.W. Development and quantitative evaluation of a high-resolution metabolomics technology. *Anal Chem* **2014**, *86*, 2175-2184, doi:10.1021/ac403845u.
381. Sands, C.J.; Gómez-Romero, M.; Correia, G.; Chekmeneva, E.; Camuzeaux, S.; Izzi-Engbeaya, C.; Dhillo, W.S.; Takats, Z.; Lewis, M.R. Representing the Metabolome with High Fidelity: Range and Response as Quality Control Factors in LC-MS-Based Global Profiling. *Anal Chem* **2021**, *93*, 1924-1933, doi:10.1021/acs.analchem.0c03848.
382. Annesley, T.M. Ion suppression in mass spectrometry. *Clin Chem* **2003**, *49*, 1041-1044, doi:10.1373/49.7.1041.
383. Cech, N.B.; Enke, C.G. Practical implications of some recent studies in electrospray ionization fundamentals. *Mass Spectrom Rev* **2001**, *20*, 362-387, doi:10.1002/mas.10008.
384. King, R.; Bonfiglio, R.; Fernandez-Metzler, C.; Miller-Stein, C.; Olah, T. Mechanistic investigation of ionization suppression in electrospray ionization. *J Am Soc Mass Spectrom* **2000**, *11*, 942-950, doi:10.1016/s1044-0305(00)00163-x.
385. Wu, Z.; Gao, W.; Phelps, M.A.; Wu, D.; Miller, D.D.; Dalton, J.T. Favorable effects of weak acids on negative-ion electrospray ionization mass spectrometry. *Anal Chem* **2004**, *76*, 839-847, doi:10.1021/ac0351670.
386. Cheng, W.L.; Markus, C.; Lim, C.Y.; Tan, R.Z.; Sethi, S.K.; Loh, T.P. Calibration Practices in Clinical Mass Spectrometry: Review and Recommendations. *Ann Lab Med* **2023**, *43*, 5-18, doi:10.3343/alm.2023.43.1.5.
387. Jeanne Dit Fouque, D.; Maroto, A.; Memboeuf, A. Internal Standard Quantification Using Tandem Mass Spectrometry of a Tryptic Peptide in the Presence of an Isobaric Interference. *Anal Chem* **2018**, *90*, 14126-14130, doi:10.1021/acs.analchem.8b05016.
388. Tkalec, Ž.; Koudelka, Š.; Klánová, J.; Price, E.J. Dual LC column characterization for mass spectrometry-based small molecule profiling of human plasma and serum. *Anal Chim Acta* **2025**, *1356*, 343942, doi:10.1016/j.aca.2025.343942.
389. Wuli, W.; Tsai, S.T.; Chiou, T.W.; Harn, H.J. Human-Induced Pluripotent Stem Cells and Herbal Small-Molecule Drugs for Treatment of Alzheimer's Disease. *Int J Mol Sci* **2020**, *21*, doi:10.3390/ijms21041327.

 doi:10.20944/preprints202601.0822.v1

390. Zhang, T.; Noll, S.E.; Peng, J.T.; Klair, A.; Tripka, A.; Stutzman, N.; Cheng, C.; Zare, R.N.; Dickinson, A.J. Chemical imaging reveals diverse functions of tricarboxylic acid metabolites in root growth and development. *Nat Commun* **2023**, *14*, 2567, doi:10.1038/s41467-023-38150-z.
391. Vass, A.; Robles-Molina, J.; Pérez-Ortega, P.; Gilbert-López, B.; Dernovics, M.; Molina-Díaz, A.; García-Reyes, J.F. Study of different HILIC, mixed-mode, and other aqueous normal-phase approaches for the liquid chromatography/mass spectrometry-based determination of challenging polar pesticides. *Anal Bioanal Chem* **2016**, *408*, 4857-4869, doi:10.1007/s00216-016-9589-6.
392. Buszewski, B.; Noga, S. Hydrophilic interaction liquid chromatography (HILIC)--a powerful separation technique. *Anal Bioanal Chem* **2012**, *402*, 231-247, doi:10.1007/s00216-011-5308-5.
393. Kohler, I.; Verhoeven, M.; Haselberg, R.; Gargano, A.F. Hydrophilic interaction chromatography–mass spectrometry for metabolomics and proteomics: state-of-the-art and current trends. *Microchemical Journal* **2022**, *175*, 106986.
394. Zhang, K.; Liu, X. Mixed-mode chromatography in pharmaceutical and biopharmaceutical applications. *J Pharm Biomed Anal* **2016**, *128*, 73-88, doi:10.1016/j.jpba.2016.05.007.
395. Iwasaki, Y.; Sawada, T.; Hatayama, K.; Ohyagi, A.; Tsukuda, Y.; Namekawa, K.; Ito, R.; Saito, K.; Nakazawa, H. Separation technique for the determination of highly polar metabolites in biological samples. *Metabolites* **2012**, *2*, 496-515, doi:10.3390/metabo2030496.
396. Chapel, S.; Rouvière, F.; Guillarme, D.; Heinisch, S. Reversed HILIC Gradient: A Powerful Strategy for On-Line Comprehensive 2D-LC. *Molecules* **2023**, *28*, doi:10.3390/molecules28093907.
397. Grübner, M.; Dunkel, A.; Steiner, F.; Hofmann, T. Comparative evaluation of comprehensive offline 2D-LC strategies coupled to MS for untargeted metabolomic studies of human urine. *Anal Bioanal Chem* **2025**, doi:10.1007/s00216-025-06195-2.
398. Papatheocharidou, C.; Samanidou, V. Two-Dimensional High-Performance Liquid Chromatography as a Powerful Tool for Bioanalysis: The Paradigm of Antibiotics. *Molecules* **2023**, *28*, doi:10.3390/molecules28135056.
399. Aly, A.A.; Górecki, T. Two-dimensional liquid chromatography with reversed phase in both dimensions: A review. *J Chromatogr A* **2024**, *1721*, 464824, doi:10.1016/j.chroma.2024.464824.
400. Lu, Y.; Qin, Q.; Pan, J.; Deng, S.; Wang, S.; Li, Q.; Cao, J. Advanced applications of two-dimensional liquid chromatography in quantitative analysis of natural products. *J Chromatogr A* **2025**, *1743*, 465662, doi:10.1016/j.chroma.2025.465662.
401. Ortmayr, K.; Hann, S.; Koellensperger, G. Complementing reversed-phase selectivity with porous graphitized carbon to increase the metabolome coverage in an on-line two-dimensional LC-MS setup for metabolomics. *Analyst* **2015**, *140*, 3465-3473, doi:10.1039/c5an00206k.
402. Willemse, C.M.; Stander, M.A.; Tredoux, A.G.; de Villiers, A. Comprehensive two-dimensional liquid chromatographic analysis of anthocyanins. *J Chromatogr A* **2014**, *1359*, 189-201, doi:10.1016/j.chroma.2014.07.044.
403. Nell, E.H.J.; Muller, M.; de Villiers, A. Advances in Online Comprehensive Two-Dimensional Liquid Chromatography Method Development. *Annu Rev Anal Chem (Palo Alto Calif)* **2025**, *18*, 359-381, doi:10.1146/annurev-anchem-071524-090321.
404. Pardon, M.; Reis, R.; de Witte, P.; Chapel, S.; Cabooter, D. Detailed comparison of in-house developed and commercially available heart-cutting and selective comprehensive two-dimensional liquid chromatography systems. *J Chromatogr A* **2024**, *1713*, 464565, doi:10.1016/j.chroma.2023.464565.
405. Malerod, H.; Lundanes, E.; Greibrokk, T. Recent advances in on-line multidimensional liquid chromatography. *Analytical Methods* **2010**, *2*, 110-122.
406. Wernisch, S.; Pennathur, S. Evaluation of coverage, retention patterns, and selectivity of seven liquid chromatographic methods for metabolomics. *Anal Bioanal Chem* **2016**, *408*, 6079-6091, doi:10.1007/s00216-016-9716-4.
407. Aarika, K.; Rajyalakshmi, R.; Nalla, L.V.; Gajula, S.N.R. From complexity to clarity: expanding metabolome coverage with innovative analytical strategies. *Journal of Separation Science* **2025**, *48*, e70099.

 doi:10.20944/preprints202601.0822.v1

408. Xu, K.; Berthiller, F.; Metzler-Zebeli, B.U.; Schwartz-Zimmermann, H.E. Development and Validation of Targeted Metabolomics Methods Using Liquid Chromatography-Tandem Mass Spectrometry (LC-MS/MS) for the Quantification of 235 Plasma Metabolites. *Molecules* **2025**, *30*, doi:10.3390/molecules30030706.
409. Basov, N.V.; Rogachev, A.D.; Aleshkova, M.A.; Gaisler, E.V.; Sotnikova, Y.S.; Patrushev, Y.V.; Tolstikova, T.G.; Yarovaya, O.I.; Pokrovsky, A.G.; Salakhutdinov, N.F. Global LC-MS/MS targeted metabolomics using a combination of HILIC and RP LC separation modes on an organic monolithic column based on 1-vinyl-1,2,4-triazole. *Talanta* **2024**, *267*, 125168, doi:10.1016/j.talanta.2023.125168.
410. Lu, W.; Bennett, B.D.; Rabinowitz, J.D. Analytical strategies for LC-MS-based targeted metabolomics. *J Chromatogr B Analyt Technol Biomed Life Sci* **2008**, *871*, 236-242, doi:10.1016/j.jchromb.2008.04.031.
411. Gamoh, K.; Saitoh, H.; Wada, H. Improved liquid chromatography/mass spectrometric analysis of low molecular weight carboxylic acids by ion exclusion separation with electrospray ionization. *Rapid communications in mass spectrometry* **2003**, *17*, 685-689.
412. Zeki Ö, C.; Eylem, C.C.; Nemutlu, E. Optimization of GC-MS run time for untargeted metabolomics: Trade-offs between speed, coverage, and repeatability. *J Pharm Biomed Anal* **2025**, *266*, 117068, doi:10.1016/j.jpba.2025.117068.
413. Pinto, F.G.; Giddey, A.D.; Mohamed, N.; Almarri, R.S.B.; Murtaza, M.; Nassir, N.; Alkhnbashi, O.S.; Uddin, M.J.; Soares, N.C. Repurposing proteomic nanoLC-MS platforms for untargeted metabolomics: evaluating DIA and polarity switching performance in human plasma. *Expert Rev Proteomics* **2025**, *22*, 307-314, doi:10.1080/14789450.2025.2537210.
414. Skogvold, H.B.; Sandås, E.M.; Østeby, A.; Løkken, C.; Rootwelt, H.; Rønning, P.O.; Wilson, S.R.; Elgstøen, K.B.P. Bridging the Polar and Hydrophobic Metabolome in Single-Run Untargeted Liquid Chromatography-Mass Spectrometry Dried Blood Spot Metabolomics for Clinical Purposes. *J Proteome Res* **2021**, *20*, 4010-4021, doi:10.1021/acs.jproteome.1c00326.
415. Gika, H.G.; Theodoridis, G.A.; Vrhovsek, U.; Mattivi, F. Quantitative profiling of polar primary metabolites using hydrophilic interaction ultrahigh performance liquid chromatography-tandem mass spectrometry. *J Chromatogr A* **2012**, *1259*, 121-127, doi:10.1016/j.chroma.2012.02.010.
416. Violi, J.P.; Phillips, C.R.; Gertner, D.S.; Westerhausen, M.T.; Padula, M.P.; Bishop, D.P.; Rodgers, K.J. Comprehensive untargeted polar metabolite analysis using solvent switching liquid chromatography tandem mass spectrometry. *Talanta* **2025**, *287*, 127610, doi:10.1016/j.talanta.2025.127610.
417. Chen, L.; Zhong, F.; Zhu, J. Bridging Targeted and Untargeted Mass Spectrometry-Based Metabolomics via Hybrid Approaches. *Metabolites* **2020**, *10*, doi:10.3390/metabo10090348.
418. Cochran, D.; NourEldein, M.; Bezdekova, D.; Schram, A.; Howard, R.; Powers, R. A Reproducibility Crisis for Clinical Metabolomics Studies. *Trends Analyt Chem* **2024**, *180*, doi:10.1016/j.trac.2024.117918.
419. Ivanisevic, J.; Zhu, Z.J.; Plate, L.; Tautenhahn, R.; Chen, S.; O'Brien, P.J.; Johnson, C.H.; Marletta, M.A.; Patti, G.J.; Siuzdak, G. Toward 'omic scale metabolite profiling: a dual separation-mass spectrometry approach for coverage of lipid and central carbon metabolism. *Anal Chem* **2013**, *85*, 6876-6884, doi:10.1021/ac401140h.
420. Arrivault, S.; Guenther, M.; Fry, S.C.; Fuenfgeld, M.M.; Veyel, D.; Mettler-Altmann, T.; Stitt, M.; Lunn, J.E. Synthesis and Use of Stable-Isotope-Labeled Internal Standards for Quantification of Phosphorylated Metabolites by LC-MS/MS. *Anal Chem* **2015**, *87*, 6896-6904, doi:10.1021/acs.analchem.5b01387.
421. Ulvik, A.; McCann, A.; Midttun, Ø.; Meyer, K.; Godfrey, K.M.; Ueland, P.M. Quantifying Precision Loss in Targeted Metabolomics Based on Mass Spectrometry and Nonmatching Internal Standards. *Anal Chem* **2021**, *93*, 7616-7624, doi:10.1021/acs.analchem.1c00119.
422. Mahmud, I.; Wei, B.; Veillon, L.; Tan, L.; Martinez, S.; Tran, B.; Raskind, A.; de Jong, F.; Liu, Y.; Ding, J.; et al. Ion suppression correction and normalization for non-targeted metabolomics. *Nat Commun* **2025**, *16*, 1347, doi:10.1038/s41467-025-56646-8.
423. Ćeranić, A.; Bueschl, C.; Doppler, M.; Parich, A.; Xu, K.; Lemmens, M.; Buerstmayr, H.; Schuhmacher, R. Enhanced Metabolome Coverage and Evaluation of Matrix Effects by the Use of Experimental-Condition-Matched (13)C-Labeled Biological Samples in Isotope-Assisted LC-HRMS Metabolomics. *Metabolites* **2020**, *10*, doi:10.3390/metabo10110434.
424. Bueschl, C.; Krska, R.; Kluger, B.; Schuhmacher, R. Isotopic labeling-assisted metabolomics using LC-MS. *Anal Bioanal Chem* **2013**, *405*, 27-33, doi:10.1007/s00216-012-6375-y.

425. Bruheim, P.; Kvitvang, H.F.; Villas-Boas, S.G. Stable isotope coded derivatizing reagents as internal standards in metabolite profiling. *J Chromatogr A* **2013**, *1296*, 196-203, doi:10.1016/j.chroma.2013.03.072.
426. Zhao, S. Development and Application of Chemical Isotope Labeling Methods and Metabolite Identification Solution for Liquid Chromatography-Mass Spectrometry-Based Metabolomics. **2018**.
427. Mathon, C.; Bovard, D.; Dutertre, Q.; Sendyk, S.; Bentley, M.; Hoeng, J.; Knorr, A. Impact of sample preparation upon intracellular metabolite measurements in 3D cell culture systems. *Metabolomics* **2019**, *15*, 92, doi:10.1007/s11306-019-1551-0.
428. Sysi-Aho, M.; Katajamaa, M.; Yetukuri, L.; Oresic, M. Normalization method for metabolomics data using optimal selection of multiple internal standards. *BMC Bioinformatics* **2007**, *8*, 93, doi:10.1186/1471-2105-8-93.
429. Boysen, A.K.; Heal, K.R.; Carlson, L.T.; Ingalls, A.E. Best-Matched Internal Standard Normalization in Liquid Chromatography-Mass Spectrometry Metabolomics Applied to Environmental Samples. *Anal Chem* **2018**, *90*, 1363-1369, doi:10.1021/acs.analchem.7b04400.
430. Wu, Y.; Li, L. Sample normalization methods in quantitative metabolomics. *J Chromatogr A* **2016**, *1430*, 80-95, doi:10.1016/j.chroma.2015.12.007.
431. Gu, H.; Zhao, Y.; DeMichele, M.; Zheng, N.; Zhang, Y.J.; Pillutla, R.; Zeng, J. In-Sample Calibration Curve Using Multiple Isotopologue Reaction Monitoring of a Stable Isotopically Labeled Analyte for Instant LC-MS/MS Bioanalysis and Quantitative Proteomics. *Anal Chem* **2019**, *91*, 2536-2543, doi:10.1021/acs.analchem.8b05656.
432. Mani, D.R.; Abbatiello, S.E.; Carr, S.A. Statistical characterization of multiple-reaction monitoring mass spectrometry (MRM-MS) assays for quantitative proteomics. *BMC Bioinformatics* **2012**, *13 Suppl 16*, S9, doi:10.1186/1471-2105-13-s16-s9.
433. Beger, R.D.; Goodacre, R.; Jones, C.M.; Lippa, K.A.; Mayboroda, O.A.; O'Neill, D.; Najdekr, L.; Ntai, I.; Wilson, I.D.; Dunn, W.B. Analysis types and quantification methods applied in UHPLC-MS metabolomics research: a tutorial. *Metabolomics* **2024**, *20*, 95, doi:10.1007/s11306-024-02155-6.
434. Verhaeghe, T. Systematic internal standard variability and issue resolution: two case studies. *Bioanalysis* **2019**, *11*, 1685-1692, doi:10.4155/bio-2019-0165.
435. Liao, H.W.; Cheng, Y.W.; Tang, S.C.; Kuo, C.H. Bias caused by incomplete metabolite extraction and matrix effect: Evaluation of critical factors for plasma sample preparation prior to metabolomics. *J Pharm Biomed Anal* **2022**, *219*, 114930, doi:10.1016/j.jpba.2022.114930.
436. Gao, S.; Wang, X.; Huang, J.; Zhu, Y.; Zhang, R.; He, J.; Abliz, Z. Development and validation of a sensitive and reliable targeted metabolomics method for the quantification of cardiovascular disease-related biomarkers in plasma using ultrahigh-performance liquid chromatography-tandem mass spectrometry. *Rapid Commun Mass Spectrom* **2022**, *36*, e9292, doi:10.1002/rcm.9292.
437. Begou, O.; Gika, H.G.; Theodoridis, G.A.; Wilson, I.D. Quality Control and Validation Issues in LC-MS Metabolomics. *Methods Mol Biol* **2018**, *1738*, 15-26, doi:10.1007/978-1-4939-7643-0_2.
438. González-Domínguez, Á.; Estanyol-Torres, N.; Brunius, C.; Landberg, R.; González-Domínguez, R. QComics: Recommendations and Guidelines for Robust, Easily Implementable and Reportable Quality Control of Metabolomics Data. *Anal Chem* **2024**, *96*, 1064-1072, doi:10.1021/acs.analchem.3c03660.
439. Li, S.; Looby, N.; Chandran, V.; Kulasingam, V. Challenges in the Metabolomics-Based Biomarker Validation Pipeline. *Metabolites* **2024**, *14*, doi:10.3390/metabo14040200.
440. Furlanello, T.; Bertolini, F.M.; Zoia, A.; Sanchez Del Pulgar, J.; Masti, R. Establishment and Validation of Sensitive Liquid Chromatography-Tandem Mass Spectrometry Method for Aldosterone Quantification in Feline Serum with Reference Interval Determination. *Animals (Basel)* **2025**, *15*, doi:10.3390/ani15121687.
441. Brêtas, J.M.; César, I.C.; Brêtas, C.M.; Teixeira Lde, S.; Bellorio, K.B.; Mundim, I.M.; Pianetti, G.A. Development and validation of an LC-ESI-MS/MS method for the simultaneous quantification of naproxen and sumatriptan in human plasma: application to a pharmacokinetic study. *Anal Bioanal Chem* **2016**, *408*, 3981-3992, doi:10.1007/s00216-016-9488-x.
442. Prakash, K.; Adiki, S.K.; Kalakuntla, R.R. Development and validation of a liquid chromatography-mass spectrometry method for the determination of zileuton in human plasma. *Sci Pharm* **2014**, *82*, 571-583, doi:10.3797/scipharm.1402-19.

443. Nandania, J.; Peddinti, G.; Pessia, A.; Kokkonen, M.; Velagapudi, V. Validation and Automation of a High-Throughput Multitargeted Method for Semiquantification of Endogenous Metabolites from Different Biological Matrices Using Tandem Mass Spectrometry. *Metabolites* **2018**, *8*, doi:10.3390/metabo8030044.
444. Godoy, A.T.; Eberlin, M.N.; Simionato, A.V.C. Targeted metabolomics: Liquid chromatography coupled to mass spectrometry method development and validation for the identification and quantitation of modified nucleosides as putative cancer biomarkers. *Talanta* **2020**, *210*, 120640, doi:10.1016/j.talanta.2019.120640.
445. Luo, B.; Groenke, K.; Takors, R.; Wandrey, C.; Oldiges, M. Simultaneous determination of multiple intracellular metabolites in glycolysis, pentose phosphate pathway and tricarboxylic acid cycle by liquid chromatography-mass spectrometry. *J Chromatogr A* **2007**, *1147*, 153-164, doi:10.1016/j.chroma.2007.02.034.
446. Matuszewski, B.K.; Constanzer, M.L.; Chavez-Eng, C.M. Strategies for the assessment of matrix effect in quantitative bioanalytical methods based on HPLC-MS/MS. *Anal Chem* **2003**, *75*, 3019-3030, doi:10.1021/ac020361s.
447. Steiner, D.; Krska, R.; Malachová, A.; Taschl, I.; Sulyok, M. Evaluation of Matrix Effects and Extraction Efficiencies of LC-MS/MS Methods as the Essential Part for Proper Validation of Multiclass Contaminants in Complex Feed. *J Agric Food Chem* **2020**, *68*, 3868-3880, doi:10.1021/acs.jafc.9b07706.
448. Cortese, M.; Gigliobianco, M.R.; Magnoni, F.; Censi, R.; Di Martino, P.D. Compensate for or Minimize Matrix Effects? Strategies for Overcoming Matrix Effects in Liquid Chromatography-Mass Spectrometry Technique: A Tutorial Review. *Molecules* **2020**, *25*, doi:10.3390/molecules25133047.
449. Taylor, P.J. Matrix effects: the Achilles heel of quantitative high-performance liquid chromatography-electrospray-tandem mass spectrometry. *Clin Biochem* **2005**, *38*, 328-334, doi:10.1016/j.clinbiochem.2004.11.007.
450. Gika, H.G.; Theodoridis, G.A.; Wilson, I.D. Liquid chromatography and ultra-performance liquid chromatography-mass spectrometry fingerprinting of human urine: sample stability under different handling and storage conditions for metabonomics studies. *J Chromatogr A* **2008**, *1189*, 314-322, doi:10.1016/j.chroma.2007.10.066.
451. van de Merbel, N.; Savoie, N.; Yadav, M.; Ohtsu, Y.; White, J.; Riccio, M.F.; Dong, K.; de Vries, R.; Diancin, J. Stability: recommendation for best practices and harmonization from the Global Bioanalysis Consortium Harmonization Team. *Aaps j* **2014**, *16*, 392-399, doi:10.1208/s12248-014-9573-z.
452. Briscoe, C. Assessing stability in bioanalysis: reflections on the last 10 years. *Bioanalysis* **2019**, *11*, 579-582, doi:10.4155/bio-2019-0043.
453. Eilertsen, H.C.; Huseby, S.; Degerlund, M.; Eriksen, G.K.; Ingebrigtsen, R.A.; Hansen, E. The effect of freeze/thaw cycles on reproducibility of metabolic profiling of marine microalgal extracts using direct infusion high-resolution mass spectrometry (HR-MS). *Molecules* **2014**, *19*, 16373-16380, doi:10.3390/molecules191016373.
454. Lee, J.E.; Kim, S.Y.; Shin, S.Y. Effect of Repeated Freezing and Thawing on Biomarker Stability in Plasma and Serum Samples. *Osong Public Health Res Perspect* **2015**, *6*, 357-362, doi:10.1016/j.phrp.2015.11.005.
455. Tiwari, G.; Tiwari, R. Bioanalytical method validation: An updated review. *Pharm Methods* **2010**, *1*, 25-38, doi:10.4103/2229-4708.72226.
456. Theodorsson, E.; Magnusson, B. Full method validation in clinical chemistry. *Accreditation and Quality Assurance* **2017**, *22*, 235-246.
457. Gika, H.G.; Theodoridis, G.A.; Earll, M.; Wilson, I.D. A QC approach to the determination of day-to-day reproducibility and robustness of LC-MS methods for global metabolite profiling in metabonomics/metabolomics. *Bioanalysis* **2012**, *4*, 2239-2247, doi:10.4155/bio.12.212.
458. Hoffman, D. Statistical considerations for assessment of bioanalytical incurred sample reproducibility. *Aaps j* **2009**, *11*, 570-580, doi:10.1208/s12248-009-9134-z.
459. Ermer, J. Validation in pharmaceutical analysis. Part I: an integrated approach. *J Pharm Biomed Anal* **2001**, *24*, 755-767, doi:10.1016/s0731-7085(00)00530-6.
460. Verch, T.; Campa, C.; Chéry, C.C.; Frenkel, R.; Graul, T.; Jaya, N.; Nakhle, B.; Springall, J.; Starkey, J.; Wypych, J.; et al. Analytical Quality by Design, Life Cycle Management, and Method Control. *Aaps j* **2022**, *24*, 34, doi:10.1208/s12248-022-00685-2.

461. Paglia, G.; Astarita, G. A High-Throughput HILIC-MS-Based Metabolomic Assay for the Analysis of Polar Metabolites. *Methods Mol Biol* **2022**, *2396*, 137-159, doi:10.1007/978-1-0716-1822-6_11.
462. Spagou, K.; Tsoukali, H.; Raikos, N.; Gika, H.; Wilson, I.D.; Theodoridis, G. Hydrophilic interaction chromatography coupled to MS for metabonomic/metabolomic studies. *J Sep Sci* **2010**, *33*, 716-727, doi:10.1002/jssc.200900803.
463. Kopaciewicz, W.; Regnier, F.E. Mobile phase selection for the high-performance ion-exchange chromatography of proteins. *Anal Biochem* **1983**, *133*, 251-259, doi:10.1016/0003-2697(83)90251-8.
464. Choy, D.Y.; Creagh, A.L.; Haynes, C. Improved isoelectric focusing chromatography on strong anion exchange media via a new model that custom designs mobile phases using simple buffers. *Biotechnol Bioeng* **2014**, *111*, 552-564, doi:10.1002/bit.25122.
465. Jaćkowska, M.; Bocian, S.; Kosobucki, P.; Buszewski, B. Polymeric Functionalized Stationary Phase for Separation of Ionic Compounds by IC. *Chromatographia* **2010**, *72*, 611-616, doi:10.1365/s10337-010-1753-0.
466. Studzińska, S.; Bocian, S.; Kilanowska, A.; Buszewski, B. Dendrimer Anion-Exchange Stationary Phase for Separation of Oligonucleotides. *Molecules* **2022**, *27*, doi:10.3390/molecules27051491.
467. Law, B.; Hussain, M.A. Re-evaluation of anion-exchange HPLC for the analysis of acidic compounds. *J Pharm Biomed Anal* **2000**, *22*, 149-154, doi:10.1016/s0731-7085(99)00284-8.
468. Ikeda, K.; Takahashi, M.; Bamba, T.; Izumi, Y. Comparison of Amine-Modified Polymeric Stationary Phases for Polar Metabolomic Analysis Based on Unified-Hydrophilic Interaction/Anion Exchange Liquid Chromatography/High-Resolution Mass Spectrometry (Unified-HILIC/AEX/HRMS). *Mass Spectrom (Tokyo)* **2024**, *13*, A0143, doi:10.5702/massspectrometry.A0143.
469. Tang, D.Q.; Zou, L.; Yin, X.X.; Ong, C.N. HILIC-MS for metabolomics: An attractive and complementary approach to RPLC-MS. *Mass Spectrom Rev* **2016**, *35*, 574-600, doi:10.1002/mas.21445.
470. Yang, Q.; Zhang, A.H.; Miao, J.H.; Sun, H.; Han, Y.; Yan, G.L.; Wu, F.F.; Wang, X.J. Metabolomics biotechnology, applications, and future trends: a systematic review. *RSC Adv* **2019**, *9*, 37245-37257, doi:10.1039/c9ra06697g.
471. Castelli, F.A.; Rosati, G.; Moguet, C.; Fuentes, C.; Marrugo-Ramírez, J.; Lefebvre, T.; Volland, H.; Merkoçi, A.; Simon, S.; Fenaille, F.; et al. Metabolomics for personalized medicine: the input of analytical chemistry from biomarker discovery to point-of-care tests. *Anal Bioanal Chem* **2022**, *414*, 759-789, doi:10.1007/s00216-021-03586-z.
472. Peng, B.; Li, H.; Peng, X.X. Functional metabolomics: from biomarker discovery to metabolome reprogramming. *Protein Cell* **2015**, *6*, 628-637, doi:10.1007/s13238-015-0185-x.
473. Li, K.; Naviaux, J.C.; Bright, A.T.; Wang, L.; Naviaux, R.K. A robust, single-injection method for targeted, broad-spectrum plasma metabolomics. *Metabolomics* **2017**, *13*, 122, doi:10.1007/s11306-017-1264-1.
474. Hosseinkhani, F.; Huang, L.; Dubbelman, A.C.; Guled, F.; Harms, A.C.; Hankemeier, T. Systematic Evaluation of HILIC Stationary Phases for Global Metabolomics of Human Plasma. *Metabolites* **2022**, *12*, doi:10.3390/metabo12020165.
475. Fisher-Wellman, K.H.; Davidson, M.T.; Narowski, T.M.; Lin, C.T.; Koves, T.R.; Muoio, D.M. Mitochondrial Diagnostics: A Multiplexed Assay Platform for Comprehensive Assessment of Mitochondrial Energy Fluxes. *Cell Rep* **2018**, *24*, 3593-3606.e3510, doi:10.1016/j.celrep.2018.08.091.
476. Mordaunt, D.; Cox, D.; Fuller, M. Metabolomics to Improve the Diagnostic Efficiency of Inborn Errors of Metabolism. *Int J Mol Sci* **2020**, *21*, doi:10.3390/ijms21041195.
477. Peters, F.T.; Drummer, O.H.; Musshoff, F. Validation of new methods. *Forensic Sci Int* **2007**, *165*, 216-224, doi:10.1016/j.forsciint.2006.05.021.
478. Viswanathan, C.T.; Bansal, S.; Booth, B.; DeStefano, A.J.; Rose, M.J.; Sailstad, J.; Shah, V.P.; Skelly, J.P.; Swann, P.G.; Weiner, R. Quantitative bioanalytical methods validation and implementation: best practices for chromatographic and ligand binding assays. *Pharm Res* **2007**, *24*, 1962-1973, doi:10.1007/s11095-007-9291-7.
479. Shah, V.P.; Midha, K.K.; Findlay, J.W.; Hill, H.M.; Hulse, J.D.; McGilveray, I.J.; McKay, G.; Miller, K.J.; Patnaik, R.N.; Powell, M.L.; et al. Bioanalytical method validation--a revisit with a decade of progress. *Pharm Res* **2000**, *17*, 1551-1557, doi:10.1023/a:1007669411738.

480. Van Eeckhaut, A.; Lanckmans, K.; Sarre, S.; Smolders, I.; Michotte, Y. Validation of bioanalytical LC-MS/MS assays: evaluation of matrix effects. *J Chromatogr B Analyt Technol Biomed Life Sci* **2009**, *877*, 2198-2207, doi:10.1016/j.jchromb.2009.01.003.
481. Trufelli, H.; Palma, P.; Famiglini, G.; Cappiello, A. An overview of matrix effects in liquid chromatography-mass spectrometry. *Mass Spectrom Rev* **2011**, *30*, 491-509, doi:10.1002/mas.20298.
482. Peters, F.T.; Remane, D. Aspects of matrix effects in applications of liquid chromatography-mass spectrometry to forensic and clinical toxicology--a review. *Anal Bioanal Chem* **2012**, *403*, 2155-2172, doi:10.1007/s00216-012-6035-2.
483. Kostiainen, R.; Kauppila, T.J. Effect of eluent on the ionization process in liquid chromatography-mass spectrometry. *J Chromatogr A* **2009**, *1216*, 685-699, doi:10.1016/j.chroma.2008.08.095.
484. Li, W.; Zhang, J.; Francis, L. Handbook of LC-MS bioanalysis: best practices, experimental protocols, and regulations. **2013**.
485. Jemal, M.; Schuster, A.; Whigan, D.B. Liquid chromatography/tandem mass spectrometry methods for quantitation of mevalonic acid in human plasma and urine: method validation, demonstration of using a surrogate analyte, and demonstration of unacceptable matrix effect in spite of use of a stable isotope analog internal standard. *Rapid Commun Mass Spectrom* **2003**, *17*, 1723-1734, doi:10.1002/rcm.1112.
486. Want, E.J.; Wilson, I.D.; Gika, H.; Theodoridis, G.; Plumb, R.S.; Shockcor, J.; Holmes, E.; Nicholson, J.K. Global metabolic profiling procedures for urine using UPLC-MS. *Nat Protoc* **2010**, *5*, 1005-1018, doi:10.1038/nprot.2010.50.
487. Dunn, W.B.; Erban, A.; Weber, R.J.; Creek, D.J.; Brown, M.; Breitling, R.; Hankemeier, T.; Goodacre, R.; Neumann, S.; Kopka, J. Mass appeal: metabolite identification in mass spectrometry-focused untargeted metabolomics. *Metabolomics* **2013**, *9*, 44-66.
488. Liu, H.; Ding, L.; Zhang, H.; Mellor, D.; Wu, H.; Zhao, D.; Wu, C.; Lin, Z.; Yuan, J.; Peng, D. The Metabolic Factor Kynurenic Acid of Kynurenine Pathway Predicts Major Depressive Disorder. *Front Psychiatry* **2018**, *9*, 552, doi:10.3389/fpsyt.2018.00552.
489. Pan, J.X.; Xia, J.J.; Deng, F.L.; Liang, W.W.; Wu, J.; Yin, B.M.; Dong, M.X.; Chen, J.J.; Ye, F.; Wang, H.Y.; et al. Diagnosis of major depressive disorder based on changes in multiple plasma neurotransmitters: a targeted metabolomics study. *Transl Psychiatry* **2018**, *8*, 130, doi:10.1038/s41398-018-0183-x.
490. Bi, Q.; Zhao, J.; Nie, J.; Huang, F. Metabolic pathway analysis of tumors using stable isotopes. *Semin Cancer Biol* **2025**, *113*, 9-24, doi:10.1016/j.semcancer.2025.05.002.
491. Emwas, A.H.; Szczepski, K.; Al-Younis, I.; Lachowicz, J.I.; Jaremko, M. Fluxomics—New Metabolomics Approaches to Monitor Metabolic Pathways. *Front Pharmacol* **2022**, *13*, 805782, doi:10.3389/fphar.2022.805782.
492. Fan, T.W.; Lorkiewicz, P.K.; Sellers, K.; Moseley, H.N.; Higashi, R.M.; Lane, A.N. Stable isotope-resolved metabolomics and applications for drug development. *Pharmacol Ther* **2012**, *133*, 366-391, doi:10.1016/j.pharmthera.2011.12.007.
493. Liu, K.H.; Nellis, M.; Uppal, K.; Ma, C.; Tran, V.; Liang, Y.; Walker, D.I.; Jones, D.P. Reference Standardization for Quantification and Harmonization of Large-Scale Metabolomics. *Anal Chem* **2020**, *92*, 8836-8844, doi:10.1021/acs.analchem.0c00338.
494. Gáspár, R.; Halmi, D.; Demján, V.; Berkecz, R.; Pipicz, M.; Csont, T. Kynurenine Pathway Metabolites as Potential Clinical Biomarkers in Coronary Artery Disease. *Front Immunol* **2021**, *12*, 768560, doi:10.3389/fimmu.2021.768560.
495. Tan, Y.Q.; Wang, Y.N.; Feng, H.Y.; Guo, Z.Y.; Li, X.; Nie, X.L.; Zhao, Y.Y. Host/microbiota interactions-derived tryptophan metabolites modulate oxidative stress and inflammation via aryl hydrocarbon receptor signaling. *Free Radic Biol Med* **2022**, *184*, 30-41, doi:10.1016/j.freeradbiomed.2022.03.025.
496. Birch, P.J.; Grossman, C.J.; Hayes, A.G. Kynurenate and FG9041 have both competitive and non-competitive antagonist actions at excitatory amino acid receptors. *Eur J Pharmacol* **1988**, *151*, 313-315, doi:10.1016/0014-2999(88)90814-x.
497. Sawa-Wejksza, K.; Parada-Turska, J.; Turski, W. The Pharmacological Evidences for the Involvement of AhR and GPR35 Receptors in Kynurenic Acid-Mediated Cytokine and Chemokine Secretion by THP-1-Derived Macrophages. *Molecules* **2025**, *30*, doi:10.3390/molecules30153133.

498. Villani, S.; Fallarini, S.; Rezzi, S.J.; Di Martino, R.M.C.; Aprile, S.; Del Grosso, E. Selective inhibition of indoleamine and tryptophan 2,3-dioxygenases: Comparative study on kynurenine pathway in cell lines via LC-MS/MS-based targeted metabolomics. *J Pharm Biomed Anal* **2024**, *237*, 115750, doi:10.1016/j.jpba.2023.115750.
499. Zhao, S.; Luo, X.; Li, L. Chemical Isotope Labeling LC-MS for High Coverage and Quantitative Profiling of the Hydroxyl Submetabolome in Metabolomics. *Anal Chem* **2016**, *88*, 10617-10623, doi:10.1021/acs.analchem.6b02967.
500. Schönberger, K.; Mitterer, M.; Glaser, K.; Stecher, M.; Hobitz, S.; Schain-Zota, D.; Schuldes, K.; Lämmermann, T.; Rambold, A.S.; Cabezas-Wallscheid, N.; et al. LC-MS-Based Targeted Metabolomics for FACS-Purified Rare Cells. *Anal Chem* **2023**, *95*, 4325-4334, doi:10.1021/acs.analchem.2c04396.
501. Nadour, Z.; Simian, C.; Laprévote, O.; Loriot, M.A.; Larabi, I.A.; Pallet, N. Validation of a liquid chromatography coupled to tandem mass spectrometry method for simultaneous quantification of tryptophan and 10 key metabolites of the kynurenine pathway in plasma and urine: Application to a cohort of acute kidney injury patients. *Clin Chim Acta* **2022**, *534*, 115-127, doi:10.1016/j.cca.2022.07.009.
502. Liu, Z.; Ma, Z.; Jin, L.; Nizhamuding, X.; Zeng, J.; Zhang, T.; Zhang, J.; Wang, J.; Zhao, H.; Zhou, W.; et al. Altered neopterin and IDO in kynurenine metabolism based on LC-MS/MS metabolomics study: Novel therapeutic checkpoints for type 2 diabetes mellitus. *Clin Chim Acta* **2024**, *557*, 117859, doi:10.1016/j.cca.2024.117859.
503. Pang, Z.; Xu, L.; Viau, C.; Lu, Y.; Salavati, R.; Basu, N.; Xia, J. MetaboAnalystR 4.0: a unified LC-MS workflow for global metabolomics. *Nat Commun* **2024**, *15*, 3675, doi:10.1038/s41467-024-48009-6.
504. Chen, J.; Zhang, P.; Qin, S.; Tan, B.; Li, S.; Tang, S.; Liao, C.; Zhang, Y.; Zhang, Z.; Xu, F. Stepwise solid phase extraction integrated with chemical derivatization for all-in-one injection LC-MS/MS analysis of metabolome and lipidome. *Anal Chim Acta* **2023**, *1241*, 340807, doi:10.1016/j.aca.2023.340807.
505. Saigusa, D.; Okamura, Y.; Motoike, I.N.; Katoh, Y.; Kurosawa, Y.; Saijyo, R.; Koshiba, S.; Yasuda, J.; Motohashi, H.; Sugawara, J.; et al. Establishment of Protocols for Global Metabolomics by LC-MS for Biomarker Discovery. *PLoS One* **2016**, *11*, e0160555, doi:10.1371/journal.pone.0160555.
506. Joisten, N.; Ruas, J.L.; Braidy, N.; Guillemin, G.J.; Zimmer, P. The kynurenine pathway in chronic diseases: a compensatory mechanism or a driving force? *Trends Mol Med* **2021**, *27*, 946-954, doi:10.1016/j.molmed.2021.07.006.
507. Braidy, N.; Berg, J.; Clement, J.; Khorshidi, F.; Poljak, A.; Jayasena, T.; Grant, R.; Sachdev, P. Role of Nicotinamide Adenine Dinucleotide and Related Precursors as Therapeutic Targets for Age-Related Degenerative Diseases: Rationale, Biochemistry, Pharmacokinetics, and Outcomes. *Antioxid Redox Signal* **2019**, *30*, 251-294, doi:10.1089/ars.2017.7269.
508. Wee, H.N.; Liu, J.J.; Ching, J.; Kovalik, J.P.; Lim, S.C. The Kynurenine Pathway in Acute Kidney Injury and Chronic Kidney Disease. *Am J Nephrol* **2021**, *52*, 771-787, doi:10.1159/000519811.
509. Zhai, Y.; Chavez, J.A.; D'Aquino, K.E.; Meng, R.; Nawrocki, A.R.; Pocai, A.; Wang, L.; Ma, L.J. Kynurenine 3-monooxygenase limits de novo NAD(+) synthesis through dietary tryptophan in renal proximal tubule epithelial cell models. *Am J Physiol Cell Physiol* **2024**, *326*, C1423-c1436, doi:10.1152/ajpcell.00445.2023.
510. Dehhaghi, M.; Kazemi Shariat Panahi, H.; Guillemin, G.J. Microorganisms, Tryptophan Metabolism, and Kynurenine Pathway: A Complex Interconnected Loop Influencing Human Health Status. *Int J Tryptophan Res* **2019**, *12*, 1178646919852996, doi:10.1177/1178646919852996.
511. Zhang, X.; Dong, J.; Raftery, D. Five Easy Metrics of Data Quality for LC-MS-Based Global Metabolomics. *Anal Chem* **2020**, *92*, 12925-12933, doi:10.1021/acs.analchem.0c01493.
512. Konakchieva, R.; Mladenov, M.; Konaktchieva, M.; Sazdova, I.; Gagov, H.; Nikolaev, G. Circadian Clock Deregulation and Metabolic Reprogramming: A System Biology Approach to Tissue-Specific Redox Signaling and Disease Development. *Int J Mol Sci* **2025**, *26*, doi:10.3390/ijms26136267.
513. Froy, O.; Weintraub, Y. The circadian clock, metabolism, and inflammation-the holy trinity of inflammatory bowel diseases. *Clin Sci (Lond)* **2025**, *139*, 777-790, doi:10.1042/cs20256383.
514. Moaddel, R.; Candia, J.; Ubaida-Mohien, C.; Tanaka, T.; Moore, A.Z.; Zhu, M.; Fantoni, G.; Church, S.; D'Agostino, J.; Fan, J.; et al. Healthy Aging Metabolomic and Proteomic Signatures Across Multiple Physiological Compartments. *Aging Cell* **2025**, *24*, e70014, doi:10.1111/acel.70014.

515. Overgaard, N.H.; Fan, T.M.; Schachtschneider, K.M.; Principe, D.R.; Schook, L.B.; Jungersen, G. Of Mice, Dogs, Pigs, and Men: Choosing the Appropriate Model for Immuno-Oncology Research. *Ilar j* **2018**, *59*, 247-262, doi:10.1093/ilar/ily014.
516. Guerrero-López, P.; Martín-Pardillos, A.; Bonet-Aleta, J.; Mosseri, A.; Hueso, J.L.; Santamaria, J.; Garcia-Aznar, J.M. 2D versus 3D tumor-on-chip models to study the impact of tumor organization on metabolic patterns in vitro. *Sci Rep* **2025**, *15*, 19506, doi:10.1038/s41598-025-03504-8.
517. Luan, H.; Ji, F.; Chen, Y.; Cai, Z. statTarget: A streamlined tool for signal drift correction and interpretations of quantitative mass spectrometry-based omics data. *Anal Chim Acta* **2018**, *1036*, 66-72, doi:10.1016/j.aca.2018.08.002.
518. Pedraz-Petrozzi, B.; Marszalek-Grabska, M.; Kozub, A.; Szalaj, K.; Trzpil, A.; Stachniuk, A.; Lamadé, E.K.; Gilles, M.; Deuschle, M.; Turski, W.A.; et al. LC-MS/MS-based quantification of tryptophan, kynurenine, and kynurenic acid in human placental, fetal membranes, and umbilical cord samples. *Sci Rep* **2023**, *13*, 12554, doi:10.1038/s41598-023-39774-3.
519. Wang, G.; Heijs, B.; Kostidis, S.; Mahfouz, A.; Rietjens, R.G.J.; Bijkerk, R.; Koudijs, A.; van der Pluijm, L.A.K.; van den Berg, C.W.; Dumas, S.J.; et al. Analyzing cell-type-specific dynamics of metabolism in kidney repair. *Nat Metab* **2022**, *4*, 1109-1118, doi:10.1038/s42255-022-00615-8.
520. Buergel, T.; Steinfeldt, J.; Ruyoga, G.; Pietzner, M.; Bizzarri, D.; Vojinovic, D.; Upmeier Zu Belzen, J.; Loock, L.; Kittner, P.; Christmann, L.; et al. Metabolomic profiles predict individual multidisease outcomes. *Nat Med* **2022**, *28*, 2309-2320, doi:10.1038/s41591-022-01980-3.
521. Golubova, A.; Lanekoff, I. Quantitative approaches for spatial metabolomics with isomer differentiation using surface sampling capillary electrophoresis mass spectrometry. *Talanta* **2026**, *296*, 128482, doi:10.1016/j.talanta.2025.128482.
522. van der Walt, G.; Louw, R. Novel mitochondrial and cytosolic purification pipeline for compartment-specific metabolomics in mammalian disease model tissues. *Metabolomics* **2020**, *16*, 78, doi:10.1007/s11306-020-01697-9.
523. Wang, Z.; Fu, W.; Huo, M.; He, B.; Liu, Y.; Tian, L.; Li, W.; Zhou, Z.; Wang, B.; Xia, J.; et al. Spatial-resolved metabolomics reveals tissue-specific metabolic reprogramming in diabetic nephropathy by using mass spectrometry imaging. *Acta Pharm Sin B* **2021**, *11*, 3665-3677, doi:10.1016/j.apsb.2021.05.013.
524. Knitsch, R.; AlWahsh, M.; Raschke, H.; Lambert, J.; Hergenröder, R. In Vitro Spatio-Temporal NMR Metabolomics of Living 3D Cell Models. *Anal Chem* **2021**, *93*, 13485-13494, doi:10.1021/acs.analchem.1c02221.
525. van der Walt, G.; Lindeque, J.Z.; Mason, S.; Louw, R. Sub-Cellular Metabolomics Contributes Mitochondria-Specific Metabolic Insights to a Mouse Model of Leigh Syndrome. *Metabolites* **2021**, *11*, doi:10.3390/metabo11100658.
526. Qin, S.; Gao, M.; Zhang, Q.; Xiao, Q.; Fu, J.; Tian, Y.; Jiao, Y.; Zhang, Z.; Zhang, P.; Xu, F. High-Coverage Strategy for Multi-Subcellular Metabolome Analysis Using Dansyl-Labeling-Based LC-MS/MS. *Anal Chem* **2023**, *95*, 10034-10043, doi:10.1021/acs.analchem.3c01343.
527. More, T.H.; Hiller, K. Complexity of subcellular metabolism: strategies for compartment-specific profiling. *Curr Opin Biotechnol* **2022**, *75*, 102711, doi:10.1016/j.copbio.2022.102711.
528. Talmor-Barkan, Y.; Bar, N.; Shaul, A.A.; Shahaf, N.; Godneva, A.; Bussi, Y.; Lotan-Pompan, M.; Weinberger, A.; Shechter, A.; Chezar-Azerrad, C.; et al. Metabolomic and microbiome profiling reveals personalized risk factors for coronary artery disease. *Nat Med* **2022**, *28*, 295-302, doi:10.1038/s41591-022-01686-6.
529. Geier, B.; Sogin, E.M.; Michellod, D.; Janda, M.; Kompauer, M.; Spengler, B.; Dubilier, N.; Liebeke, M. Spatial metabolomics of in situ host-microbe interactions at the micrometre scale. *Nat Microbiol* **2020**, *5*, 498-510, doi:10.1038/s41564-019-0664-6.
530. Yu, Y.; Zhang, N.; Mai, Y.; Ren, L.; Chen, Q.; Cao, Z.; Chen, Q.; Liu, Y.; Hou, W.; Yang, J.; et al. Correcting batch effects in large-scale multiomics studies using a reference-material-based ratio method. *Genome Biol* **2023**, *24*, 201, doi:10.1186/s13059-023-03047-z.
531. Viant, M.R.; Ebbels, T.M.D.; Beger, R.D.; Ekman, D.R.; Epps, D.J.T.; Kamp, H.; Leonards, P.E.G.; Loizou, G.D.; MacRae, J.I.; van Ravenzwaay, B.; et al. Use cases, best practice and reporting standards for metabolomics in regulatory toxicology. *Nat Commun* **2019**, *10*, 3041, doi:10.1038/s41467-019-10900-y.

 doi:10.20944/preprints202601.0822.v1

532. Nian, M.; Chen, X.; Fang, M. Addressing Pitfalls of Metabolomics for Toxicology: A Call for Standardization, Reproducibility and Data Sharing. *Chem Res Toxicol* **2025**, *38*, 1150-1156, doi:10.1021/acs.chemrestox.4c00555.
533. Rampler, E.; Abiead, Y.E.; Schoeny, H.; Rusz, M.; Hildebrand, F.; Fitz, V.; Koellensperger, G. Recurrent Topics in Mass Spectrometry-Based Metabolomics and Lipidomics-Standardization, Coverage, and Throughput. *Anal Chem* **2021**, *93*, 519-545, doi:10.1021/acs.analchem.0c04698.
534. Garrett, R.; Ptolemy, A.S.; Pickett, S.; Kellogg, M.D.; Peake, R.W.A. Untargeted Metabolomics for Inborn Errors of Metabolism: Development and Evaluation of a Sustainable Reference Material for Correcting Inter-Batch Variability. *Clin Chem* **2024**, *70*, 1452-1462, doi:10.1093/clinchem/hvae141.
535. Long, N.P.; Nghi, T.D.; Kang, Y.P.; Anh, N.H.; Kim, H.M.; Park, S.K.; Kwon, S.W. Toward a Standardized Strategy of Clinical Metabolomics for the Advancement of Precision Medicine. *Metabolites* **2020**, *10*, doi:10.3390/metabo10020051.
536. Malinowska, J.M.; Whelan, M. The important role of standards for the uptake of transcriptomics and metabolomics based in vitro methods in regulatory toxicology. *Arch Toxicol* **2025**, *99*, 3865-3875, doi:10.1007/s00204-025-04119-8.
537. Liu, J. Computational aspects of psychometric methods with R by Patricia Martinková and Adéla Hladká, Chapman & Hall/CRC, 2023, ISBN: 9781003054313, https://doi.org/10.1201/9781003054313. *Biometrics* **2025**, doi:10.1093/biomtc/ujaf132.
538. Harada, S.; Iida, M.; Miyagawa, N.; Hirata, A.; Kuwabara, K.; Matsumoto, M.; Okamura, T.; Edagawa, S.; Kawada, Y.; Miyake, A.; et al. Study Profile of the Tsuruoka Metabolomics Cohort Study (TMCS). *J Epidemiol* **2024**, *34*, 393-401, doi:10.2188/jea.JE20230192.
539. Sturm, G.; Monzel, A.S.; Karan, K.R.; Michelson, J.; Ware, S.A.; Cardenas, A.; Lin, J.; Bris, C.; Santhanam, B.; Murphy, M.P.; et al. A multi-omics longitudinal aging dataset in primary human fibroblasts with mitochondrial perturbations. *Sci Data* **2022**, *9*, 751, doi:10.1038/s41597-022-01852-y.
540. Dukovski, I.; Bajić, D.; Chacón, J.M.; Quintin, M.; Vila, J.C.C.; Sulheim, S.; Pacheco, A.R.; Bernstein, D.B.; Riehl, W.J.; Korolev, K.S.; et al. A metabolic modeling platform for the computation of microbial ecosystems in time and space (COMETS). *Nat Protoc* **2021**, *16*, 5030-5082, doi:10.1038/s41596-021-00593-3.
541. Ma, Y.; Jin, J.; Xue, Z.; Zhao, J.; Cai, W.; Zhang, W. Integrated multi-omics analysis and machine learning developed a prognostic model based on mitochondrial function in a large multicenter cohort for Gastric Cancer. *J Transl Med* **2024**, *22*, 381, doi:10.1186/s12967-024-05109-7.
542. Weiss, E.; de la Peña-Ramirez, C.; Aguilar, F.; Lozano, J.J.; Sánchez-Garrido, C.; Sierra, P.; Martin, P.I.; Diaz, J.M.; Fenaille, F.; Castelli, F.A.; et al. Sympathetic nervous activation, mitochondrial dysfunction and outcome in acutely decompensated cirrhosis: the metabolomic prognostic models (CLIF-C MET). *Gut* **2023**, *72*, 1581-1591, doi:10.1136/gutjnl-2022-328708.
543. Xu, Y.; Ritchie, S.C.; Liang, Y.; Timmers, P.; Pietzner, M.; Lannelongue, L.; Lambert, S.A.; Tahir, U.A.; May-Wilson, S.; Foguet, C.; et al. An atlas of genetic scores to predict multi-omic traits. *Nature* **2023**, *616*, 123-131, doi:10.1038/s41586-023-05844-9.
544. Alston, C.L.; Stenton, S.L.; Hudson, G.; Prokisch, H.; Taylor, R.W. The genetics of mitochondrial disease: dissecting mitochondrial pathology using multi-omic pipelines. *J Pathol* **2021**, *254*, 430-442, doi:10.1002/path.5641.
545. Lane, A.N.; Tan, J.; Wang, Y.; Yan, J.; Higashi, R.M.; Fan, T.W. Probing the metabolic phenotype of breast cancer cells by multiple tracer stable isotope resolved metabolomics. *Metab Eng* **2017**, *43*, 125-136, doi:10.1016/j.ymben.2017.01.010.
546. Roci, I.; Gallart-Ayala, H.; Schmidt, A.; Watrous, J.; Jain, M.; Wheelock, C.E.; Nilsson, R. Metabolite Profiling and Stable Isotope Tracing in Sorted Subpopulations of Mammalian Cells. *Anal Chem* **2016**, *88*, 2707-2713, doi:10.1021/acs.analchem.5b04071.
547. Timón-Gómez, A.; Doerrier, C.; Sumbalová, Z.; Garcia-Souza, L.F.; Baglivo, E.; Cardoso, L.H.D.; Gnaiger, E. Bioenergetic profiles and respiratory control in mitochondrial physiology: Precision analysis of oxidative phosphorylation. *Exp Physiol* **2025**, doi:10.1113/ep092792.

 doi:10.20944/preprints202601.0822.v1

548. Seifert, J.; Taubert, M.; Jehmlich, N.; Schmidt, F.; Völker, U.; Vogt, C.; Richnow, H.H.; von Bergen, M. Protein-based stable isotope probing (protein-SIP) in functional metaproteomics. *Mass Spectrom Rev* **2012**, *31*, 683-697, doi:10.1002/mas.21346.
549. Rodriguez, P.; Laskowski, L.J.; Pallais, J.P.; Bock, H.A.; Cavalco, N.G.; Anderson, E.I.; Calkins, M.M.; Razzoli, M.; Sham, Y.Y.; McCorvy, J.D.; et al. Functional profiling of the G protein-coupled receptor C3aR1 reveals ligand-mediated biased agonism. *J Biol Chem* **2024**, *300*, 105549, doi:10.1016/j.jbc.2023.105549.
550. Hilmas, C.; Pereira, E.F.; Alkondon, M.; Rassoulpour, A.; Schwarcz, R.; Albuquerque, E.X. The brain metabolite kynurenic acid inhibits alpha7 nicotinic receptor activity and increases non-alpha7 nicotinic receptor expression: physiopathological implications. *J Neurosci* **2001**, *21*, 7463-7473, doi:10.1523/jneurosci.21-19-07463.2001.
551. Sapko, M.T.; Guidetti, P.; Yu, P.; Tagle, D.A.; Pellicciari, R.; Schwarcz, R. Endogenous kynurenate controls the vulnerability of striatal neurons to quinolinate: Implications for Huntington's disease. *Exp Neurol* **2006**, *197*, 31-40, doi:10.1016/j.expneurol.2005.07.004.
552. Bock, A.; Bermudez, M. Allosteric coupling and biased agonism in G protein-coupled receptors. *Febs j* **2021**, *288*, 2513-2528, doi:10.1111/febs.15783.
553. Cadenas, S. Mitochondria rescue cells from ischemic injury. *Science* **2022**, *377*, 579-580, doi:10.1126/science.add4629.
554. Erhardt, S.; Schwieler, L.; Imbeault, S.; Engberg, G. The kynurenine pathway in schizophrenia and bipolar disorder. *Neuropharmacology* **2017**, *112*, 297-306, doi:10.1016/j.neuropharm.2016.05.020.
555. Zielonka, J.; Joseph, J.; Sikora, A.; Hardy, M.; Ouari, O.; Vasquez-Vivar, J.; Cheng, G.; Lopez, M.; Kalyanaraman, B. Mitochondria-Targeted Triphenylphosphonium-Based Compounds: Syntheses, Mechanisms of Action, and Therapeutic and Diagnostic Applications. *Chem Rev* **2017**, *117*, 10043-10120, doi:10.1021/acs.chemrev.7b00042.
556. Singh, A.; Faccenda, D.; Campanella, M. Pharmacological advances in mitochondrial therapy. *EBioMedicine* **2021**, *65*, 103244, doi:10.1016/j.ebiom.2021.103244.
557. Stone, T.W.; Williams, R.O. Tryptophan metabolism as a 'reflex' feature of neuroimmune communication: Sensor and effector functions for the indoleamine-2, 3-dioxygenase kynurenine pathway. *J Neurochem* **2024**, *168*, 3333-3357, doi:10.1111/jnc.16015.